UNIVERSITY OF READING

Department of Meteorology

School of Mathematical, Physical and

Computational Sciences

Drivers and feedbacks impacting the Caspian Sea hydroclimate

SIFAN A. KORICHE

A thesis submitted for the degree of Doctor of Philosophy

February 2021

Declaration

I confirm that this is my own work and the use of all material from other sources has been properly and fully acknowledged.

Sifan A. Koriche

Dedicated to the memory of my son, my mother, my sister,

and to all martyred Oromoo Qeerroo and Qarree!

May their souls rest in peace and power!

ODAA: the symbol of Oromoo and Oromummaa!

"Gabrummaa hiddaan buqqifna;

dadhabnu ilmaan itti guddifna!"

J/Waaqoo Guutuu

Abstract

The Caspian Sea is the world's largest land-locked lake. It plays a key role in the Pontocaspian region, with a unique ecosystem providing numerous ecosystem services to millions of people. Large variations in Caspian Sea level have occurred in the past and are projected for the future. However, there is considerable debate about the importance of different drivers and feedbacks leading to these variations. The primary aim of this thesis is to use a modelling approach to improve our understanding of Caspian Sea hydroclimate and sea level from the late Quaternary to the end of the 21st century.

Firstly, contributions to Caspian Sea level from glacial-interglacial climate change, topographic changes due to ice-sheet loading, and ice-sheet meltwater were explored by combining climate model simulations and ice-sheet reconstructions to drive a hydrological model. The results show that the reorganization of river drainage systems due to Fennoscandian ice-sheet growth and retreat played the dominant role in the variation of the Caspian Sea level in the late glacial high-stand, while hydroclimate change was the major factor leading to the early Holocene low-stand.

Secondly, given that large changes in Caspian Sea area will accompany changes in sea level, a separate climate model experiment examined the extent and magnitude of subsequent climate feedbacks. Results indicate an important local negative lake surface-evaporation feedback and remote teleconnections, impacting as far as the North Pacific. This also demonstrates the need for accurate representation of the Caspian Sea in climate models.

Finally, a hydrological balance model was used to explore future Caspian Sea level changes based on multi-model climate projections from the Coupled Model Intercomparison Project (CMIP5 and CMIP6) and idealized water extraction scenarios. The combined impacts of anthropogenic warming and water withdrawals will lead to a decline in Caspian Sea level and the desiccation of the shallow northern Caspian Sea before 2100. This will have multifaceted implications for the surrounding communities, increasing freshwater scarcity, transforming ecosystems, and impacting the climate system.

Axareeraa

Haroon 'Caspian Sea' haroowwan addunyaa irratti argman keessaa bal'inaan sadarkaa tokkoffaa irrattii argama. Haroon kun 'Pontocaspian' keessatti shoora ol aanaa qaba. Lammiilee kitila hedduu biyyoota baha Awurooppaa, lixaafi giddugaleessa Eeshiyaa keessatti argamaniif dhimmoota adda addaaf fayyada (fkf., oomisha qurxummiif). Haroon 'Caspian Sea' takka guutee, yeroo biraa ammoo hir'atee, addummaa guddaa agarsiisee jira. Kun akka fuuldurattis ta'u tilmaamamee jira. Haa ta'u malee, qorannoowwan adda addaa wantoonni guutuufi hir'achuu haroo kanaaf gumaachan falmisiisoo ta'uu mul'isu. Kanaafuu, kaayyoon qoraannoo kanaa, inni jalqabaa, waggoota kumootan lakka'amanii kaasee hanga dhuma jaarraa 21ffaatti qorachuun maddaafi sababaalee jijjiirama haala qilleensaafi hir'achuufi guutuu 'Caspian Sea'-iif kanneen gumaachan xiinxalee jira.

Jalqaba irratti, haroo 'Caspian Sea' hir'isuufi guutuuf maddaafi sababii ta'uu danda'u jedhamuun kanneen tilmaamaman keessaa kan akka jijjiirama haala qilleensaa yeroo dachiin cabbiin uwwifamtee ('glacial')-fi ho'inni dachii dabalu ('interglacial'), jijjiirama taa'umsa lafaa kuufama cabbii irraa ka'eefi baqinsa cabbiin walqabate xiinxaluun moodela jijjiirama haroo 'Caspian Sea' kan waggootii kumaataman lakka'amaniif hojjechuufi xiinxaluu ture. Haaluma kanaan, maddi jijjiirama 'Caspian Sea' caalmaatti sababa kuufamaafi baqinsa cabbii 'Fennoscandian ice-sheet' kan ture ta'uu bu'aan qorannoo kanaa agarsiisa. Itti aanun jijjiiramni haala qilleensaas hir'isuufi guutuu haroo kanaaf gumaachee jira.

Lammaffarratti, moodela haala qilleensaa qorachuuf gargaaru fayyadamuun gahee guutuufi hir'achuun haroo 'Caspian Sea' qilleensa jijjiiruu irratti qabu adda baasuuf qorannoon kun xiinxalee jira. Guutuufi hir'achuun 'Caspian Sea' qilleensa naannoo jijjiiruuf shooraa guddaa gumaacha. Kana irra darbees, iddoowwan haroo kana irraa fagoo, kanneen akka giddu-galeessa Eeshiiyaafi kaaba garba Paasifik, ta'anittillee qilleensa jijjiiruu danda'a.

Dhumarratti, qorannoon kun gahee jijjiirama haala qilleensaafi itti fayyadamni bishaanii hanga dhumaa jaarraa 21ffaatti haroo 'Caspian Sea' irratti qabaachuu danda'an xiinxalee jira. Haaluma kanaan, sababoonni armaan olitti ibsaman lamaan, hir'achuu haroo kanaaf shoora ol'aanaa akka gumaachan xiinxalli kun agarsiisa. Dhuma jaarraa 21ffaan duraa, bal'inni haroo

kanaa harka sadii keessaa harki tokko akka goguu danda'u qorannoon kun nimul'isa. Kun immoo lammiilee haroo kana qarqara jiraataniifi kanneen diinagdee irratti bu'ureffataniifi uumamaa guddaa miidhuu danda'a. Dabalataan jijjiirama haala qilleensaas fiduu danda'a.

Authorship of papers

The papers listed below have been included in this thesis in the format that they were submitted to their respective journals for publication. The first and second papers are under review at JGR-Atmospheres and Quaternary Science Review respectively. The third paper is accepted at Environmental Research Letters. The fourth paper was published in 2019 at Earth-Science Reviews (accessible at https://doi.org/10.1016/j.earscirev.2018.10.013). The Supplementary Information for the first, second, and third papers can be found in the Appendices.

(1) **Koriche**, S. A., Singarayer, J.S., Cloke, H.L., Valdes, P.J., Wesselingh, F.P., Kroonenberg, S.B., Wickert, A.D. and Yanina, T.A. (2020). What are the drivers of Caspian Sea level variation during the late Quaternary? Under review at Journal of Quaternary Science Review. [S.A.K. c*ontribution= 90%]*

(2) **Koriche**, S. A., Nandini-Weiss, S. D., Prange. M., Singarayer, J.S., Arpe, K., Cloke, H.L., Schul, M., Bakker, P., Leroy, S.A.G. and Coe, M.T. (2020). Impacts of variations in Caspian Sea surface area on catchment-scale and large-scale climate. Under review at JGR-Atmospheres. [*S.A.K. contribution= 65%]*

(3) **Koriche**, S. A., Singarayer, J.S. and Cloke, H.L. (2021). The fate of Caspian Sea under projected climate change and water extraction during the 21st century. Submitted to Environmental Research Letters. [S.A.K. c*ontribution= 90%]*

(4) Krijgsman, W., Tesakov, A., Yanina, T., Lazarev, S., Danukalova, G., Van Baak, C.G.C., Agustí, J., Alçiçek, M.C., Aliyeva, E., Bista, D., Bruch, A., Büyükmeriç, Y., Bukhsianidze, M., Flecker, R., Frolov, P., Hoyle, T.M., Jorissen, E.L., Kirscher, U., **Koriche**, S.A., Kroonenberg, S.B., Lordkipanidze, D., Oms, O., Rausch, L., Singarayer, J., Stoica, M., van de Velde, S., Titov, V.V. and Wesselingh, F.P., 2019. Quaternary time scales for the Pontocaspian domain: Interbasinal connectivity and faunal evolution. Earth-Science Reviews 188, 1-40. 10.1016/j.earscirev.2018.10.013. [S.A.K. c*ontribution= 15%]*

Acknowledgements

Contents

List of Figures

List of Tables

1. CHAPTER ONE: Introduction

1.1 Background and motivation

The 'Pontocaspian' region encompasses the world's largest basins: the closed basin of the Caspian Sea and two currently open basins connecting to the global ocean, the Black Sea and the Sea of Azov (Fig. 1.1). The region has unique endemic aquatic biota including fish, molluscs, crustaceans and planktonic groups (Grigorovich et al., 2003; Marret et al., 2004) that are adapted to the unusual salinity regimes of these basins. Many of these Pontocaspian species have been facing severe declines in population and even extinction since the 1930s. This is due to pressures from anthropogenic activities such as water extraction, oil exploration, and global shipping leading to habitat degradation, pollution, and invasive species introduced either accidentally via shipping or intentionally for fisheries (Grigorovich et al., 2003; Latypov, 2015). Over the last one hundred years, the species diversity of the Caspian Sea fauna has considerably decreased from abundant endemic faunal species (Fig. 1.2a) to one dominated by a few invasive species (Fig. 1.2b).

Figure 1.1. Present-day drainage area of the Pontocaspian region. The red and pink outlines are catchment areas of the Caspian Sea and Black Sea basins. Shaded relief, water, and drainages are made with Natural Earth (Free vector and raster map data @ naturalearthdata.com). (Key: KBG – Kara-Bogaz-Gol lagoon)

The region has a dynamic history of basin development and biotic evolution. During the Quaternary period (the last 2.5 million years) it was dominated by major changes in water (lake and sea) levels resulting in a pulsating system of connected and isolated basins (Bezrodnykh et al., 2004; Rychagov, 1997b; Svitoch, 2013; Yanina, 2012) (Fig. 1.3), which affected the biodiversity of the system, as a number of paleoenvironmenal records suggest (Krijgsman et al., 2019; Nevesskaja, 2007; Svitoch and Yanina, 2001; Yanina, 2014). Consequently, many episodes of biodiversity crises were recorded during the Quaternary period (e.g. the last natural turnover occurred in the early Holocene between 10–8 kyr; Krijgsman et al., 2019) during which there was diversification and extinction, as well as geographical contraction and expansion of Pontocaspian biota.

Figure 1.2. Caspian faunas about (a) 100 years ago and (b) present day (©Frank Wesselingh)

The geological history of the Pontocaspian basin and the paleontological record of the biota makes this an ideal system to investigate the relationship between biodiversity turnover and external drivers such as climate change, lake geochemistry, nutrient dynamics, as well as invasive species. Understanding past causes and consequences of biodiversity change will enhance our understanding of the current biodiversity crisis. A major industrial-academic partnership project was set up to tackle this research gap, and was funded by the EU Marie Curie-Sklodowska Innovative Training Network (ITN) scheme. The multi-disciplinary research project involved climate-, earth-, and bio-sciences and was entitled 'Drivers of Pontocaspian biodiversity Rise and Demise' (PRIDE). PRIDE sought to contextualise the present biodiversity crisis of endemic fauna in the Pontocaspian basin within longer term changes to climate, geology, and biology that have driven previous variations in Pontocaspian basin biodiversity. The programme was organised in three research/training work packages. The first work package concerned Quaternary Pontocaspian lake system evolution. The second work package dealt with the documentation of biodiversity change in the Quaternary record, and the third work package targeted the Anthropocene biodiversity crisis. In each work package, there were five projects, and a description of all 15 projects can be found at https://www.pontocaspian.eu. The research presented in this doctoral thesis forms part of the first work package.

The first work package was to study the Pontocaspian lake system's evolution, with a goal to understand and identify drivers of development of lake basins (and their biota) in the Quaternary. This involved modelling of the climate system and the lake basin, characterization of the drivers and change indicators based on geochemical and biological analysis, and creation of an updated Pontocaspian stratigraphic framework. As part of the first work package, the particular focus of this study is the Caspian Sea basin. The Caspian Sea, part of a closed basin, has experienced large variations of water level on various time scales and is sensitive to changes induced by hydroclimatological and geophysical processes, therefore, playing a main role during episodes of connections with the Black sea basin, as various palaeo-environmental records indicate (Krijgsman et al., 2019; Leroy et al., 2020). This study investigates the influence of climate on Caspian Sea level through the changing balance of evaporation, precipitation, and drainage patterns, considering the various potential driving processes and the environmental setting of a closed basin.
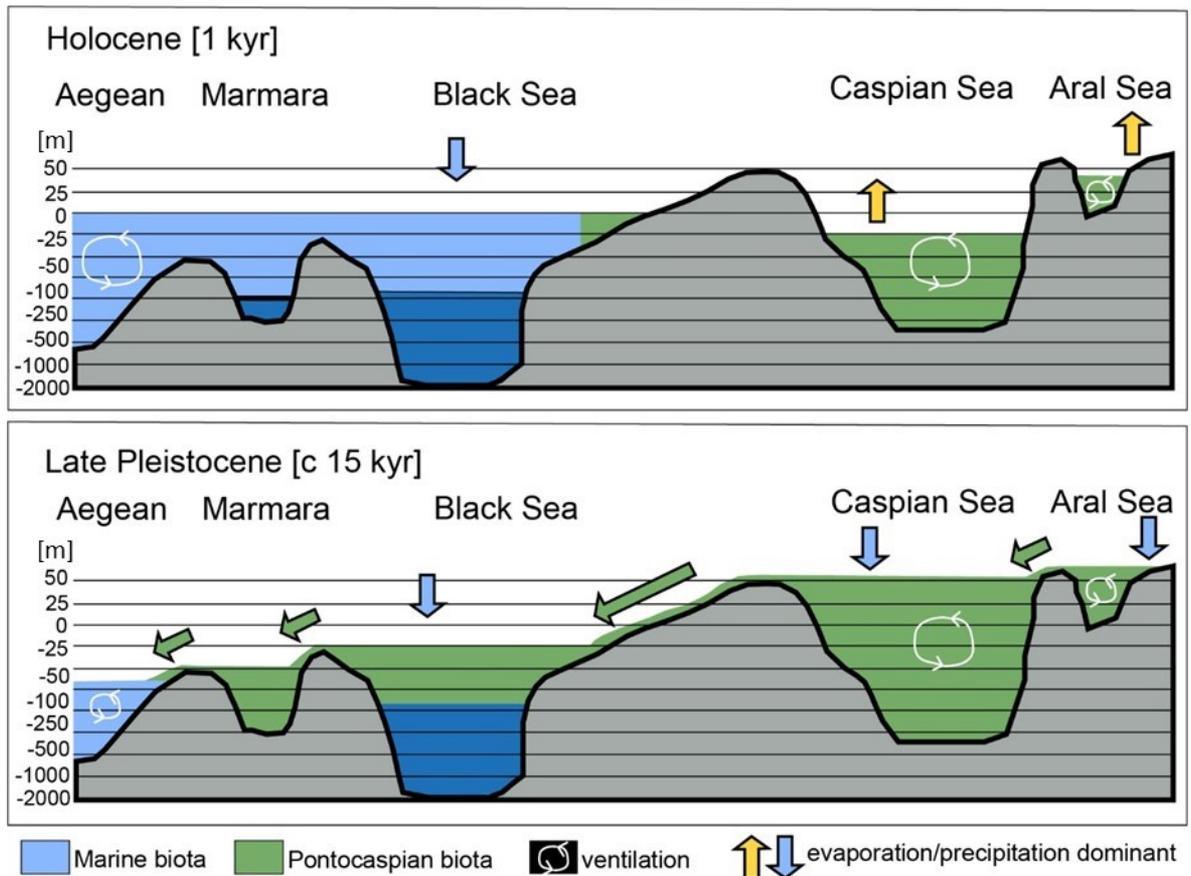
Figure 1.3. Evolution of sea level in the different basins of the Pontocaspian region illustrating the changing nature of connectivity between the basins (redrawn from PRIDE project proposal – https://www.pontocaspian.eu/).

1.2 The Caspian Sea

The Caspian Sea, which lies between the Caucasus Mountains and the Central Asian Steppe, is by far the largest inland waterbody and third deepest lake in the world with about 7000 km of coastline. The lake has three parts, based on the depth of water (Fig. 1.4). One third of the lake, the northern part, is shallow and has an average depth of ~6 m. The average depth of the middle part of the lake is ~200 m, while the southern part is very deep with maximum depth reaching 1025 m. Currently, the water level is at 28 m below mean sea level with surface area of ~371000 km^2 (excluding the Kara-Bogaz-Gol lagoon) and volume equal 78200 km^3 (Kosarev, 2005; Leroy et al., 2020).

The Caspian Sea is part of the largest internally drained basin in the world. Its drainage basin integrates the hydrological budget over a vast area of around 3x10^6 km^2, from high

northern latitudes to the Middle East covering nine countries (Fig. 1.1). The drainage basin encompasses different climatic zones. The northern part is located in a zone of temperate continental climate with humid mid-latitudes and some arid regions, while the western part is characterized by a moderately warm and dry climate (Leroy et al., 2020). A subtropical humid climatic zone dominates the southwestern and the southern part of the basin, whereas, the eastern part of the basin is desert (Leroy et al., 2020).

Currently, over a hundred rivers flow into the sea, with the Volga contributing >80% of the total inflow (Leroy et al., 2020; Rodionov, 1994). The only outflows from the Caspian Sea are the evaporation at the surface and artificially altered connection to the Kara-Bogez-Gol (KBG) lagoon, although it has formerly been connected to the global ocean (e.g. c 15 kyr ago, Fig. 1.3) via connection through the Black Sea and Sea of Azov at various times in prehistory (Krijgsman et al., 2019; Leroy et al., 2020; Yanina, 2014). As a closed basin, the Caspian Sea level is controlled by the inflows from the contributing rivers, and precipitation and evaporation over the sea, which make it very sensitive to changes in climate and human interventions.
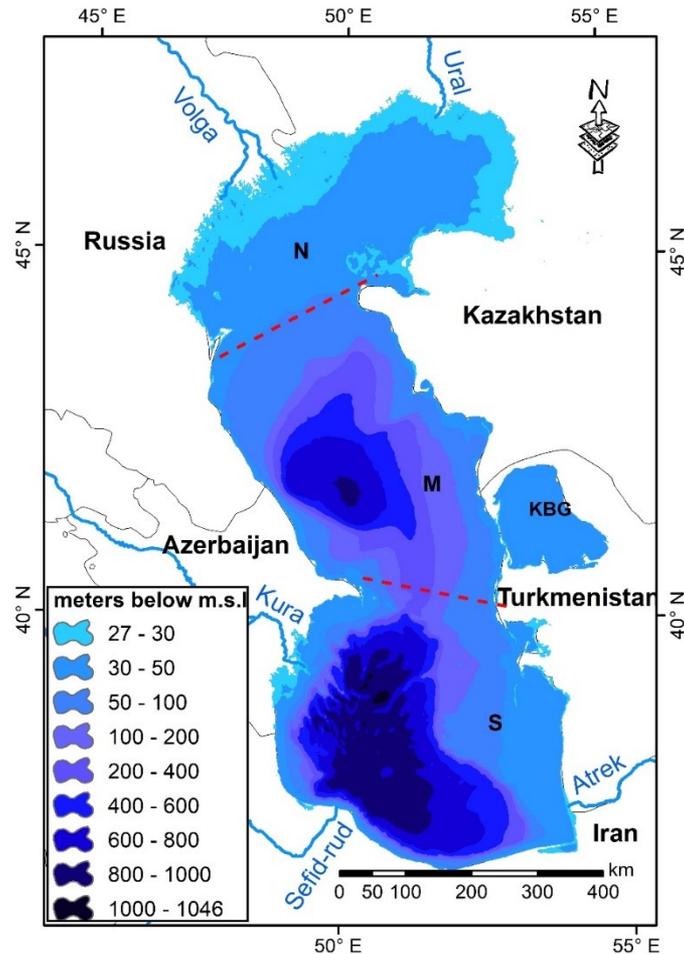
Figure 1.4. Bathymetry of the Caspian Sea based on the General Bathymetric Chart of the Oceans (GEBCO) gridded merged topographic and bathymetric data set (GEBCO, 2019). The sea has the shallow depth (~6 m average depth) in the northern part, and two deeper parts middle and southern basins. (N, M and S stands for North, Middle, South; KBG stands for Kara-Bogez-Gol lagoon).

1.2.1   The Caspian Sea hydroclimate during the Quaternary

The Quaternary is most noted for its periodic variation of climate between long cold, glacial phases and short, warm interglacial phases driven by changes in Earth's orbit around the sun, which have been termed Milankovitch Cycles. The ultimate cause of Milankovitch cycles is changes in the configuration of the Earth's orbit around the Sun, which create small variations in the seasonality of the amount of solar insolation (Berger and Loutre, 1991; Hays et al., 1976). Glacial periods are characterized by the growth of ice-sheets, favoured by the decrease in the summer isolation leading to more accumulation of snowfalls and dry climate,

whereas the interglacial periods are related to increased summer insolation and wetter climate (NOAA, n.d.; PAGES, 2016). Consequently, the global ocean has experienced substantial environmental and hydroclimatic changes during the Quaternary mainly due to changes in mass balance related to the growth and retreat of ice-sheets (e.g. Bamber et al., 2009; Ritz et al., 2015), and due to the geophysical changes affected by tectonics and isostatic rebound (e.g. Love et al., 2016).

The rate and magnitude of the sea level changes are not globally uniform, with considerable regional variation. The Caspian Sea has experienced large variations in sea level, and its water level variability through time does not follow the global ocean or other marginal seas because of its location in an internally drained basin. Its water level variations during the Quaternary reached an amplitude of around 150 m, with transgressive stages (sea level rises relative to the land) reaching up to 50 m above sea level during interglacial periods and regressive stages (sea level declines relative to the land) of ~113 m below mean sea level during glacial periods (Krijgsman et al., 2019; Leroy et al., 2020 and references therein).

The water level evolution of the Caspian Sea is very complex, resulting from different driving processes and settings. Previous studies have suggested that the water level variations of the Caspian Sea have depended on (1) geophysical processes including tectonics, deposition and erosion affecting the Manych-Kerch gateway (Belousov and Enman, 1999; Le Pichon et al., 2016; Svitoch, 2013; Svitoch and Makshaev, 2011) with the marine realm (e.g. to the Black Sea), and (2) hydro-climatological processes resulting in water balance changes within Caspian Sea catchment with significant contributions during periods of glacial and permafrost development and melt (Kroonenberg et al., 2008; Rodionov, 1994; Yanina et al., 2018; Yanina, 2012, 2014). However, there is no consensus among various studies on the chronologies, driving mechanisms, and sources of the runoff causing the corresponding transgressive and regressive stages. Therefore, different opinions exist on the importance of particular drivers of lake level change in the Caspian Basin during the late Quaternary (see § 2.2 for further details).

Furthermore, ice-sheet growth and retreat are also vital contributors to the re-organization and expansion/contraction of the drainage basin, which affects the total amount of runoff delivery (Wickert, 2016). Wickert (2016) has demonstrated that the North American

ice-sheet complex played a vital role in restructuring rivers and drainage basin systems of Northern America by altering the topography of the Earth's surface. The same processes would likely be important to the Caspian Sea basin due to the growth and retreat of the Fennoscandian ice-sheet, which would modify the geography of the drainage basin and alter runoff to the Caspian Sea. However, this has not been addressed in any of the previous studies of the Caspian Sea. In addition to climate change and drainage basin dynamics, the changes in the topography of the Manych-Kerch strait (Fig. 1.1) either due to ice-sheet loading/unloading or sedimentation, would have played a vital role in the connection of the Caspian Sea with the marine realm. The latest Caspian Sea level connection with the Black Sea occurred during the late deglaciation (~15 kyr ago), though there exist differences in the chronology (Krijgsman et al., 2019 and references therein). The level of the Manych-Kerch strait now is ~40 m above mean sea level, which is ~62 m above the current Caspian Sea level. This level has varied in the past due to topographic changes as a result of ice-sheet loading/unloading, and this has major implications for the bio-ecosystem of the Caspian Sea. Therefore, it is vital to evaluate the impacts of the ice-sheet on, and the mechanisms leading to, past sea level variations for understanding the sensitivity of the lake system to large climate changes, and the respective impacts on bio-ecosystem over longer time scales. This can help contextualize the recent changes and the associated biodiversity crises and support appropriate conservation measures for future biodiversity.

1.2.2   The Caspian Sea hydroclimate during the historical period

The Caspian Sea has undergone large interannual fluctuations in sea level during the 20th century. During this period, the water level varied between -26 m and -29 m (currently ~-28 m) based on observed data. This included two periods of rapid change when sea level decreased and increased by 2.5-3 m in less than ten years in the 1930s and 1970s respectively.

The majority of the fluctuations have been attributed to climate-driven changes of the basin's hydrologic regime, as illustrated by different authors (Arpe et al., 2000; Chen et al., 2017a; Golitsyn, 1995; Rodionov, 1994). Currently, water supply to the Caspian Sea is mostly controlled by runoff contributions from the Volga River, with some additional contributions from the other smaller rivers and the direct contribution of rain over the Caspian Sea. The river runoff is determined by regional climate systems and responds to global climate change.

The work of Elguindi and Giorgi (2006b) has shown that the shift and rapid rise of Caspian Sea level that occurred during the 1970s was due to changes in the climatology of the Caspian Sea basin, particularly due to an increase in precipitation over the northern basin and a decrease in evaporation. The climatic phenomena in the Caspian basin can be linked to the Northern Atlantic Oscillation (Nandini-Weiss et al., 2020; Pokhrel et al., 2012) and the El Nino Southern Oscillation (ENSO) (Arpe et al., 2000). Variations of these oscillations have the potential to affect temperatures, moisture, and winter storms across Europe including the Volga basin, as well as rainfall patterns over the Caspian basin (Arpe et al., 2000; Panin and Diansky, 2014). Apart from climate driven changes, increased water consumption for agricultural and human use, the construction of dams across rivers feeding the Caspian Sea (particularly over the Volga) since the 1940s, and the artificial connection of the Caspian Sea with the Kara-Bogez-Gol lagoon (in 1983 to decelerate the fall of Caspian Sea and in 1992 to minimise the increase in salinity of the lagoon) have contributed to further lowering of the Caspian Sea level (Akbari et al., 2020; Kosarev et al., 2009).

Large variations in water level of the Caspian Sea can result in enormous surface area change. In particular, the impact is larger over the northern part of the lake as this is the shallowest area of the lake with ~6 m average depth (Fig. 1.4), where small changes in water level would result in large variation of the lake area. This can significantly affect the energy and water budget by altering the albedo, evaporative fluxes, and near-(surface) temperatures. Previous modelling studies have shown that the change in lake surface area has potential impacts on the climate in the regional catchment and on the large-scale circulation patterns (Arpe et al., 2019; Nicholls and Toumi, 2014; Tsuang et al., 2001). Their experiments were either based on relatively low spatial resolution models or based on regional climate models constrained by the lateral boundary conditions. Therefore, the potential impacts on regional and large-scale hydroclimate are not well understood. On the other hand, most climate models poorly prescribe the actual Caspian Sea area, which can result in over/underestimation of water budget of the Caspian Sea basin. Despite the clear potential for these variations to impact regional and large-scale climate, this remains an overlooked element of current global climate model simulations that requires further exploration with a global, state-of-the-art model.

1.2.3   The future Caspian Sea hydroclimate

The Caspian Sea delivers a wide variety of vital ecosystem services to more than 14 million people (Leroy et al., 2020), and with its catchment encompassing 43 urban centres larger than 300,000 inhabitants (Hampton et al., 2018) from parts of Europe, Russia and Middle East. There are a number of reservoirs used for ecosystem services such as hydropower generation, fishery, irrigation, and drinking water (Akbari et al., 2020; Rodionov, 1994). Fishing and tourism play vital roles in the economies of the surrounding nations, in addition to oil and natural gas extraction from the Caspian Sea bed. However, close to 25000 km^2 (~7% of the Caspian Sea surface area) of the coastline area is potentially vulnerable to Caspian Sea level fluctuations in terms of desiccation, based on 20th century Caspian Sea level observations (Akbari et al., 2020). Desiccation would cause significant impacts on the economies, environment, and resources of the coastal countries in the future with projected changes due to climate and human interventions. Given the economic and geopolitical importance of the Caspian and the strong dependence of Caspian Sea level on climate, the potential for impacts from future anthropogenic climate change make it imperative to better understand the relationship between the two. Hence, it is vital to understand how Caspian Sea level will vary in future due to the impact of climate change and change in future water demand.

A few previous studies have addressed the impacts of future climate change on Caspian Sea level either constrained by single climate model (Arpe and Leroy, 2007; Renssen et al., 2007; Roshan et al., 2012) or Climate Model Intercomparison Project 3 (CMIP3) simulated projections from multiple models (Elguindi and Giorgi, 2006b, 2007), which are not the latest multi-model projections. Furthermore, the impacts of human water extractions were not considered in any of the previous studies. Therefore, this study has considered the latest climate projections from Coupled Model Intercomparison Project (CMIP5 and CMIP6), and the impact of human interventions.

1.3   Thesis aims and structure

The primary aim of this thesis is to improve our understanding of the drivers and feedbacks impacting the Caspian Sea hydroclimate and to investigate the influence of climate on Caspian Sea level and its connectivity to the Black Sea through the changing balance of evaporation,

precipitation, and drainage patterns from the late Quaternary to the end of the 21st century. This was achieved through a climate and hydrological modelling approach, combined with palaeodata synthesis in order to perform model-data comparisons, and by designing scenarios of future changes of water use for understanding the impacts on the ecosystem services of the Caspian Sea. The results are presented as stand-alone papers in three chapters in the format that they were submitted to their respective journals for publication. The remainder of the thesis is structured as outlined below.

Chapter 2 has been reviewed for Quaternary Science Reviews and is currently in the process of corrections. The main objective of this paper is the identification and assessment of the drivers of Caspian Sea level variations during the late Quaternary. Contributions from potential driving forces of glacial-interglacial climate change, topographic changes due to ice-sheet loading, and ice-sheet meltwater were considered. A synthesis of palaeo lake level data covering the last 25 kyr BP is performed and compared with lake level estimates based on climate simulations using Hadley Centre coupled atmosphere-ocean-vegetation climate model (HadCM3; Gordon et al., 2000; Pope et al., 2000) and palaeo ice-sheet reconstructions based on postglacial rebound model (ICE-6G_C; Argus et al., 2014; Peltier et al., 2015), which enabled the evaluation of the relative impacts of ice-sheet growth and retreat in-relation to the catchment dynamics and meltwater contributions, and the impacts of hydro-climatological changes over the Caspian Sea basin. The different components are integrated into a hydrological model to calculate Caspian Sea level and volume. Here, the following specific research questions are addressed:

- What are the drivers and the mechanisms involved in the changes in the hydroclimate and catchment dynamics of the Caspian Sea basin during the late Quaternary?
- What are the sources of runoff to the Caspian Sea during the late Quaternary and their relative contributions and cumulative impacts to the Caspian Sea level change?

Chapter 3 has been reviewed for the Journal of Geophysical Research: Atmospheres and corrections have been addressed. Currently, the manuscript is awaiting the reviewers' and editor's decision. In this chapter the impacts of the Caspian Sea area change on the

hydroclimate within its catchment and across the northern hemisphere are evaluated and investigated using a state-of-the-art climate model (Community Earth System Model: CESM1.2.2), in which different sizes of the Caspian Sea are specified in order to examine how the climate changes as its area increases. A hydrological model (Terrestrial Hydrological Model: THMB) is driven with the climate model outputs to assess the impact of the prescribed Caspian Sea representation in the model on the catchment water balance. This chapter aims to address the following questions:

- How much does the regional water budget change with increasing Caspian Sea surface area?

- How significant are the impacts of the Caspian Sea surface area change on the large-scale hydroclimate, and how far do the impacts reach?

Chapter 4 has been accepted for publication in Environmental Research Letters. The main objective of this paper is to assess the impacts of projected 21st climate change on Caspian Sea level variation and explore the implications for human water extraction in the coming century. Here, multi-model climate projections from the Coupled Model Intercomparison Project (CMIP5 and CMIP6) were used to drive the same lake level model as used in Chapter 2 in order to quantify the sensitivity of the Caspian Sea level to medium (4.5 Wm^{-2}) and extreme (8.5 Wm^{-2}) radiative forcing by the 21st century and assess the spread of model projections. The lake level model is then used to examine idealized future water extractions in the context of anthropogenic climate change to assess the potential for increasing water insecurity in the catchment. In this final results chapter, the following questions are addressed:

- How sensitive is the Caspian Sea level to projected climate change of medium and extreme emission scenarios?

- How much do climate change projections exacerbate issues of potential Caspian Sea desiccation due to human water extraction in the 21st Century?

Chapter 5 summarises the principal conclusions and identifies possible areas of future work.

2. CHAPTER TWO: What are the drivers of Caspian Sea level variation during the late Quaternary?

Sifan A. Koriche, Joy S. Singarayer, Hannah L. Cloke, Paul J. Valdes, Frank P. Wesselingh, Salomon B. Kroonenberg, Andrew D. Wickert, Tamara A.Yanina,

Key points

- The Fennoscandian ice-sheet significantly impacted Caspian Sea level at the last deglaciation
- Ice-sheet loading and damming increased the Caspian drainage basin area by 60-70%
- Southward redirection of north-flowing rivers increased runoff to the Caspian Basin
- Runoff increase (not including ice melt) led to overflow to Black Sea at the Last Glacial Maximum (~21 kyr)
- Ice melt extended the period of Caspian Sea connection to Black Sea to ~15kyr BP

Abstract

Quaternary Caspian Sea level variations depended on geophysical processes (affecting the opening and closing of gateways and basin size/shape) and hydro-climatological processes (affecting water balance). Disentangling the drivers of past Caspian Sea level variation, as well as the mechanisms by which they impacted the Caspian Sea level variation, is much debated. In this study we examine the relative impacts of hydroclimatic change, ice-sheet accumulation and melt, and isostatic adjustment on Caspian Sea level change. We performed model analysis of ice-sheet and hydroclimate impacts on Caspian Sea level and compared these with newly collated published palaeo-Caspain sea level data for the last glacial cycle. We used palaeoclimate model simulations from a global coupled ocean-atmosphere-vegetation climate model, HadCM3, and ice-sheet data from the ICE-6G_C glacial isostatic adjustment model. Our results show that ice-sheet meltwater during the last glacial cycle played a vital role in Caspian Sea level variations, which is in agreement with hypotheses based on palaeo-Caspian sea level information. The effect was directly linked to the reorganization and

expansion of the Caspian Sea palaeo-drainage system resulting from topographic change. The combined contributions from meltwater and runoff from the expanded basin area were primary factors in the Caspian Sea transgression during the deglaciation period between 20 and 15 kyr BP. Their impact on the evolution of Caspian Sea level lasted until around 13 kyr BP. Millennial scale events (Heinrich events and the Younger Dryas) negatively impacted the surface water budget of the Caspian Sea but their influence on Caspian Sea level variation was short-lived and was outweighed by the massive combined meltwater and runoff contribution over the expanded basin.

Keywords: Caspian Sea level, Fennoscandian ice sheet, meltwater, palaeo-drainage, climate change

2.1 Introduction

Understanding drivers and future trajectories of sea and lake level change is of paramount significance for mitigating future socio-economic disasters and for planning conservation measures. Long-term changes are partly related to geophysical processes altering the shape and size of sea/lake basins. Changes to the volume of water held within those basins also impact sea/lake level. Volume changes result from either density-driven variation (salinity and/or temperature changes), or from changes in mass (e.g., due to variation in water locked up in ice-sheets and glaciers). Human interference with water storage on land for agriculture, industry, and direct human consumption also has the potential to contribute to current sea level change (Pokhrel et al., 2012).

The Caspian Sea is an endorheic long-lived lake with sea-like features (saline, marine like faunas), whose magnitude of water level variations has been larger and of higher frequency compared to the marine realm (Kroonenberg et al., 2000; Kroonenberg et al., 1997) (Fig. 2.1). Large population are reliant on the water resource within the drainage basin for irrigation, industry, and domestic uses. Understanding the natural and anthropogenic controls on Caspian Sea level is therefore of critical importance. Using past variations in sea level can help understand drivers (processes and settings) that affect Caspian Sea level dynamics. However, scarcity/ambiguity of age and sea level data in the Pontocaspian region (Black Sea and Caspian

Sea basins) have made it difficult to identify consistent periods of sea level change in the palaeo-environmental record (Krijgsman et al., 2019).

During the Quaternary, the record suggests there were typically extended periods of isolation and short intervals of connection between lake basins in the Pontocaspian domain (Bezrodnykh et al., 2004; Rychagov, 1997b; Svitoch, 2013). In particular, the Caspian Sea experienced large variations in sea level from tens to hundreds of meters on various time scales (Bezrodnykh et al., 2004; Svitoch, 2010; Varuschenko et al., 1987; Yanina, 2014) (Fig. 2.1). Several prolonged highstand phases (e.g. Apsheronian, Bakunian, Khazarian, and Khvalynian) have been distinguished in the Quaternary (Forte and Cowgill, 2013; Krijgsman et al., 2019; Kroonenberg et al., 1997; Yanina, 2012).
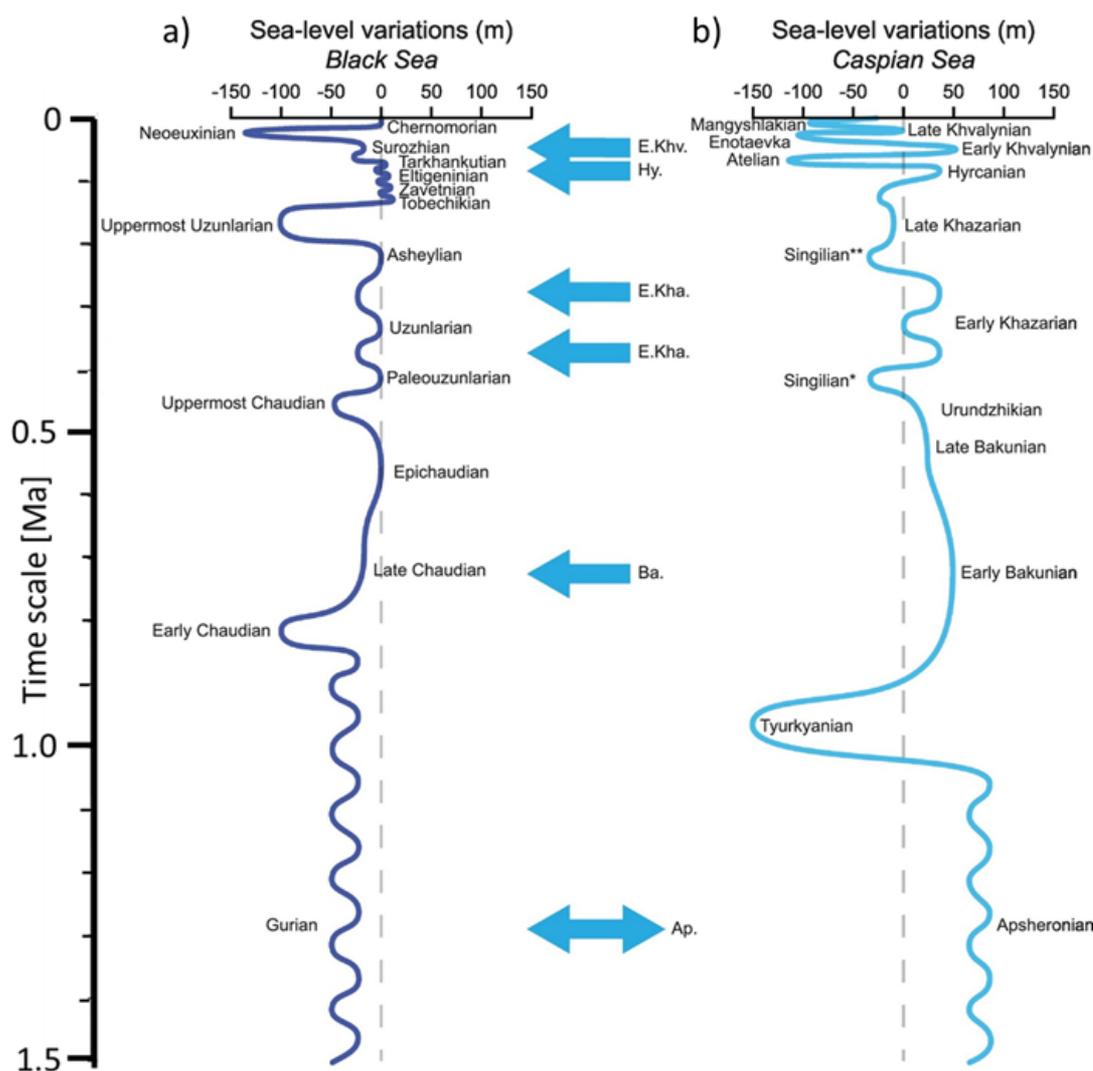
Figure 2.1. Adapted from Figure 6 of Krijgsman et al. (2019). a) Black Sea and b) Caspian Sea level reconstruction from Pleistocene to Holocene. Water flux between Caspian Sea and Black Sea are indicated by blue arrows facing to the left (or both ways for bi-directional flow). The sea level curves are reconstructed based on various palaeo-environmental records. The uncertainty may depend on the dating method employed and the bias in the quantification of the sea level variation. For example, a broad array of fauna and flora are used as sea-level indicators from coastal regions (e.g., corals, benthic foraminifers, ostracods, diatoms and mangroves) and from marine terraces (e.g., sedimentary and or stratigraphic features), which are dependent on the palaeo period considered and the regional environmental setup.

Caspian Sea level variation is unique in nature and its evolution is complex, due to the various driving processes and the environmental setting as part of a closed basin. Understanding the relative contributions of the different drivers of Caspian Sea level change requires a multi-disciplinary approach (e.g., hydroclimate modelling as well as geological and geomorphological analysis). A considerable number of studies have explored various aspects of Caspian Sea changes (e.g., Arpe et al., 2014; Arslanov et al., 2016; Kislov and Toropov, 2007; Kislov et al., 2014; Rychagov, 1997b; Tudryn et al., 2013; Yanina, 2014). However, there are conflicting ideas concerning the relative importance of different factors driving past Caspian Sea level variability (discussed in §2.2), as well as the mechanisms by which they impacted basin connectivity and Caspian Sea level variation. Below, we outline plausible sources of runoff and flow directions (see Fig. 2.2; sources are indicated by the numbers in a square brackets) that potentially played a role in controlling Caspian Sea level variation during the Quaternary (especially during glacial/deglacial periods):

- meltwater from the Eurasian (Fennoscandian) Ice-sheet (Fig. 2.2, [1]);
- river basin and drainage reorganization due to ice-sheet damming and accumulation;
- expansion of river basin area due to topographic change produced as a result of ice-sheet loading/unloading;
- formation of closed depressions and proglacial lakes outburst (Fig. 2.2, [2] and [4]);
- glacial melting (Fig. 2.2, [3]) and hydroclimate change in the neighbouring Himalayan and Amu-Darya basins, that were likely hydrologically connected to the Caspian basin at various times;

- sedimentation and structural change of spillways due to isostatic rebound (e.g. Manych-Kerch) (Fig. 2.2 [5] and [6]);

Any of the above changes would have been in addition to the hydroclimate variation (precipitation-evaporation balance) controlled by glacial-interglacial cycles and millennial scale forcing.

We anticipate that Caspian Sea level variations originate from the sources of runoff and changes in drainage extent outlined in the list above. To disentangle these factors and understand their relative importance, we firstly performed a synthesis of palaeo lake level data covering the last 25 kyr (see §2.4.1). Secondly, we examined the impacts of hydro-climatological changes using palaeoclimate model simulations (see §2.4.2). Thirdly, we evaluated the impact of the Fennoscandian ice-sheet on catchment dynamics and meltwater contributions (see §2.4.3). Finally, we constructed a model of Caspian Sea level in order to quantify the cumulative impact of the different drivers (see §2.4.4).
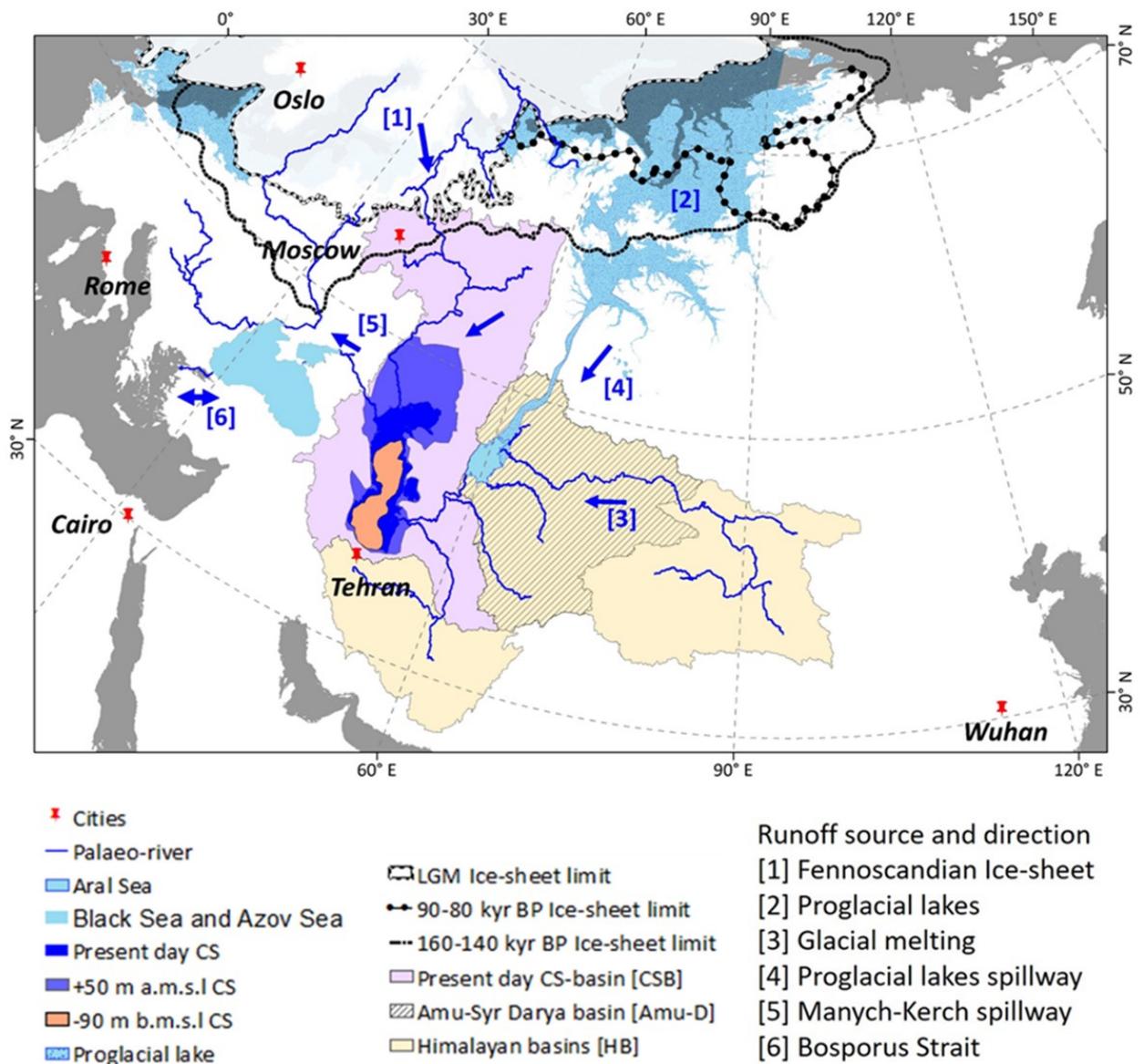
Figure 2.2. Study area map showing key palaeo and present-day features, including runoff sources and drainage directions, ice-sheet limits, Caspian Sea basin limits, and neighbouring drainage basins. Plausible runoff sources and directions to Black and Caspian Seas (indicated by blue arrows and numbers from 1-6); Limits of Last Glacial Maximum after Hughes et al. (2016) (shown by black and white line), Late Saalian [160-140 kyr BP, thick black line], and Early Weichselian glacial maximum [90–80 kyr BP; line with black circles] after Svendsen et al. (2004); Present day Caspian Sea [CSB; dark blue area], Amu-Syr Darya [AmuD; yellow hashed area] and Himalaya-Internal drainage [HB; yellow areas] basin outlines; Palaeo and present day river network [blue solid line] and Caspian Sea extents. The pro-glacial lakes locations are hypothesised after various sources (e.g., Mangerud et al., 2001; Mangerud et al., 2004;

Yanchilina et al., 2019). Grey shaded areas are present day global oceans. (Key: CSB – Caspian Sea Basin)

2.2 Previous studies

As previously indicated, Caspian Sea level has varied during the Quaternary due to both geophysical processes (that have opened and closed gateways) and hydroclimate change induced by glacial-interglacial cycles (Badertscher et al., 2011; Kroonenberg et al., 2005; Richards et al., 2017; Rodionov, 1994; Yanina et al., 2018; Yanina, 2014). The gateway that control the connection between the Ponto-Caspian seas is the Manych-Kerch (Fig. 2.2). This gateway is affected by tectonics (Le Pichon et al., 2016; Svitoch and Makshaev, 2011), deposition, and erosion (e.g., Svitoch and Makshaev, 2011); these mechanisms modify topography and therefore may lead to changes in drainage basin size or shape, or to changes in lake bathymetry. The architecture of the gateways impacts the base-level of upstream basins directly. The present rates of the tectonic movements are small (<1 mm per year) over most parts of the Manych-Kerch straits/depressions (Svitoch, 2013). However, in earlier time periods (e.g. the early Pliocene), geophysical processes (sedimentation and subsidence) played a vital role in Caspian Sea level variation (Kroonenberg et al., 2005; Nadirov et al., 1997; Richards et al., 2017; Vincent et al., 2010).

Many studies suggest that hydroclimatic processes play a significant role in controlling Caspian Sea level variation (e.g., Badertscher et al., 2011; Dolukhanov et al., 2010; Jorissen et al., 2020; Kislov and Toropov, 2007; Kislov et al., 2014; Yanina, 2012; Yanko-Hombach and Kislov, 2018). The regional water budget is mainly influenced by freshwater balance, the relationship between evaporation and lake area, melting of glaciers and/or ice-sheets, and permafrost melting (Kondratjeva et al., 1993; Kroonenberg, 2012; Rodionov, 1994; Yanina, 2012).

Present-day Caspian Sea level variation is mostly controlled by contributions from more than a hundred rivers that discharge into the Caspian, although close to 80% of the discharge originates from the Volga (Arpe et al., 2012; Rodionov, 1994). The discharge from these rivers is affected by hydroclimate processes at global and regional scales. Increased river discharge

has been reported for interglacial periods, as well as during melting of ice sheets in periods of deglaciation (Krijgsman et al., 2019 and references therein). Other additional sources of runoff during the Quaternary include previously hydrologically connected neighbouring river basins (e.g., Amu-Syr-Darya basin; Fig. 2.2) that are not connected in the present day (Kroonenberg et al., 2005; Leroy et al., 2013; Torres et al., 2007). For example, runoff to the Caspian Sea via the Uzboy River from the Aral Sea and Amu-Darya occurred briefly at around 5.8 to 5.2 and 4.5 to 3.8 ^{14}C kyr BP (Leroy et al., 2013 and references therein).

While it seems that palaeoclimate change dominated variations in Caspian Sea level during the Quaternary, there is disagreement about the relative importance of different mechanisms. For example, water sources driving early Khvalynian: ~35–25 ka BP and late Khvalynian: ~17–12 ka BP highstands are debated (Komatsu et al., 2016; Svitoch, 2009; Tudryn et al., 2016; Yanchilina et al., 2019; Yanko-Hombach and Kislov, 2018). The water source for the Khvalynian transgression has variously been associated with melting of ice sheets along the Russian Plain joining the Caspian basin via the Volga catchment (Fig. 2.2 [1]), and/or via pro-glacial lakes towards the south of the Siberian ice-sheets (Fig. 2.2 [4]), and/or runoff from Amu-Syr Darya basin (Fig. 2.2 [3]) (Svitoch, 2009; Tudryn et al., 2016; Yanko-Hombach and Kislov, 2018).

According to Mangerud et al. (2004), the Caspian Sea received significant discharge from ice-dammed proglacial lake outbursts from the south of the Siberian (Barents–Kara) ice-sheet via the Aral Sea during 90 – 80 kyr BP and around 18 – 17 kyr BP. Svitoch (2009) alternatively suggested that the Khvalynian transgression was never as a result of ice-dammed proglacial lake outbursts, but fed by discharge from Amu-Syr Darya drainage basin through Lake Sarykamysh (located approximately midway between the Caspian Sea and the Aral Sea). He also points that, this runoff source was not significant and had contributed very low to the Khvalynian transgression. This is also supported by review by Panin et al. (2020) on the routes of runoff to Caspian Sea. They also suggest that the amount of runoff that joined Caspian Sea via Lake Sarykamysh (Uzboi valley) would have only raised Caspian to -22 m above sea level, which corresponds to the maximum Holocene sea level, but cannot explain the Pleistocene sea level changes indicating that this route can be ruled out as the source of runoff for the Khvalynian transgressions.

Tudryn et al. (2016) indicated that the Caspian Sea acted as a final trap for south-eastern Scandinavian ice-sheet meltwaters during the last deglaciation. The meltwater discharge joined the Caspian Sea via the Volga River from the LGM until ~13.8 cal kyr BP, as suggested by Tudryn et al. (2016) and Soulet et al. (2013). Most of the late Pleistocene and Holocene water level fluctuations of Caspian Sea are thought to be due to hydroclimate change (Krijgsman et al., 2019; Yanchilina et al., 2019; Yanina et al., 2018). This is also supported by various palaeoclimate model studies (Kislov and Toropov, 2007; Renssen et al., 2007). Runoff from the catchment was found to be the primary driver of Caspian Sea level variation during the mid-Holocene and LGM, based on Palaeoclimate Model Intercomparison Project 3 (PMIP3) models (Kislov and Toropov, 2007).

In summary, although a considerable number of studies have focussed on exploring the main source of Caspian Sea level variation, it is likely that there have been a number of contributing mechanisms. In this study, we build on previous work to consider the cumulative impacts of the various potential drivers of Caspian Sea level variation and changes in their relative contributions through the last deglaciation.

2.3 Materials and methods

2.3.1 Study area

The Caspian Sea formed as an isolated closed basin in the early Pliocene (Popov et al., 2006; van Baak et al., 2016). It is the largest inland water body in the world and has a present-day catchment area of approximately 3.6 Mkm^2 (see Fig. 2.2 key palaeo and present-day features). The vast catchment covers a number of climatic zones, from a temperate continental climatic zone over the Volga basin, to moderately warm climate over the western area, subtropical humid climate over the southwestern and the southern regions, and semi-arid climate over the eastern part (Chen and Chen, 2013; Kosarev, 2005; Leroy et al., 2020; Leroy et al., 2007). Currently, Caspian Sea level is ~28 m below mean sea level. The Caspian system is very sensitive to changes in evaporation over the sea (Arpe et al., 2012; Chen et al., 2017a; Rodionov, 1994). Due to the shape of the lake bathymetry, as Caspian Sea level changes (between -100 m and +50 m above mean sea level), its surface area changes

significantly and non-linearly (Fig. 2.3). This has important implications for determining the amount of evaporation from the sea (a larger surface area often corresponds to strongly increased evaporation), as well as climate feedbacks with the atmosphere. Climate impacts occur in both the local-scale atmospheric water-balance and large-scale atmospheric circulation patterns (Koriche, Nandini-Weiss et al., 2020b). The relationship between Caspian Sea volume, surface area, and water level is used within the hydrological model developed and outlined in the next section.
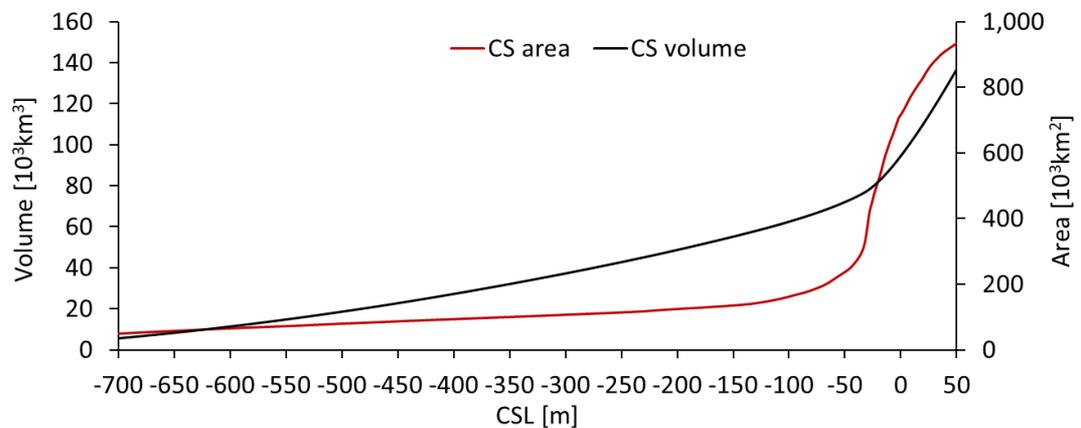
Figure 2.3. Relationship between Caspian Sea level, surface area, and water volume. Both curves are produced using the General Bathymetric Chart of the Oceans (GEBCO) gridded merged topographic and bathymetric data set (GEBCO, 2019), and the Surface Area-Volume (3D Analyst) tool of ArcScene geo-spatial package in ArcGIS-Desktop software (@esri.com).

2.3.2   Research methods

In this section we present the datasets used, hydrological modelling scheme implemented, and methods used for data analysis. The first part of the study focuses on a synthesis of Caspian Sea level data from the literature. The second part involves analysis of hydroclimate evolution over the Caspian Sea basin based on climate model simulations of the last glacial cycle (120 – 0 kyr BP). The third section looks at the impact of the Fennoscandian ice-sheet on the re-organization of the Caspian Sea drainage system and its contribution of meltwater to the basin over the last 25 kyr. The fourth part describes a hydrological model that we constructed to explore the cumulative impact of hydroclimate change, meltwater input, and river drainage system rearrangement on Caspian Sea level. The potential contribution due to

ice-sheet meltwater via Aral Sea and the east of the Caspian Sea were not examined in this study as the topographic information is only based on coarse (1^0) resolution, which limits the routing of runoff (the right amount of meltwater) over the palaeo period.

2.3.2.1 Reconstruction of palaeo-Caspian Sea level

We reconstructed Caspian Sea level over the last glacial cycle based on the limited available palaeo-environmental records from published studies. Table 2.1 contains details of the data sources and methods used to infer past Caspian Sea level as well as stratigraphic time data. We used the original chronologies associated with each dataset. Data points with age uncertainties of +/- 5 kyr or larger were excluded, though these data sources are included in the Supplementary information, Table S6.1, for completeness. Consequently, only Caspian Sea level reconstruction points covering the last 25 kyr were suitable for inclusion in the final compiled dataset, presented in §2.4.1.

2.3.2.2 Palaeoclimate modelling

Climate model data was extracted from snapshot simulations covering the last 120 kyr BP (Davies-Barnard et al., 2017; Singarayer and Valdes, 2010; Singarayer et al., 2017) performed using the Hadley Centre coupled atmosphere-ocean-vegetation climate model, HadCM3 (Gordon et al., 2000; Pope et al., 2000). The simulations included the MOSES2.1 (Met Office Surface Exchange Scheme) land surface scheme and the TRIFFID (Top-down Representation of Interactive Foliage and Flora Including Dynamics) dynamic vegetation model (Cox et al., 1999). The model experiment produced 65 climate snapshots over the last 120 kyr BP, as producing a global time series using a fully coupled complex climate model transient simulation is far too computationally expensive. Each was forced with boundary conditions pertinent to the time period being simulated, including insolation seasonality, atmospheric greenhouse gas concentrations based on ice-core data, and ice sheets. From $120 - 80$ kyr BP, simulations were performed at intervals of 4 kyr; between $80 - 22$ kyr BP simulations were performed at 2 kyr intervals; and then simulations were created for every 1000 years from $22 - 0$ kyr BP (Singarayer and Valdes, 2010; Singarayer et al., 2017). The key assumption in snapshot experiments is that the climate is in equilibrium with the boundary conditions, and that the final climate is largely independent of the initial conditions. Both of these

assumptions can be challenged during the late Pleistocene period (last deglaciation period) as the time is characterised by rapid climate change like the Heinrich event and Younger Dryas where the changes were happening in a few years(Steffensen et al., 2008). However, the use of freshwater hosing simulations for these particular periods (where equilibrium is not reached before taking the mean climatologies) somewhat corrects for this.

In addition, we incorporated millennial-scale forcing of freshwater into the North Atlantic to simulate iceberg influx during Heinrich event 2, Heinrich event 1, and the Younger Dryas. During such millennial-scale Heinrich events, palaeodata indicate that the Atlantic Meridional Overturning Circulation (AMOC) collapsed (Seidov and Maslin, 1999), resulting in cooler temperatures and drier conditions over Europe and much of the northern hemisphere (e.g., Sánchez-Goñi et al., 2000) over an extended period of time (>1000 years). Such events therefore had the potential to influence the surface water balance over the Caspian basin due to changes in precipitation and evaporation, and as a result, impact Caspian Sea level. In HadCM3 the influx of iceberg discharge is simulated as a negative salinity flux equivalent to the addition of 0.3 Sv over the surface of the North Atlantic (between 50-70°N). The result of this is a reduction in AMOC overturning strength. A limitation of this technique is that it assumes that all millennial scale variability is driven by changes in the AMOC. The decrease in AMOC strength varies depending on the background climate state. For the Younger Dryas simulation, the AMOC experiences a reduction from 18 Sv to 5 Sv on average.

The glacial cycle HadCM3 simulations have been evaluated by model-data comparisons in a number of studies covering various climate fields and geographical regions (e.g., Hoogakker et al., 2016; Singarayer and Burrough, 2015; Singarayer and Valdes, 2010; Singarayer et al., 2017). The modelled global average glacial-interglacial temperature change in this version of HadCM3 is 5.5 °C, which is in the middle of the range inferred from palaeodata (Masson-Delmotte et al., 2013). Polar temperature trends compare well to ice core records, although the magnitude of change is underestimated (Singarayer and Valdes, 2010), as it is in most climate models. Temporal variations in large-scale circulation such as the position of the intertropical convergence zone and monsoon intensity at locations from East Africa to China are well simulated by HadCM3 (Singarayer and Burrough, 2015; Singarayer et al., 2017). The glacial-interglacial changes in climate have been used to drive biome simulations that match

well with biome reconstructions from pollen over Europe and Asia (Hoogakker et al., 2016). Comparison with modern observations is described in Valdes et al. (2017). HadCM3 compares well with newer state-of-the-art models and is many times faster to run, therefore making it useful for simulating palaeoclimate scenarios over multiple time periods.

Note that HadCM3 does not include interactive ice sheets or carbon cycle. Thus, the ice-sheet evolution and greenhouse gases have to be prescribed (Singarayer and Valdes, 2010). In these simulations (with HadCM3), the ice sheet is based on ICE-5G (Peltier, 2004). Prescribing ice-sheet evolution helps to appropriately represent ice-sheet extent and palaeo-topography. However, representing the actual ice-sheet meltwater and its contribution to the basin water budget is vital and is not included in the HadCM3 climate simulations. Therefore, we separately estimated the meltwater contribution to Caspian Sea level using ice-sheet reconstructions from ICE-6G_C (Argus et al., 2014; Peltier et al., 2015).

We carried out a model-data comparison of the surface water balance in the present day to assess whether it was appropriate to incorporate a bias correction into our analysis. Prior to bias correction, the model *P-E* (precipitation minus evaporation) outputs were downscaled from the standard HadCM3 resolution ($3.75° \times 2.5°$) to 6 arcminutes by a first-order conservative interpolation method (remapcon) using the Climate-Data-Operator (CDO) software. The conservative interpolation method works well for flux conservation and interpolation to higher resolution (Jones, 1999). Three different sources of data were then used to estimate observational surface water balance over the Caspian basin. These include: (1) the 20th century observed mean Caspian Sea level change record (where average year-to-year variations in Caspian Sea level give the annual water balance) combined with average human water use from during the 20th century based on the work of Rodionov (1994) and Shiklomanov (1981); (2) the ECMWF 20th century reanalysis (ERA-20C; Poli et al., 2016); and (3) the 5th generation ECMWF reanalysis data (ERA5; Copernicus Climate Change Service (C3S), 2017; Hersbach et al., 2020). By using these three observational datasets for bias correction we were able to quantify a measure of uncertainty in the observed annual water budget for the Caspian basin. Results are described in §2.4.2.

Since there are no direct observational datasets to use for bias correction of the palaeo-time slices, we computed the mean annual water balance (*P-E*) anomaly by subtracting the pre-industrial *P-E* from the *P-E* at each palaeo-time slice. The assumption is that, the difference between the present-day mean P-E (~2950 m^3s^{-1}) and pre-industrial HadCM3 P-E (~3300 m^3s^{-1}) is small. Therefore, the observed present-day water balance was added to each of the palaeo P-E anomalies. As indicated above, due to shortage of observed palaeo datasets, this approach assumes that the bias is constant throughout all palaeo-time slices, however, this is not necessarily the case in the reality, as the climate over this period varied due to differences in the forcing and boundary conditions. We compare results with and without bias correction. The results are discussed further in §2.4.4.

Table 2.1. Data sources used to reconstruct palaeo Caspian Sea level in Fig. 2.5 (* the sources are more than one).

	Proxy (data type used to infer palaeo Caspian sea level)	Method used	Dating technique (s)	Reconstruction period (kyr BP)	Reference
[a]	Species of molluscs (*Didacna*) and fragment of bone (*Equus sp.*)	Geochronological study (age of deposits, its stages and phases)	^{14}C and ^{230}Th/^{234}U	Late-Pleistocene: ~31 to ~11	Arslanov et al. (2016)
[b]	Shells (e.g. *Cerastoderma glaucum s.l.*)	Sediment cores, Historical documents and geological records	^{14}C	Last Millennium	Naderi Beni et al. (2013)
[c]	Shell and organic matter	lithological descriptions (Sedimentary log of outcrops, image processing, old maps interpretation and field observations)	^{14}C	Holocene	Kakroodi et al. (2012)
[d]	Mollusc shells (e.g. *Cardidae*) and organic matter	outcrop, coring and ground-penetrating radar (GPR) profiling	^{14}C and ^{210}Pb	Late-Holocene: ~2.5 to 0.5	Lahijani et al. (2009)
[e], [f]	Mollusc shells	geophysical survey, Shallow Seismic, sedimentology, biostratigraphy	^{14}C	Holocene	Kroonenberg et al. (2008)
[g]	Multiple sources*			Early Holocene: 12 to 7.5 (Mangyshlak regression)	Bezrodnykh et al. (2020); Bezrodnykh et al. (2004); Bezrodnykh and Sorokin (2016); Kroonenberg et al. (2005); Kroonenberg et al. (2008); Sorokin (2011); Tudryn et al. (2013)
[h]	Multi-proxy (foraminifera, Diatoms, organic matter)	coring, sedimentological analysis and bio-facies	^{14}C	LGM and mid-Holocene	Kakroodi et al. (2015)

	Proxy (data type used to infer palaeo Caspian sea level)	Method used	Dating technique (s)	Reconstruction period (kyr BP)	Reference
[i]	Marine shells	analysis of the geology and geomorphology terraces; levelling of terraces and related shore-lines,	^{14}C	Holocene	Rychagov (1997b)
[j]	?	?	?	During LGM: 18	Harrison et al. (1991) based on the work of Kvasov, (1975)
[k]	Multiple sources*			During LGM: 24 to 17 (Enotaevkan regression)	Krijgsman et al. (2019); Mamedov (1997); Sorokin (2011); Tudryn et al. (2013)
[l]	stalagmite	Stable isotope measurements (oxygen)	^{230}Th/^{234}U	Mid-Pleistocene to present: ~700 to 0	Badertscher et al. (2011)

2.3.2.3 Palaeo drainage basin characterization

Ice sheets play an important role in reshaping the river drainage system. They also contribute vast quantities of meltwater during deglaciation periods, resulting in abrupt sea level and climate change. We evaluated the impact of the Fennoscandian ice-sheet on the dynamics of Caspian Sea drainage area evolution and its meltwater contribution. The drainage basin and the associated palaeo-rivers were reconstructed by combining a high resolution (0.5 arcminutes) digital elevation model (DEM) from the General Bathymetric Chart of the Oceans (GEBCO) gridded merged topographic and bathymetric data set (GEBCO, 2019) and palaeo ice-sheet reconstruction based on postglacial rebound model ICE-6G_C (Argus et al., 2014; Peltier et al., 2015). ICE-6G_C is a global ice-sheet and glacial isostatic adjustment (GIA) reconstruction created by combining geological data and geophysical model (Argus et al., 2014; Peltier et al., 2015). It has shown better performance compared to its predecessors (ICE-3G, ICE-5G) and closer to glacial geological data over the Laurentide icesheet (Wickert, 2016). Over the Fennoscandian, the ICE-6G_C total volume is 15% lesser than ICE-5G during 21 kyr BP and early deglaciation period (Fig. 2.4a). As shown in Fig. 2.4b, the magnitude of meltwater contribution differ during the LGM and early deglaciation period.
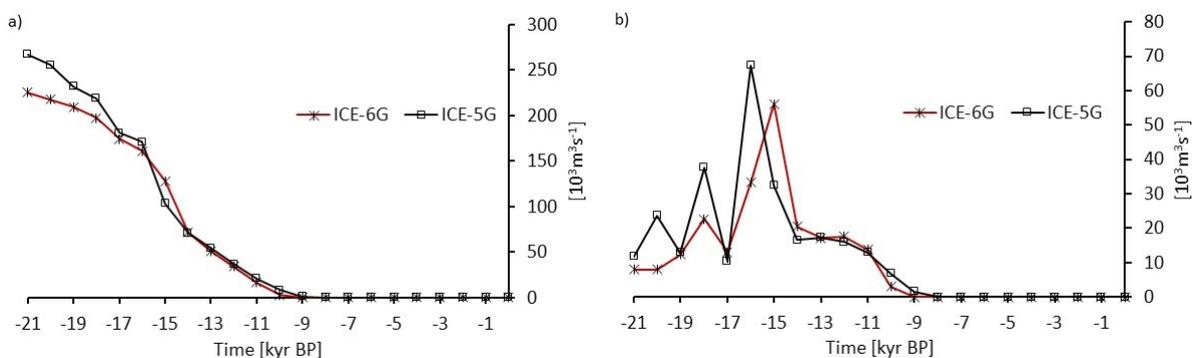
Figure 2.4. Fennoscandian ice-sheet a) volume, and b) meltwater contribution based on ICE-6G_C and ICE-5G.

Two sets of palaeo-topography were created based on 1) including ice-sheet thickness without GIA, and 2) including the topographic anomalies from present day where both ICE-6G_C ice-sheet thickness and GIA were considered. Since the reconstructed ice-sheet geometry was only available at a relatively coarse resolution (1º x 1º), combination with high-

resolution elevation data was necessary as some topographical features cannot otherwise be sufficiently well represented, such as the valleys of major river systems. High-resolution elevation data is only available from present-day observations. In order to combine both data sets, the coarse resolution ice-sheet palaeo time slices were interpolated using an iterative (7 steps) bi-linear method to help remove stepwise discontinuities that may introduce unrealistic flow direction during drainage basin creation (Wickert, 2016). High-resolution anomalies of palaeo-time slices minus pre-industrial time slices were then added on to the high-resolution modern topographic data to create the 0.5 arc-minute resolution palaeo-topographic maps.

The characterization of the drainage of the Caspian Sea basin was performed by employing Geographic Resources Analysis Support System (GRASS) software (Metz et al., 2011; Neteler et al., 2012) and using the high resolution palaeo-topographies as key inputs. GRASS is an open-source geospatial analysis software recommended for characterizing hydrologically linked drainage basins. From this analysis, drainage basin area and the associated river networks covering the period from 25 kyr to present were created. The derived drainage extent was used to perform analysis of palaeo-water budget and ice-sheet meltwater contributions.

2.3.2.4   Caspian Sea level modelling

Caspian Sea volume and level were simulated by integrating all the plausible sources of runoff due to palaeoclimate change, drainage river system rearrangement, and ice-sheet meltwater contributions to the water budget. Here, the Caspian Sea model (Eq. 2.1 and 2.2) is based on fluxes of precipitation minus evaporation (P-E) over the Caspian Sea drainage basin and meltwater from the ice sheet within the drainage basin. However, abrupt climate change and/or high discharges of meltwater can increase Caspian Sea level enough that water starts to spill over to the hydrologically linked neighbouring basin (the Black Sea) via the Manych-Kerch spillway. Equally, there is a lower volume limit set of 0 m³, which may be reached over time given sufficiently negative fluxes. These limits are expressed in Equation 2.2.

$$\Delta CSV^t = [(P_{land}^t - E_{land}^t)A_{land}^{t-1} + (P_{sea}^t - E_{sea}^t)A_{sea}^{t-1} + M^t + B]\Delta t \qquad [2.1]$$

$$CSV^t = max\big(0, min([CSV^{t-1} + \Delta CSV^t], CS\_max)\big) \hspace{3cm} [2.2]$$

where: *CSV* is Caspian sea volume, *P* is precipitation, *E* is evaporation (from canopy, soil and water body), *A* is surface area over the land or sea part of the basin, *M* is the ice-sheet meltwater flux, *B* is a bias correction based on modern day observations, *Δt* is the time step, and *CS_max* is the maximum volume in the Caspian Sea before overspill occurs. Once *CSV* is calculated, the Caspian Sea level at each time step is calculated by interpolation of the volume-sea level curve in Fig. 2.3.

As mentioned previously, the area of the Caspian Sea varies considerably with changing Caspian Sea level (Fig. 2.3). Any changes in sea surface area would significantly impact the total evaporation per time step. Accordingly, we use a variable area (calculated from the volume at the current time step) and multiply the water balance (*P-E*) over the sea by the sea area (at the previous time step; Eq. 2.1), and similar for the land area water balance. In order to avoid numerical instabilities, we used a time step (*Δt*) of 20 years. As the simulated climate and ice-sheet states are averages at 1000-year intervals, the precipitation, evaporation, and ice-sheet meltwater fluxes were linearly interpolated to 20-year intervals.

Previous studies have shown that the contribution of groundwater to the Caspian Sea in the late Quaternary is estimated to be small (Golovanova, 2015; Zekster, 1995). Therefore, we assume that there is no significant groundwater reservoir on these timescales and have not included a groundwater component in the water balance analysis.

2.4 Results

2.4.1 Synthesis of palaeo lake lave data

As previously outlined, present day Caspian Sea level is at an elevation of ~28 m below mean sea level and the water balance is controlled mainly by inflow from major rivers, such as the Volga, Kura, and Ural, balanced by evaporation over the sea (Arpe et al., 2014; Chen et al., 2017a; Rodionov, 1994). Over the last thousand years the Caspian Sea level varied between 19 and 28 m below mean sea level, based on Caspian Sea level reconstruction from combined historical documents and geological records by Naderi Beni et al. (2013) (Table 2.1).

CHAPTER TWO: What are the drivers of Caspian Sea level variation during the late Quaternary?

The rate of Caspian Sea level change earlier in the Holocene was much higher compared to present-day Caspian Sea level change (variation of around 3 m in the 20th Century). The deepest lowstand recorded (referred to as the Mangyshlak regression) for the Caspian Sea during our time frame of interest was during the early Holocene (Fig. 2.5). This lowstand was approximately 80-113 m below mean sea level (Kroonenberg et al., 2008 and references therein). The timing of the Mangyshlak lowstand varies between studies from 12 kyr BP to 8 kyr BP (e.g., Bezrodnykh and Sorokin, 2016; Kroonenberg, 2012; Yanina, 2014) (Fig. 2.5). For instance, Bezrodnykh and Sorokin (2016) indicated that the start of the Mangyshlak regression was at around 12.4 kyr with a level of around -40 m which then dropped rapidly by 40-44 m over 700-1000 years, and they indicate an end of the regression around 9.5 kyr BP (see Table S6.1 for other sources). However, Rychagov (1997a) suggests that maximum lowstand was around 12 kyr BP. The second lowest Caspian Sea level recorded in the Holocene was during the warm medieval period (at -42 m a.s.l), around 1.4 kyr BP (Kakroodi et al., 2012). Numerous highstands of up to 25 m below mean sea level were also recorded semi-regularly throughout the Holocene (Kakroodi et al., 2012; Rychagov, 1997b).

A series of palaeo-geographic events took place during late Pleistocene, including the Late Khazarian, early Khvalynian and late Khvalynian transgressive stages, and the Atelian, Enotaevka and Mangyshlak regression stages (see Fig. 2.1 and Table S6.1 for suggested age and the corresponding Caspian Sea level). During these periods, the Caspian Sea experienced extreme water level change, ranging from +50 m to ~-130 m above mean sea level. Various studies explored timing and magnitude of Caspian Sea level events from depositional records (e.g., Bezrodnykh et al., 2015; Bezrodnykh et al., 2004; Mamedov, 1997; Shkatova, 2010; Sorokin, 2011; Tudryn et al., 2013; Yanina et al., 2018; Yanina, 2014) but no consensus exists over the Caspian Sea level curves. The ages of the Atelian regression and the early Khvalynian transgression are still controversial (Krijgsman et al., 2019; Yanina et al., 2018). Many authors (e.g., Dolukhanov et al., 2010; Kroonenberg et al., 1997; Tudryn et al., 2013; Yanina, 2014) reported the existence of a +50 m highstand of the Caspian Sea for the early Khvalynian transgression with age estimates ranging between >40 kyr BP to 17 kyr BP (see Table S6.1).

In summary, the Caspian Sea level variation during the late Pleistocene glacial period was much larger than the Holocene, with the potential of overspill periods to the Black Sea basin

(Fig. 2.5). The variation reached more than 70 m of water level change. The extreme (Mangyshlak) lowstand at the Pleistocene-Holocene transition suggests that the climate rapidly became drier. This was then followed by transgressive and regressive phases ranging from -19 to -41 m a.s.l., controlled by hydroclimate change over the Caspian Sea basin (Bezrodnykh et al., 2020; Kroonenberg et al., 2008) combined with intermittent contributions from hydrologically linked basins such as the Amu-Syr Darya river basin around 4 ^{14}C kyr BP (Leroy et al., 2013).
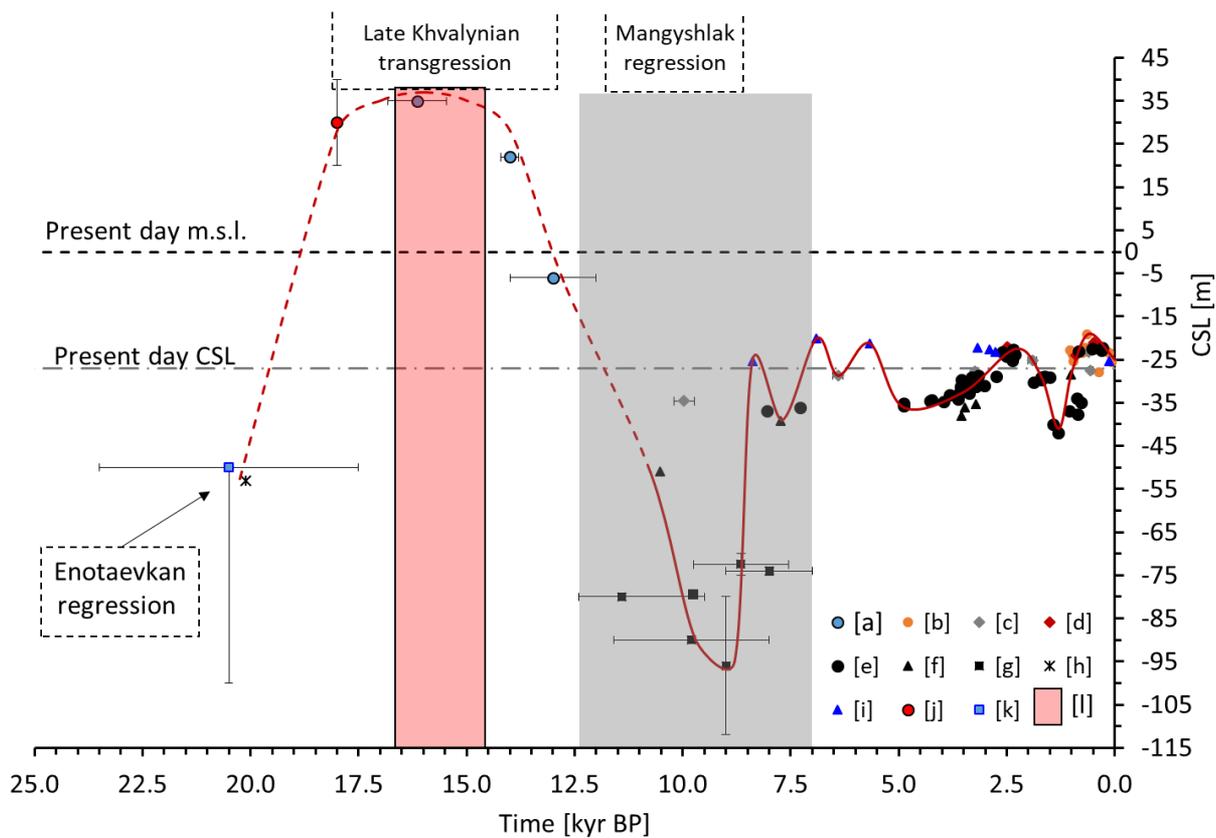
Figure 2.5. Caspian Sea level (CSL) based on various palaeo-environmental records from published works (see Table 2.1 and listed below). The error bars indicate the uncertainty in the reported age records except for 'Enotaevkan' regressions, where various studies reported different lowstand timings, which are combined into a single uncertainty bar for age and Caspian Sea level. The grey-shaded bar indicates the period 'Mangyshlak' regression lasted based on various studies (see Table S6.1). The pink- shaded bar indicates Caspian Sea overflow into the Black Sea basin according to Badertscher et al. (2011). The legend labels [a], [b], [c], [d], [e], [f], [g], [h], [i], [j], [k] and [l] refer to the source of the data presented in Table 2.1. The

red line shows interpolated Caspian Sea level. The solid line represents the Holocene where the resolution of Caspian Sea level record is relatively high and the chronology more precise than the earlier part of the record. The dashed line represents the late Pleistocene period where there is larger uncertainty in the Caspian Sea level record and fewer data points.

2.4.2 Hydroclimate analysis based on HadCM3 simulations

Until recently, palaeoclimate model simulations were typically focused on snapshot simulations of a few well-studied periods, such as the LGM and Mid-Holocene, which have been the focus of international modelling efforts as part of the PMIP collaboration (Braconnot et al., 2012). However, here we want to understand the cumulative impact of changing climate conditions over the late Quaternary. In order to advance our understanding of the impact of climate change on Caspian Sea level evolution, we have analysed the basin water budget variation during the last 25 kyr using simulations from a global coupled ocean-atmosphere-vegetation climate model (HadCM3), based on 25 time-slice simulations (as described in §2.3). The modelled annual mean water budget variations presented in Fig. 2.6a (black sold line) are integrated over the present-day Caspian Sea basin.

We observe that the pre-industrial (0 kyr BP) model estimate of P-E over the present Caspian Sea basin is higher than the rest of the time slices considered. The P-E balance is generally positive in interglacial periods (see Fig. S6.1 for model simulation results covering the last 120 kyr) and then lower during the glacial period (Fig. 2.6a). The spatial pattern (Fig. S6.2) of precipitation and evaporation change is somewhat heterogeneous and varies between time slices, but there are common features. In general, both precipitation and evaporation over land in the drainage basin decrease during glacial times compared with the pre-industrial. However, precipitation declines to a greater extent than evaporation, resulting in drier conditions (an overall decrease in P-E). Over the northern Caspian Sea itself and surrounding land, both precipitation and evaporation increase in the modelled glacial time slices compared to the pre-industrial, primarily as result of an expansion of the prescribed lake grid cells. However, in this region the increase in evaporation is larger than that of precipitation due to the inundation of the land by the Caspian Sea, and so here also the change in P-E is negative (i.e. drier conditions). Over the southern lake grid cells glacial P-E is

higher than pre-industrial. Here, there is no expansion of the lake to replace land grid cells, and while precipitation decreases, the evaporation decrease is greater due to reduced glacial-stage temperatures (Fig. 2.6a).

The rapid climate change events that are simulated (Heinrich events 1 and 2, and the Younger Dryas) produce drier conditions (negative change in P-E) that is roughly half of the total glacial-interglacial amplitude, but on a shorter timescale. The freshwater flux forcing introduced in the North Atlantic induces a rapid collapse of the AMOC and reduced meridional heat transport, which produces widespread temperature decreases throughout the northern hemisphere. The temperature reductions over Europe and the Caspian basin result in decreases in both evaporation and precipitation. As with the multi-millennial scale changes, the reduction in evaporation is not as large as precipitation, producing an overall drying (i.e. negative change in P-E). Despite each of the simulated millennial events being forced with the same magnitude of freshwater flux, the magnitude of the P-E impacts varies. This is likely due to a dependence of the response on the background climate state (e.g., Gong et al., 2013), although further exploration of this is beyond the scope of this study.

In Fig. 2.6b, we present the annual mean HadCM3 P-E, adjusted using bias correction (as described in §2.3.2.4), and a plausible range of uncertainty of P-E for the present-day Caspian Sea basin. The mean annual P-E with bias correction from ERA5 (Hersbach et al., 2020) is given as the middle line in Fig. 2.6b (black solid line). The upper bound of the uncertainty region (shown in grey shading) is given by the annual mean water budget (~6835 m^3s^{-1}) derived from historical Caspian Sea level records combined with an average annual rate of human water extraction (as described in §2.3.2.2). The lower bound is a plausible minimum value (~778 m^3s^{-1}) that is obtained by considering present day observed mean annual Caspian Sea level change without any human extraction (i.e. assuming that either human extraction is negligible or that all human water extraction flows directly back into the Caspian Sea). The raw pre-industrial modelled P-E is closest to the surface water budget calculated from ERA5 and sits in the middle of the uncertainty bounds.

The simulated water budget based on the climate model P-E does not match with the palaeodata based Caspian Sea level graph in Fig. 2.5. Caspian sea level data suggest a strong

positive water budget with a period of Caspian Sea over-spill to the Black Sea during the deglaciation period (20-14 kyr BP), whereas the modelled P-E suggests that the glacial and deglacial are considerably drier than the Holocene. Of course, the Caspian Sea level record is integrating year-to-year changes in budget through time and so we would not expect the temporal evolution of the modelled P-E to produce a direct correspondence with it. However, there is no suggestion that the climate change driven changes in the water budget within the current extent of the Caspian Sea basin resulted in over-spill of the Caspian Sea in the early deglaciation phase. One interpretation of the model-data difference is that there are missing components in the modelled water budget. Potential contributions could come from (1) ice-sheet meltwater (that is neither prescribed nor modelled interactively in the climate model) and/or (2) the impact of topography changes (due to isostatic adjustment and ice-sheet configuration) on drainage system reorganization and basin area change. These issues are addressed in §2.4.3.
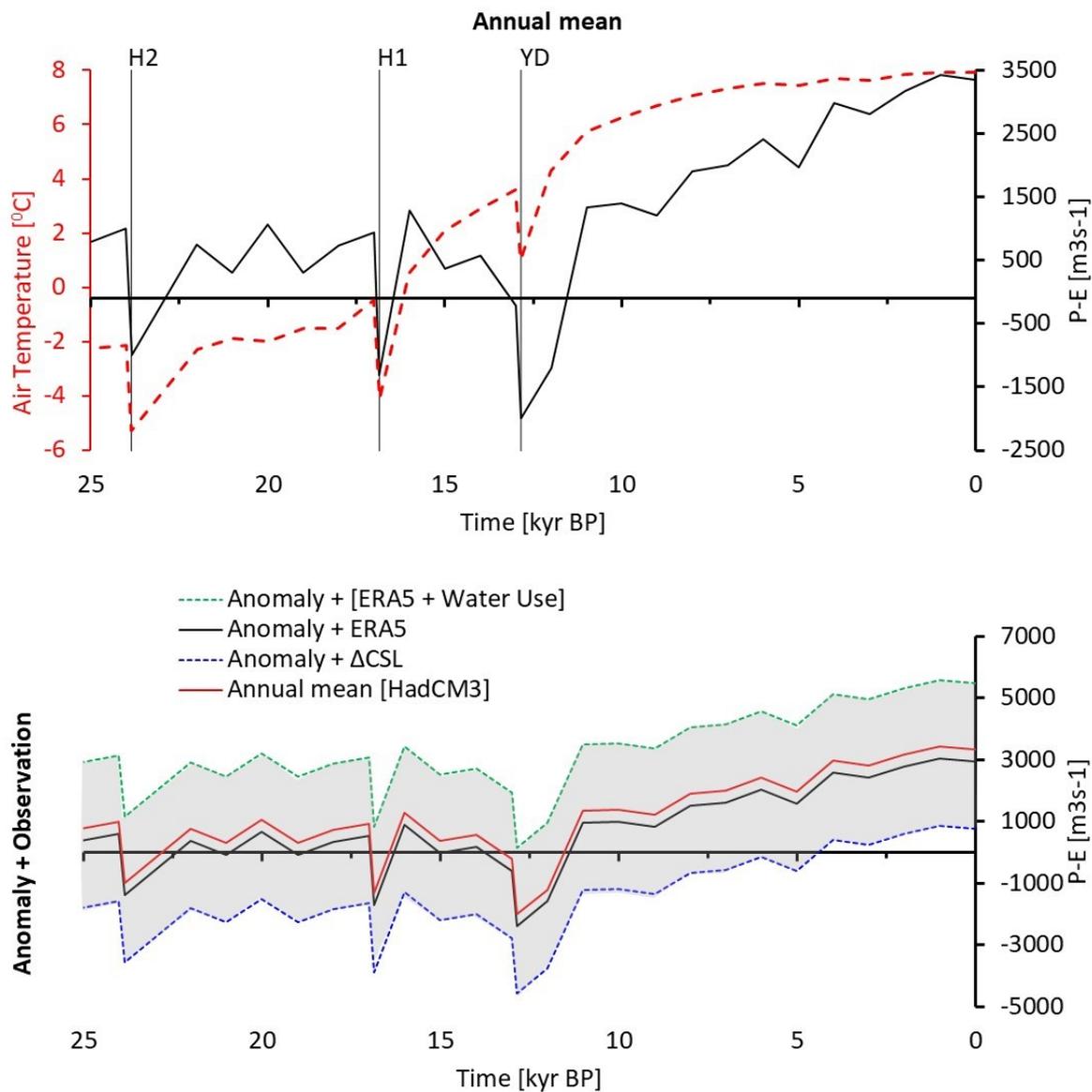
Figure 2.6. Caspian Sea basin water budget (P-E) based on HadCM3 climate for all time-slice simulations covering the last 25 kyr: a) Annual mean precipitation minus evaporation (P-E; solid black line) and annual mean surface air temperature (red dotted line), b) mean bias corrected P-E obtained by adding anomaly of annual mean P-E to the mean annual P-E from ERA5 (Copernicus Climate Change Service, 2017; Hersbach et al., 2020) in the black line. The shading shows plausible range of P-E over the present day Caspian Sea basin based on observed mean annual Caspian Sea level change and water extraction (green dotted line), or just Caspian Sea level change (blue dotted line). The raw P-E model output is shown in red for comparison. (Key: Younger Dryas – YD, and Heinrich – H). The annual mean surface air temperature and P-E are calculated over the Caspian Sea basin (Fig. 2.2).

2.4.3 Evaluation of Fennoscandian ice-sheet impact on the Caspian Sea

Previous studies (e.g., Wickert, 2016) have demonstrated that the North American ice-sheet complex played a vital role in restructuring rivers and drainage basin systems by altering the topography of the Earth's surface. Below we use similar methods to explore the impact of the Fennoscandian ice-sheet on reorganizing the palaeo-drainage of the Caspian Sea basin during the last deglaciation period. We explore the potential impact of the direct contribution of water as the ice melts. Detailed explanations are presented as follow (§2.4.3.1, §2.4.3.2).

2.4.3.1 Reconstruction of palaeo Caspian Sea drainage basin and river flow direction

Reconstruction of the palaeo-Caspian Sea basin and river flow directions was performed using the method described in §2.3 at 1000 yr intervals over 25 kyr BP to 0 kyr BP. The spatial maps presented in Fig. 2.7 show the evolution of the Caspian Sea Basin and river network for key periods, including the LGM. Readers are advised to refer to the supplementary movie showing the full time series reconstruction from 25 kyr BP to present day (accessible at link[1]). There was massive expansion of the drainage basin and river systems during the last glacial maximum and deglaciation (Fig. 2.7).
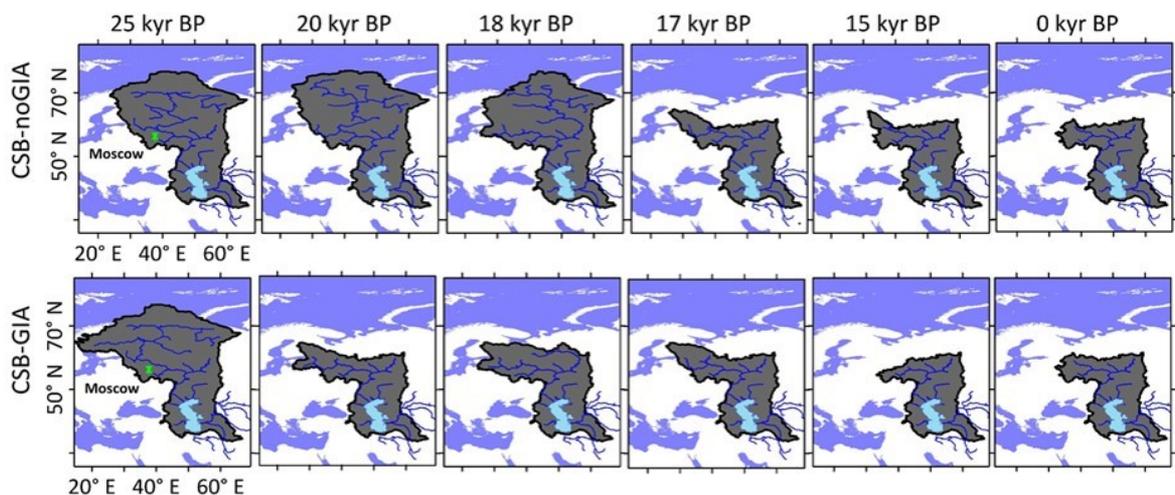
Figure 2.7. Spatial map showing Caspian Sea basin outline and river network for 0k, 15k, 17k, 18k, 20k and 25k years before present. The spatial map on the first row (a) is based on topography created by combining present day high resolution digital elevation model (DEM)

and Ice-sheet thickness from ICE-6G (Argus et al., 2014; Peltier et al., 2015; Stuhne and Peltier, 2015), and here glacial isostatic adjustment is not considered. The second row (b) is based on ICE-6G_C topography data corrected for glacial isostatic adjustment combined with present day high resolution digital elevation model (DEM). Drainage basins are delimited in dark grey shaded area and blue lines represent the respective river flow direction. The white and blue colour backgrounds are present day land and sea mask respectively. (Key: CSB – Caspian Sea Basin)

We considered two scenarios of palaeo-topography, both of which include ice-sheet topographic change but only one in which glacial isostatic adjustment is also incorporated. The spatial maps for these scenarios, presented in Fig. 2.7a-b, were constructed using the ice-sheet history from ICE-6G_C (Argus et al., 2014; Peltier et al., 2015; Stuhne and Peltier, 2015) combined with a present-day high-resolution digital elevation model (DEM). Fig. 2.7a shows spatial map of the palaeo Caspian Sea drainage system derived from topography created by combining present-day GEBCO digital elevation model (DEM) and ice-sheet thickness history from ICE-6G_C, hereafter referred as **CSB-noGIA**. In this scenario the effect of glacial isostatic adjustment is not considered. The spatial maps shown on Fig. 2.7b are derived from ICE-6G_C topography corrected for glacial isostatic adjustment (Argus et al., 2014; Peltier et al., 2015) combined with the present-day GEBCO DEM, hereafter referred as **CSB-GIA**. Another set of spatial maps (Fig. S6.3) are included in the supplementary information which are made using the same set of datasets as Fig. 2.7b, with glacial isostatic adjustment algorithm described by Kendall et al. (2005) for comparison. This third combination produced drainage basins similar to CSB-noGIA and so is not discussed in the main text.

In both scenarios (CSB-noGIA and CSB-GIA) the Caspian Sea basin expanded farther north of the present-day basin land area. The total area of the basin increased by 60-70% of current basin size (Fig. 2.8). The basin decreases in size earlier in the deglaciation when the glacial isostatic adjustment component is included. The reorganization of the Caspian Basin has implications for Caspian Sea level variation, as the drainage system experiences additional river flow and routing of meltwater into the basin with a larger drainage area.
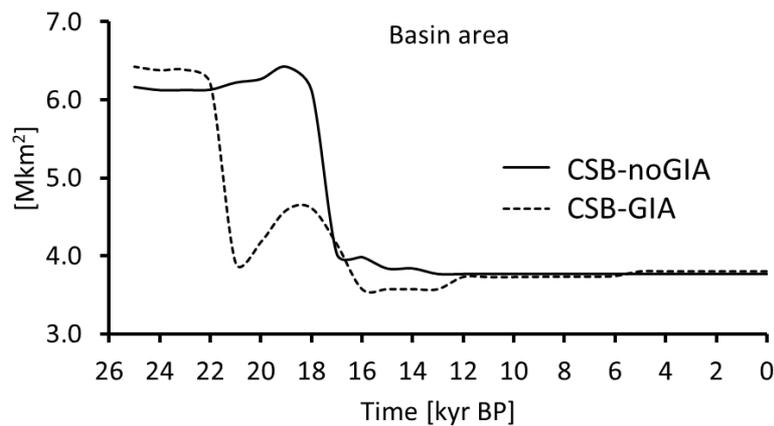
Figure 2.8. Estimate of drainage area corresponding with the two scenarios presented in Fig. 2.7.

2.4.3.2 Impact on water budget

In this section we present an evaluation of ice-sheet and topographic impacts on the palaeo-water budget of the Caspian Sea basin. Fig. 2.9a, shows the total volume of accumulated ice-sheet within the palaeo-Caspian Sea basin area (CSB-noGIA and CSB-GIA) and from the entire Fennoscandian ice-sheet. The substantial amount of ice-sheet accumulation during the glacial period resulted in an increase of elevation that caused the Caspian Sea area to expand (Fig. 2.7). North-flowing rivers were redirected southward and this led to an increase in runoff due to ice-melt and hydroclimate-based runoff (P-E).

The amount of meltwater contribution reached up to 2 Mkm^3 per thousand years during the deglaciation (Fig. 2.9b). However, the timing and magnitude of meltwater contributions are highly sensitive to the isostatic adjustment (Figs. 2.7 and 2.8). When the isostatic component is included, the contribution of ice-melt was close to 58,302 m^{3}s^{-1} at around 20 kyr BP, whereas, when isostatic component is not considered the ice-melt contribution reached a maximum of close to 36,263 m^{3}s^{-1} at around 16 kyr BP (Fig. 2.9d).

Northward expansion of the Caspian Sea drainage basin, due to elevation change caused by ice-sheet growth, also resulted in considerable positive changes to P-E. The increase in P-E between 25 – 15 kyr BP is smaller when the isostatic component is considered (CSB-GIA) than when not considered (CSB-noGIA; Fig. 2.9c). The combined contribution from both ice-sheet meltwater and meteoric (P-E) water in the expanded glacial basin was substantial and

likely the main contributor to the Caspian Sea water budget in the early deglaciation (Fig. 2.9d). The accumulated ice-melt contribution was ~17% higher than P-E from HadCM3 when the isostatic component was included (CSB-GIA), but ~33% lower when its impacts were not included (CSB-noGIA). The treatment of the isostatic adjustment is therefore an important component to consider.

The P-E water budget we considered here uses the total amount of water falling as precipitation, and this may fall as rainfall or snowfall (Fig. 2.9c-d). However, in reality, the climatic condition (very cold/dry or wet/warm) plays a significant role in how the precipitation is transformed to runoff. Snowfall may accumulate and retained as ice over prolonged periods and therefore not contribute to the water budget until the ice melts. Therefore, the climatic conditions over the ice-sheet play an important role in whether snowfall contributes to runoff. However, the model simulation output did not permit an analysis of this (only total precipitation was available), so we used the HadCM3 runoff field to integrate the various aspects of snowfall and melt (Fig. 2.9e). The modelled runoff reached its peak around ~18 – 17 kyr BP and is ~2000 m^3s^{-1} less than P-E for CSB-noGIA (Fig. 2.9e). The amount of runoff from 25 to 19 kyr BP is roughly 50% less than P-E, likely as a result of a portion of the precipitation falling as snowfall that would not have contributed to runoff formation.

Runoff (HadCM3) and meltwater (ICE-G6_C) from the expanded basin contributed substantially to the deglacial Caspian Sea water budget (Fig. 2.9f). The ice-melt contribution dominates at around 16 kyr BP and 20 kyr BP for CSB-noGIA and CSB-GIA respectively, i.e. the timing is dependent on the isostatic adjustment. The accumulated ice-melt contribution (between 25 and 12 kyr BP) was higher than runoff from expanded Caspian Sea drainage area (by ~42%) when isostatic adjustment was considered and lower (by ~ 15%) when isostatic impacts were not considered.
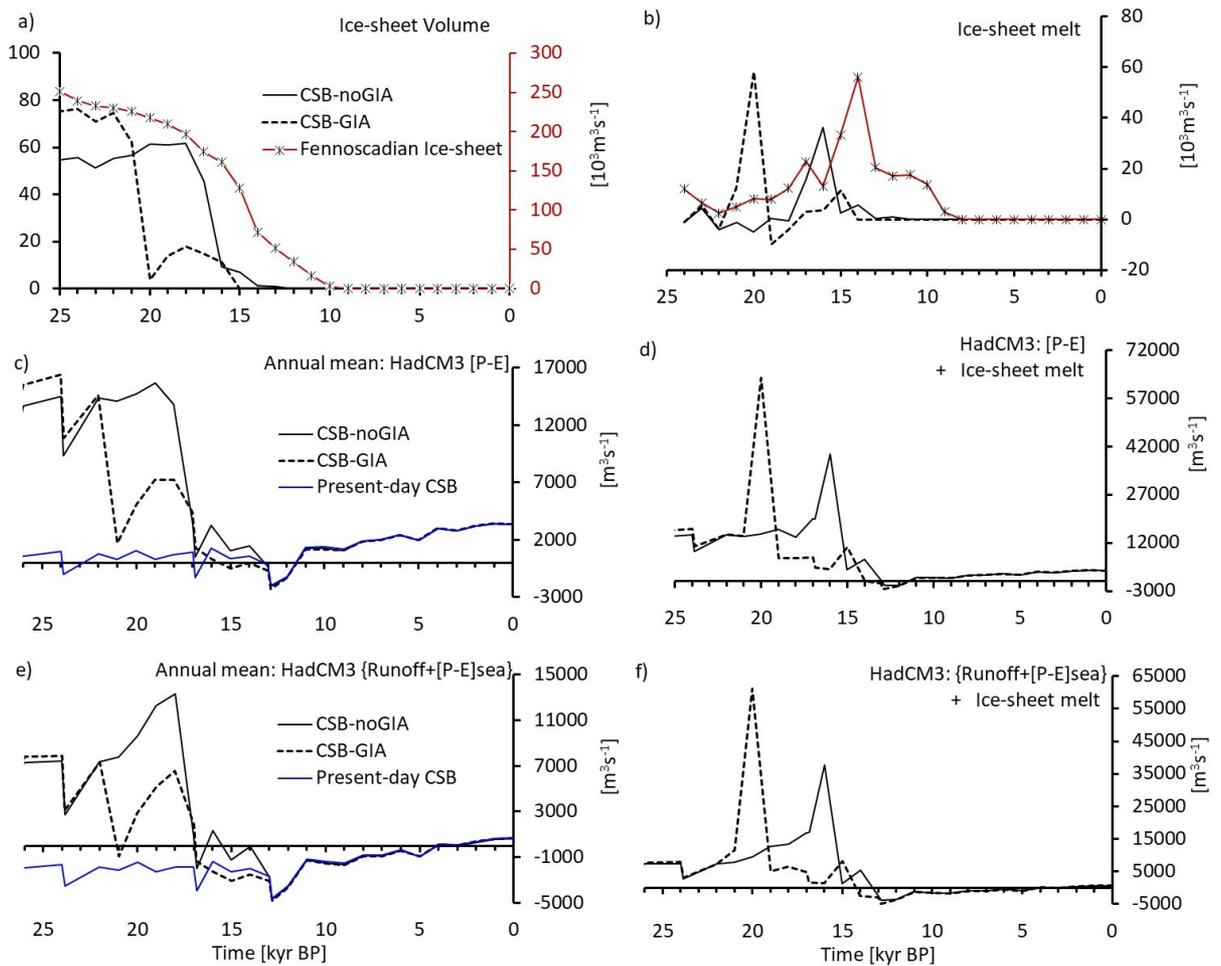
Figure 2.9. a) total ice-sheet volume, b) ice-sheet meltwater contribution, c) annual mean HadCM3 [P-E], d) annual mean HadCM3 [P-E] plus Ice-sheet melt, e) annual mean HadCM3 [runoff], and f) annual mean HadCM3 [runoff] plus ice-sheet melt. All values are integrated over catchment areas identified as Caspian Sea basins A, and B presented in Fig. 2.7.

2.4.4 Caspian Sea level variation using HadCM3 runoff, ICE-6G_C ice melt, and basin shape changes

The main drivers of Caspian Sea level variation during the last glacial period are thought to have been (1) climate change (P-E or runoff), (2) impact of ice-sheet growth/melt leading to restructuring of palaeo-drainage basin and reorganizing of the river systems, and (3) contributions of ice-sheet meltwater itself. In this section we integrate these different components into a simple model to calculate Caspian Sea level in order to explore their relative importance (as described in §2.3.2.4). We performed two sets of simulations, with

and without bias-correction, using HadCM3 runoff, ICE-6G_C ice melt, and basin shape changes, identified as CSB-noGIA and CSB-GIA in Fig. 2.7. Results are presented in Fig. 2.10 and described below using HadCM3 runoff (output from land surface process model: MOSES2.1) to drive the model, but a similar figure is included in the supplementary information for comparison where HadCM3 P-E (output from the atmospheric component) is used instead of runoff (Fig. S6.4).

A first set of simulations were performed to evaluate the combined impact of runoff and ice-sheet meltwater in the expanded Caspian basin. As can be seen in Fig. 2.10a, the contribution of meltwater combined with runoff from the expanded area substantially increases Caspian Sea level starting from 25 kyr BP and lasting through the deglaciation period until 12 kyr BP. We set a sill height in the model at 40 m above m.s.l. (Manych-Kerch spillway). The increase in water budget resulted in overspill of the Caspian Sea to Black Sea basin between 20 and 15 kyr BP when the isostatic component is not considered (CSB-noGIA), and from 19 to 15 kyr BP when the isostatic component is considered (CSB-GIA). This can be compared to the simulation in which the basin is kept at the present-day extent (blue line in Fig. 2.10), where there is no large transgression leading to overspill at any point during the last 25 kyr. In this particular simulation, we note that although P-E (or runoff) over the whole basin is lower during the glacial period than during the Holocene (see Fig. 2.6a), the modelled Caspian Sea level is higher in the glacial period. This is because the model separates the water balance over sea and land, and there is a positive anomaly in P-E during the glacial period over the sea grid points, which outweighs the lower runoff over land. We did a sensitivity analysis of the initial condition of the Caspian Sea volume (at 26 kyr BP) and found that it only impacted the Caspian Sea level evolution for ~2 kyr, and did not have a long term influence (Fig. S6.5).

A second set of simulations were based on HadCM3 runoff integrated over the CSB-noGIA and CSB-GIA without ice-sheet meltwater contribution. As can be seen on Fig. 2.10b, runoff contribution from the expanded area alone greatly increased Caspian Sea level between 25 and 13 kyr BP when the isostatic component is not considered (CSB-noGIA), and between 25 and 16 kyr BP when the isostatic component is considered (CSB-GIA). The over-spill to the Black Sea occurred between 20 and 17 Kyr BP for CSB-noGIA, and from 19 to 17 kyr BP for

CSB-GIA. The effect of the ice-melt is also to raise the height of the lowstand around 12 kyr BP by ~23m compared to when meltwater is not included (Fig. 2.10a and b).

In both sets of simulations, the impacts of meltwater input and runoff from basin expansion essentially decrease and become negligible by the early Holocene. In the Holocene all the scenarios are essentially the same, with a slight monotonic increase in Caspian Sea level throughout the Holocene, but much smaller variation than the deglaciation. The model reaches ~28 m below m.s.l. of Caspian Sea level in the present-day even without bias correction. The simulated Caspian Sea level is ~3 m less than the observed Caspian Sea level of ~25 m below m.s.l. during pre-industrial period. This indicates that the modern-day model bias is small compared to the palaeo-changes. The bias correction (described in §2.4.2), which is applied over the whole period considered for the study has little impact on Holocene Caspian Sea level but does influence the magnitude of the extreme high and lowstands in the deglaciation, as shown in Fig. 2.10c and 2.10d.

In terms of the comparison between the model and palaeodata, both model (Fig. 2.10) and data (Fig. 2.5) suggest that there was a major transgressive episode leading to overspill into the Black Sea in the early deglaciation (19-14 kyr BP in the palaeodata). In the model, a key factor driving is the change in topography (due to ice-sheets) increasing the size of the basin. The increase in runoff/P-E into the Caspian alone is sufficient to lead to overspill in this time period (Fig. 2.10b). When ice-sheet meltwater is added this extends the timing of the connection to the Black Sea. The impact of isostatic adjustment opposes this and reduces the time interval of Caspian Sea overspill in the model (Fig. 2.10; compare dashed red line and black line). The impacts of Heinrich events (H1 in particular) on Caspian Sea level are more apparent when meltwater is not considered. Otherwise the impacts of meltwater on Caspian Sea overspill overwhelms the drying effect of the Heinrich events. The ice-sheet meltwater in the basin is immediately routed to the Caspian Sea and it is the derivative of the ice-sheet volume computed over thousand years with the assumption of a linear relationship (Fig. 2.90a). The actual variation in rate of ice-sheet melt during the thousand years was not considered as the ice-sheet reconstruction temporal resolution is very low. Therefore, what is shown in this result only reflects the volume of water that could have melted within the expended area of Caspian Sea basin leading to increased Caspian Sea level during cold dry

periods (e.g. H1). Moreover, although the snapshot simulations (equilibrium climate condition every thousand years) allow us to effectively cope with constrained computational resources and boundary conditions, consideration of transient climate simulations would likely improve the last deglaciation period simulations characterized by abrupt climate change.

Both model and data indicate much more stable sea levels during the Holocene, with the exception of the Mangyshlak regression in the early Holocene. The timing of the lowstand is earlier in the model, corresponding to the timing of the Younger Dryas, whereas in the data the average timing of the Mangyshlak is ~ 9.5 kyr BP, although within uncertainties there is overlap. The magnitude of the lowstand recorded in the palaeodata during the LGM (Enotaevkan regression) is much lower than model output. In the model, reduced Caspian Sea level at this time was a result of palaeoclimate change during Heinrich event 2.

In the Holocene there is less variation in the model than in the palaeo-Caspian Sea level data. This is expected given the way the climate model was set up to simulate regular time slice intervals (which were run to equilibrium) that were processed as climatologies rather than a transient simulation with sub-millennial forcing (e.g. solar activity or volcanic variation) or internal variability on centennial/millennial time scales. This means we have not modelled some events that may well have produced Caspian Sea level variation at these time scales during the Holocene, such as the 8.2 kyr event (Alley et al., 1997) or the Roman climatic optimum, for example.
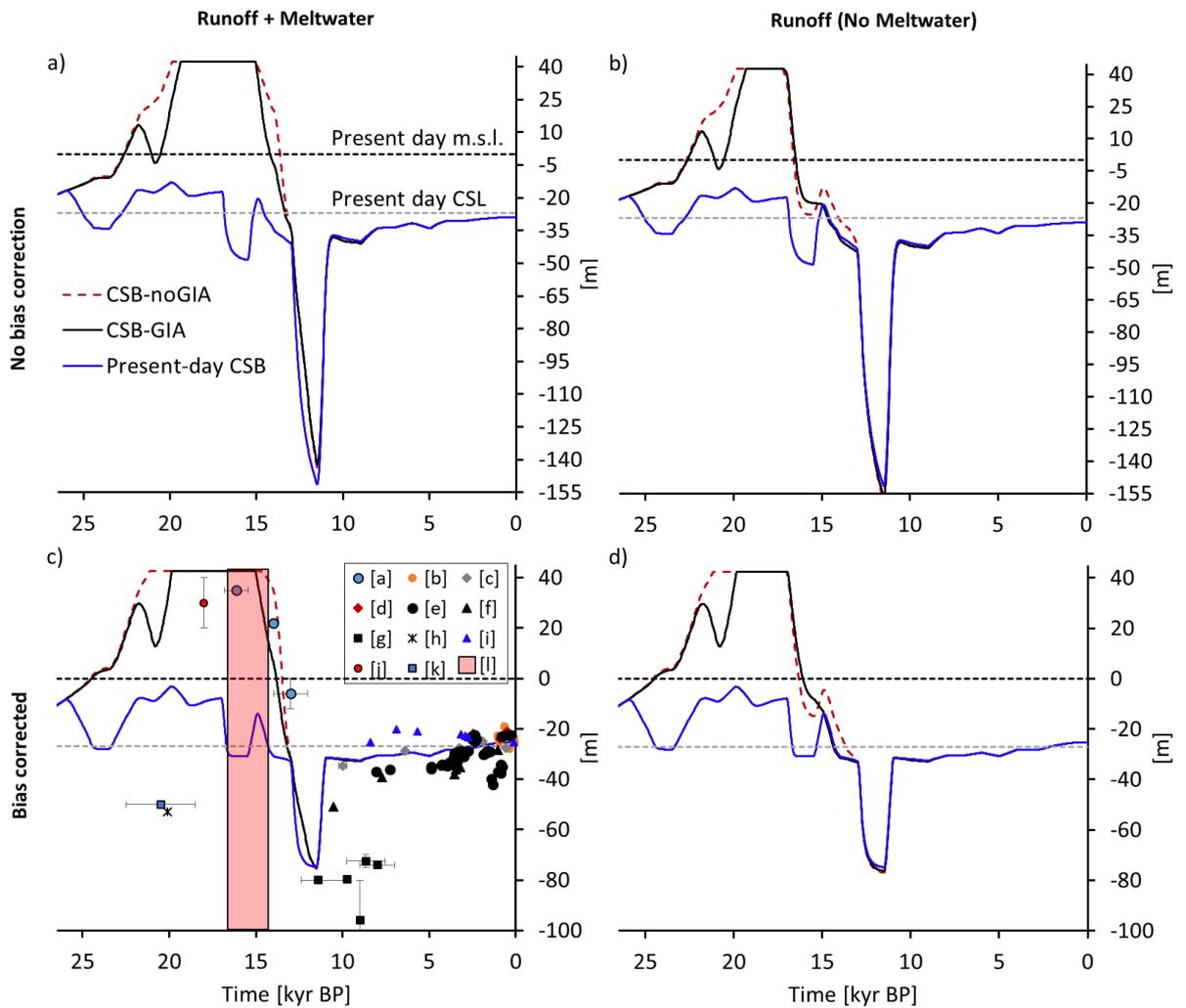
Figure 2.10. Caspian Sea level variation using HadCM3 runoff, ICE-6G_C ice melt, and basin shape changes identified as CSB-noGIA, CSB-GIA (see Fig. 2.70) and Present-day CSB (see Fig. 2.20). Without (a) and with (c) bias-correction of simulated Caspian Sea level using HadCM3 runoff integrated over palaeo CSB-noGIA and CSB-GIA plus ice-sheet melt. Without (b) and with (d) bias-correction of simulated Caspian Sea level using HadCM3 runoff integrated over palaeo CSB-noGIA and CSB-GIA without ice-sheet melt contribution. The blue line is used as control and it represents Caspian Sea level based on HadCM3 runoff within present day Caspian Sea basin. The point plots are proxy based Caspian Sea level reconstruction presented in Fig. 2.50.

2.5   Discussion and conclusions

In an attempt to identify the primary drivers of Caspian Sea level variation during the late Quaternary, we have investigated the nexus between hydro-climatological processes, ice-sheet evolution, and catchment dynamics and their potential impacts on Caspian Sea level variation. We integrated palaeoclimate model output from HadCM3 with reconstructed ice-sheet meltwater and topographic changes from ICE-6G_C to simulate Caspian Sea level over the last 25 kyr. We also collated Caspian Sea level data from published palaeo-environmental records for comparison.

Among the anticipated drivers, the Fennoscandian ice-sheet played the most substantial role on Caspian Sea level in the model by altering the topography of the earth surface and restructuring river drainage systems, increasing the area of the Caspian Sea drainage basin by 60-70% of its current size. The runoff in the expanded basin increased, despite the fact that the modelled glacial conditions were drier, due to the reorganisation of river flows. When combined with meltwater during the last deglaciation period (19 – 12 kyr BP), these were the main drivers of the highest transgression of the Caspian Sea. The model only produced overspill into the Black Sea (as seen in the palaeodata) in the scenarios with an expanded basin area, and ice-sheet meltwater was not a necessary factor to produce the overspill in the model.

The climatic impacts of Heinrich events 1 and 2 and the Younger Dryas were included in the HadCM3 simulations. Each millennial-scale event produces a decrease in the water budget (i.e. drier conditions over the basin) due to collapse of the AMOC. However, the impact of Heinrich event 1 on Caspian Sea level is overwhelmed by the influx of ice-sheet meltwater and runoff from the expanded Caspian Sea basin due to drainage reorganization at the time. This is not the case for the Younger Dryas, during which drier conditions lead to the lowest Caspian Sea level in the modelled time period. We note that, in the model, ice-sheet meltwater in the basin is immediately routed to the Caspian Sea. However, it is possible that the timing of meltwater routing may have been modified by pro-glacial lakes (Fig. 2.2[4]), which may have temporarily stored meltwater and then postponed and/or redirected its release (due to reaching overspill level, ice-damming collapse, or impact of isostatic

adjustment). There is an indication in palaeorecords of pro-glacial lake water storage at the LGM and subsequent brief overflow into the Volga basin during the early deglaciation (Lysa et al., 2011; Mangerud et al., 2004). In addition, catastrophic flooding in Siberia (due to subglacial volcanoes) might have contributed to the overspill of proglacial lakes to the Aral Sea (Mangerud et al., 2004). Moreover, as shown in Krinner et al. (2004), a number of large ice-dammed lakes, with a combined area twice that of the Caspian Sea, were formed in northern Eurasia during the last glacial period. Their result suggests that Eurasian proglacial lakes played a vital role in the reduction of ice sheet melting through strong regional summer cooling resulting in accelerated ice sheet growth and delay in ice sheet decay in Eurasia. Therefore, a careful consideration of the impacts of proglacial lakes on the Caspian Sea climate is necessary, and a spatially distributed hydrological routing model would be needed to explore the routing of the overspill that might have contributed to the Caspian Sea level.

In the literature, the timing of the Mangyshlak lowstand, and therefore the proposed cause, varies. In the model, the lowstand that resulted from Younger Dryas conditions overlaps in time with the uncertainties in the chronology of the Mangyshlak regression. The lowstand has been associated previously with the Younger Dryas (e.g., Bezrodnykh and Sorokin, 2016; Kislov, 2018) or the shift to warmer, dryer continental conditions in the early Holocene (e.g., Arslanov et al., 2016) or reduction in meltwater coupled with increased evaporation (Leroy et al., 2013). HadCM3 (and indeed most other climate models) does not produce the magnitude of warming and increased continental conditions in the early Holocene that has previously been interpreted from the palaeo-record (termed the Holocene temperature conundrum by Liu et al., 2014). However, there has been recent debate about this interpretation of the palaeodata, following another study (Marsicek et al., 2018), which used fossil pollen temperature reconstructions over Europe and North America to demonstrate a gradual warming through the Holocene, with a similar temporal signature to climate models (including HadCM3), rather than an early Holocene climatic optimum. Such climatic conditions in the model are not able produce a significant low stand in the early Holocene.

All of our hydroclimatic results are based on HadCM3, and our results could be sensitive to this choice. (Kislov and Toropov, 2007) show that a previous version of this model

performed well compared to data for the Caspian for the present day and LGM. However, Bartlein et al. (2017) report that the ensemble mean of PMIP3 models show a drying of continental Eurasia during the mid-Holocene in contrary to data, which suggest a moistening. Examination of our simulations reveals that HadCM3 shows barely any change in precipitation over Europe (aside from some increase over Italy) during the mid-Holocene (Fig. S6.2), which is closer to the data. However, the data compilation has relatively few points over the Caspian Sea catchment and the available data shows some small drying, which is in better agreement with the model.

In the present day, there is no flow from the Amu-Syr Darya/Himalayan drainage basins (Fig. 2.2) into the Caspian Sea, but there is geomorphological evidence that there have been previous short-lived connections that affected the water budget of Caspian Sea basin (Leroy et al., 2013). Palaeo-runoff from the Amu-Syr Darya basin could have potentially contributed to past Caspian Sea level variations. However, as there is insufficient detail on the timing and extent of this connection, we were unable to fully assess any potential contribution. A brief analysis suggests that if the Amu-Syr Darya and the whole Himalayan basins flowed into the Caspian Sea, they could potentially increase the water budget by 2 and 5 times respectively (Fig. S6.1). However, contributions for the present-day leads to far too high P-E and doesn't reflect the current situation, and that available palaeodata suggests only brief periods of connection in the time period we've covered. Though there was potential for a large impact during periods of suspected connection, we think it is unlikely that the contributions were long-lived based on current evidence.

The Caspian Sea surface area changes rapidly with volume when Caspian Sea level is between -50 m and +50 m above mean sea level. A larger surface area enhances evaporation from the sea, adding more moisture in the atmosphere and affecting the water budget of the region as well as large-scale hydroclimate (Koriche, Nandini-Weiss et al., 2020b). We have made a first-order attempt to account for changes in evaporation due to surface area change of the lake in the simple model to simulate Caspian Sea level (see Equation 2.1). In addition, the HadCM3 simulations have an increased lake size in the glacial compared to the present-day (see Fig. S6.2a), so there is an element of climate feedback included from the enhanced lake area, although this is prescribed and at the low-resolution of the climate model.

Improved representation and coupling of all the processes that lead to changes in Caspian Sea area (e.g. ice-sheet meltwater) could further improve the Caspian Sea level model as well as the spatial patterns of change in the climate model.

As explained in §2.2, there are competing ideas about sources and timing of runoff that caused the transgressive and regressive stages of Caspian Sea during the late Quaternary. One of the debates concerns whether the source of runoff that caused the Khvalynian transgression during the last deglaciation period was meltwater from the Fennoscandian ice-sheet via Volga river basin (e.g., Soulet et al., 2013; Tudryn et al., 2016) or glacial melting supplemented by proglacial lake outbursts from the Siberian region joining via the Aral Sea (e.g., Mangerud et al., 2004; Yanko-Hombach and Kislov, 2018). Based on our findings, the Fennoscandian ice-sheet played the vital role by altering the topography of the earth surface leading to river drainage system reorganization, and through meltwater contribution during the deglaciation period, although we cannot rule out some impacts related to pro-glacial lakes outburst and glacial melting from the Himalayan region. We find that the hydroclimate changes (P-E/runoff) at the LGM and early deglacial within the extent of the modern basin were not a dominant component in Caspian Sea level variation in our model when compared with ice-sheet related factors. This varies from the conclusions of some previous studies (Krijgsman et al., 2019; Yanchilina et al., 2019; Yanina et al., 2018). Holocene variations in Caspian Sea level were, however, dominated by hydroclimate change.

Acknowledgements

3. CHAPTER THREE: Impacts of variations in Caspian Sea surface area on catchment-scale and large-scale climate

Sifan A. Koriche, Sri D. Nandini-Weiss, Matthias Prange, Joy S. Singarayer, Klaus Arpe, Hannah L. Cloke, Michael Schulz, Pepijn Bakker, Suzanne A. G. Leroy, Michael Coe

Key points

- Caspian Sea surface area affects regional climate over the catchment as well as large-scale climate over the entire northern hemisphere

- Surface water budget over the Caspian catchment decreases as surface area increases due to negative lake surface-evaporation feedback

- A larger Caspian Sea enhances precipitation over central Asia, warms the north-western Pacific during winter, and reduces Pacific sea ice

- Accurate representation of the Caspian Sea in climate models is important to avoid creating additional biases both locally and globally

Abstract

The Caspian Sea is the largest inland lake in the world. Large variations in sea level and surface area occurred in the past and are projected for the future. The potential impacts on regional and large-scale hydroclimate are not well understood. Here, we examine the impact of Caspian Sea area on climate within its catchment and across the northern hemisphere, for the first time with a fully coupled climate model. The Community Earth System Model (CESM1.2.2) is used to simulate the climate of four scenarios: (1) larger than present Caspian Sea area, (2) current area, (3) smaller than present area, and (4) no-Caspian Sea scenario. The results reveal large changes in the regional atmospheric water budget. Evaporation (E) over the sea increases with increasing area, while precipitation (P) increases over the south-west Caspian Sea with increasing area. P-E over the Caspian Sea catchment decreases as Caspian Sea surface area increases, indicating a dominant negative lake-evaporation feedback. A larger Caspian Sea reduces summer surface air temperatures and increases winter

temperatures. The impacts extend eastwards, where summer precipitation is enhanced over central Asia and the north-western Pacific experiences warming with reduced winter sea ice. Our results also indicate weakening of the 500-hPa troughs over the northern Pacific with larger Caspian Sea area. We find a thermal response triggers a southward shift of the upper troposphere jet stream during summer. Our findings establish that changing Caspian Sea area results in climate impacts of such scope that Caspian Sea area variations should be incorporated into climate model simulations, including palaeo and future scenarios.

Keywords: Caspian Sea, Precipitation, Evaporation, CESM1.2.2 model, subtropical jet

Plain Language Summary

The Caspian Sea is the largest land-locked water body in the world. It is filled by rivers draining a vast region from northern Russia to Iran. The size of the Caspian Sea has varied considerably over recent centuries and millennia due to various factors, including changes in climate. Conversely, as the area of the sea changes it also has impacts on the climate, but there are significant questions about how and where those impacts would be felt. In this study we used a state-of-the-art climate model in which we specified different sizes of Caspian Sea in order to examine how the climate changes as its area increases. We observed that the local seasonal cycle of temperatures gets smaller, and evaporation increases, while there are more spatially complex changes in local rainfall. Furthermore, the impacts on atmospheric circulation occur as far as the north Pacific, with resulting increases in temperature and decreases in sea-ice coverage in winter as the Caspian area increases. The climate impacts are so significant and geographically extensive that climate models used to simulate climate change (both in future and past scenarios) should incorporate changes to the Caspian Sea area if they are to robustly model regional climate.

3.1 Introduction

The Caspian Sea is the world's largest inland sea, sited within a vast endorheic catchment area (3.6 Mkm^2) that is fed by 130 rivers (Rodionov, 1994). Currently, >80% of inflow contribution is from the Volga and the Caspian Sea water level is ~28 m below global mean sea level (Leroy et al., 2020). The Caspian Sea is situated amid semi-arid Central Asian regions, flat northern terrains, and humid high mountain ranges in Eurasia (Fig. 3.1). A large region

vulnerable to desertification lies west of the northern Caspian Sea (Republic of Kalmykia), and a region of high precipitation (the Hyrcanian region) is found south of the Caspian Sea (Molavi-Arabshahi et al., 2016). Given the complex orography and extensive geography, the entire Caspian Sea catchment area occupies six Köppen climatic zones (Chen and Chen, 2013).

Over the Quaternary period, the Caspian Sea experienced extreme water-level changes ranging from approximately +50 m to -90 m between transgressive and regressive periods, and variations of >3 m during the last century (Arpe and Leroy, 2007; Arslanov et al., 2016; Bezrodnykh et al., 2020; Forte and Cowgill, 2013; Kakroodi et al., 2014; Kakroodi et al., 2015; Krijgsman et al., 2019; Kroonenberg et al., 2008; Naderi Beni et al., 2013; Yanina et al., 2020; Yanina, 2014). Such large variations in water level have substantial impacts on the change in Caspian Sea surface area (Fig. 3.1). The difference in area between late Quaternary low stands and high stands is roughly equivalent to 70% of current Caspian Sea area, and this difference can potentially affect regional and large-scale hydroclimate (Arpe et al., 2019). Understanding the feedbacks of Caspian Sea area variations on the hydroclimate system is essential at both the regional and global scale, since any large waterbody like the Caspian Sea plays a significant role in affecting the energy and water budget by altering the albedo, evaporative fluxes, and near-surface temperature.
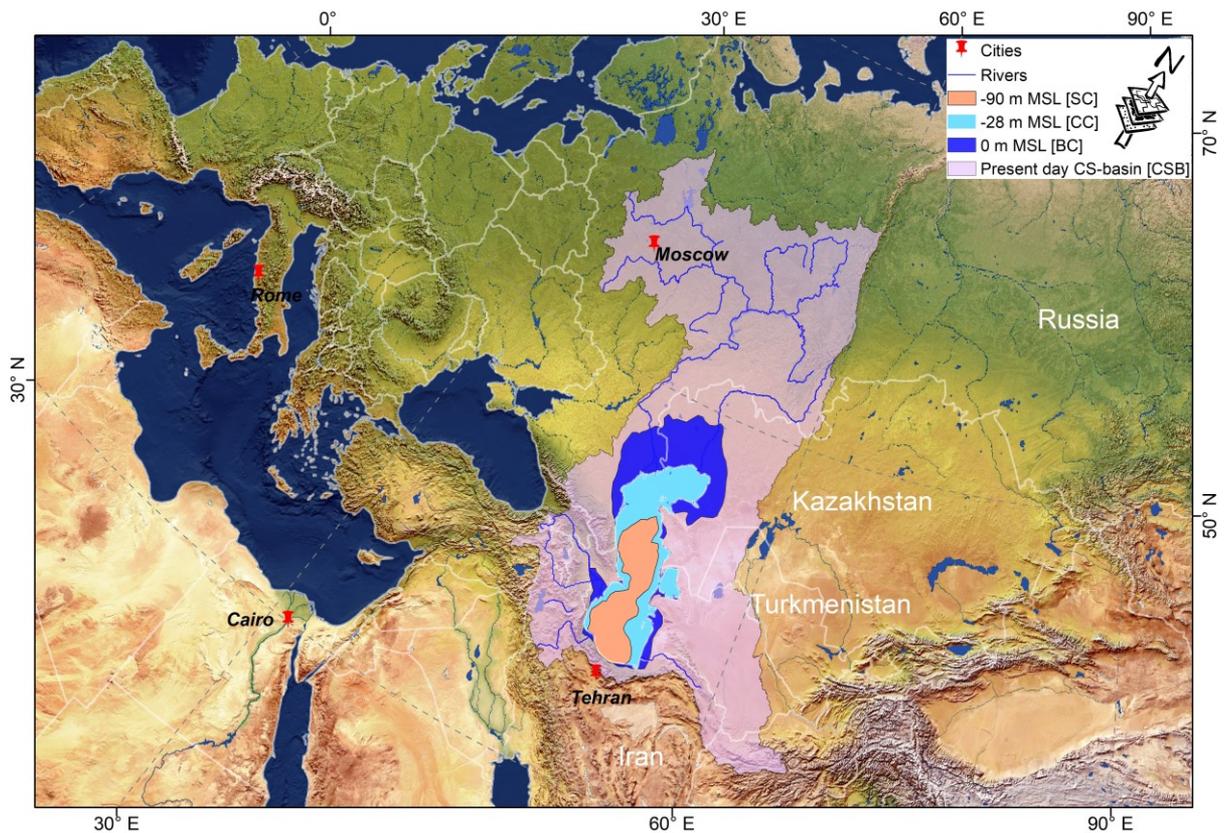
Figure 3.1. High-resolution DEM contours of Caspian Sea surface areas (shown by dark blue area (large Caspian, BC), brown area (Small Caspian, SC) and light blue area (Current Caspian, CC)). The catchment area is depicted by light purple area. Blue and white solid lines represent rivers and country borders respectively, and MSL refers to Mean Sea Level. Shaded relief, water, and drainages are made with Natural Earth (Free vector and raster map data @ naturalearthdata.com).

The influence of the presence of the Caspian Sea on regional and large-scale climate can be inferred from previous climate modelling studies. Several have examined the impacts on the Caspian Sea itself (Arpe et al., 2019; Lodh, 2015; Nicholls and Toumi, 2014) and some have examined other large lakes, e.g., mega-lake Chad (Broström et al., 1998; Coe and Bonan, 1997; Contoux et al., 2013) or the Great Lakes (Lofgren, 1997; Notaro et al., 2013; Sousounis and Fritsch, 1994). Idealized studies of the Great Lakes have noted that their presence impacts large-scale circulation patterns and the jet stream (Lofgren, 1997), with increased strength of zonal winds and enhanced cyclogenesis associated with anomalous heat and moisture transport (Sousounis and Fritsch, 1994). Another study on the effects of the Great Lakes on

large-scale circulation found that the lakes caused decreased (increased) surface pressure in winter (summer), which led to irregular cyclonicity (anticyclonicity) over the lakes (Notaro et al., 2013). However, they found no shift in the jet stream, unlike other studies (e.g., Lofgren, 1997), likely due to constraints in the regional modelling domain.

Most climate models still poorly prescribe the actual Caspian Sea area, in part due to their relatively low spatial resolutions. This may bias its climatic impacts and introduce errors in the Caspian Sea water budget (Arpe et al., 2019; Nandini-Weiss et al., 2020). Previous studies have employed global or regional climate models to understand the influence of changing Caspian Sea surface areas on regional and large-scale climate. Using a regional climate model, Tsuang et al. (2001) and Nicholls and Toumi (2014) examined the impacts of the presence of the current Caspian Sea area (when compared to no-Caspian Sea) on seasonal precipitation and atmospheric circulation patterns. Their findings suggest that the presence of the Caspian Sea leads to significant changes in surface temperatures over the Caspian Sea, which increase in winter and decrease in summer. In particular, decreases in summer temperature, due to higher air density, influence the atmosphere via changes to geopotential height extending to the top of the troposphere, and zonal winds, leading to a stronger summer jet stream over western Asia. However, these studies did not investigate how the size of the surface area of the Caspian Sea may impact climate explicitly.

On the other hand, using a global climate model, Arpe et al. (2019) examined the impacts of different Caspian Sea areas and found that changes in evaporation over the sea were linearly related to Caspian Sea surface area. They also found an increase of precipitation with in the Caspian Sea catchment area, partly compensating the impact of increased evaporation for the water budget of the Caspian Sea. Interestingly, they found that variations in Caspian Sea surface area had an impact on the large-scale atmospheric circulation as far as the northern Pacific. However, their results may be affected by low resolution (T63), which limits the actual representation of the Caspian Sea area and the topography around the Caspian Sea. In addition, prescribed sea surface temperatures were used for the global ocean, with the aim to focus more on the direct impact of the Caspian Sea area, which may limit the large-scale response to Caspian Sea area variation.

The above studies suggest that the Caspian Sea may have regional and remote effects on climate. However, there remain open questions about the manner and magnitude of the climatic feedbacks from realistic variations in Caspian Sea surface area. Here, we apply a new modelling approach, involving a global state-of-the-art climate model and a hydrological routing model, to constrain the impacts from major surface area changes of the Caspian Sea that are known to have occurred during the late Quaternary period. We use our modelling approach to investigate catchment-scale and large-scale effects of varying Caspian Sea surface areas on hydroclimate, lake level and atmospheric circulation.

3.2 Methodology and data

In this section, we describe the modelling methodology used and the data analysis performed. Firstly, we designed four scenarios of different Caspian Sea size (large, small, current and no Caspian) used to drive the Earth-system model CESM1.2.2 (Hurrell et al., 2013) to simulate the climate response. The large and small Caspian Sea scenarios are chosen to represent two cases of extreme Caspian Sea area change (as discussed in §3.1) that occurred during the paleao period, and the current Caspian Sea scenario is selected to evaluate the effect of having a 'realistic' Caspian Sea extent that represent present day area. Though the Caspian Sea has never fully desiccated since its formation, the no-Caspian Sea scenario is chosen as one of the scenario (and used as a reference) to evaluate the effect of including a Caspian Sea in a model as numerous climate models either not properly prescribe or ignore Caspian Sea.

Secondly, we examined the regional catchment anomalies in atmospheric water budget (precipitation - evaporation; P-E), surface air temperature and vertically integrated lower level (> 850 hPa) water-vapour flux of large, current and small Caspian scenarios with respect to no-Caspian Sea. The water-vapour flux was inferred from vertically integrated water-vapour transport calculated by integrating the zonal and meridional moisture fluxes via each atmospheric layer between 1000 hPa and 850 hPa. This variable is used as a measure of the horizontal transport of atmospheric moisture (Sousa et al., 2020). Thirdly, we repeated this for large-scale changes (sub-tropical jet stream, geopotential height and sea level pressure). Finally, we performed stand-alone numerical simulations of Caspian Sea level using the

Hydrological Routing Algorithm model (THMB; Coe, 1998, 2000) with climate forcing from the four scenarios in order to assess the feedback between Caspian Sea surface area change and its water budget. Statistical analyses on all four simulations include annual mean and seasonal plots of winter (December, January, February-DJF), spring (March, April, May-MAM), summer (June, July, August-JJA) and autumn (September, October, November-SON). The statistical significance of seasonal and annual mean differences was estimated using a two–tailed Student t-test with 95% confidence level.

3.2.1 CESM1.2.2 model experimental design

CESM is a fully coupled global climate model composed of five separate models simulating the Earth's atmosphere (Community Atmosphere Model, CAM5), ocean (Parallel Ocean Program, POP2), land (Community Land Model, CLM4.0), rivers (River Transport Model, RTM) and sea-ice (Community Sea Ice Model, CICE), plus one central coupler component (Hurrell et al., 2013). In this model version, the Caspian Sea is set up to be part of the ocean model component as a marginal sea. The atmosphere and land components are set to 0.9° latitude by 1.25° longitude horizontal resolution. The atmosphere component has 30 vertical levels, whereas, the ocean component has 60 vertical levels. Both ocean and sea ice components use a horizontal grid mesh of 384 by 320 cells. The total runoff from the land surface model is routed by the river transport model to either the active ocean or marginal seas which enables the hydrologic cycle to be closed (Branstetter, 2001).

Evaluation of the model version used in this study (1° version of CESM1.2.2) and a 2° version model with two different atmospheric physics components (CAM4 and CAM5), has been carried out previously in Nandini-Weiss et al. (2020). According to their results, the higher resolution model with the improvements to atmospheric physics performance was considerably better over the Caspian Sea region than the other versions, when considering surface air temperature, precipitation, and evaporation, as well as NAO teleconnections. Orography-based biases were also smallest in this version, and over all the 1° CAM5 model was deemed to have a sufficient level of skill in modelling climate in the region of the lake.

Four numerical sensitivity experiments were carried out at the North German Supercomputer HLRN3. Each simulation had pre-industrial (1850s) climate boundary conditions as this is a

standard baseline reference for most climate modelling runs. At the pre-industrial the levels of atmospheric greenhouse gases are assumed to be minimally altered by anthropogenic emissions, enabling the pre-industrial scenario to be compared to future anthropogenic or palaeo simulations, or other changes to boundary conditions. The four simulations only differ in the CS prescribed areas. Readers are advised to refer to the supplementary file, Fig. S6.6, showing the representations of Caspian Sea size for each scenarios in the ocean and land components of the CESM1.2.2 model.

Table 3.1. CESM model components and compset used in this study. We used a component set configured for pre-industrial boundary conditions, which reflects land use/cover conditions consistent with 1850.

Compset
Name: B_1850_CAM5_CN (Pre-industrial)
Boundary condition: pre-industrial
Physics: cam5 and clm4.0
NB: clm4.0 with carbon nitrogen cycle, prognostic CICE and POP2 default

3.2.2 CESM Caspian Sea areas and input data preparation

The three Caspian Sea surface areas (large, current and small; Fig. 3.1) correspond to lake levels of 0 m, -28 m and -90 m above mean sea level, respectively, and were determined using a 1 arc minute ETOPO1 Digital Elevation Model (DEM) (Amante and Eakins, 2009) and spatial analysis tools in ArcGIS 10.5.1. The resultant Caspian Sea areas were overlain onto the CESM default ocean domain file in order to identify and modify the land and ocean grid points. If the water level of a grid point (ocean grid cells) was lower than the mean bathymetry of the grid, the grid cell is set to be land. The large Caspian simulation is actually the default CESM pre-industrial simulation, which includes a Caspian Sea surface area that is larger than the present-day area.

Based on the new Caspian Sea areas, the CESM ocean bathymetry was modified for the changes made to land/ocean areas. Next, new surface-flux mapping files were generated with the NCAR Paleo toolkit software to prepare all input files, which were interpolated onto the same domain. For all four scenarios, we extrapolated the surface properties of the nearest neighbour grid cell to the new land grid cells (e.g. plant functional types and soil properties).

The land properties were recalculated for each scenario. The CESM simulations were spun up for 100 years (initialized from a standard pre-industrial control state) and the last 50 years were taken for analysis in our sensitivity study. In this study, we examined differences between all simulations with respect to a no-Caspian Sea scenario.

3.2.3   The hydrological model: THMB

The hydrological model THMB (which was formerly called HYDRA, Hydrological Routing Algorithm; Coe, 1998) was used to simulate the level of the Caspian Sea based on the outputs from the CESM climate simulations with the aim to validate the P-E that the climate model produced over the Caspian Sea drainage area. In this study the THMB hydrological model is a routing scheme and there is no transform function that converts precipitation to runoff. Therefore, the aim is to evaluate if THMB, when it is routing P-E (runoff), produces the correct Caspian Sea level, and if the water balance is right. For detailed information about THMB, readers are advised to refer to Coe (1998). Four offline simulations of the Caspian Sea level were performed using input boundary conditions derived from the large, current, small, and no-Caspian Sea climate simulations. The mean monthly climatology averaged over the last 50 years of the climate simulations was used to drive the THMB simulations. The THMB model simulations were spun up for 1000 years.

THMB simulates hydrological processes as a linked dynamic system in which locally derived runoff is transported across the land surface in rivers, lakes and wetlands, and is finally transported to the ocean or an inland lake (Coe, 1998, 2000). The model is forced with estimates of runoff over land, and precipitation and evaporation over sea, in a hydrologic network linked to a linear reservoir model (Eq. 3.1). The linear reservoir model (river water reservoir (Wr), surface runoff pool (Ws), and subsurface drainage pool (Svendsen et al.) simulates water transport based on prescribed local drainage directions derived from the local topography, residence times of water within a grid cell, and effective flow velocities, given in equation 3.1:

$$\partial[W_r]/\partial t = [W_s/T_s + W_d/T_d] * [1 - A_w] + [P_w - E_w] * A_w - [W_r/T_r] + \sum F_{in} \quad [3.1]$$

where A_w is the predicted fractional water area in the grid cell; T_s, T_d, and T_r are the residence times (s) of the water in each of the reservoirs; P_w and E_w are the precipitation and evaporation rates (m^3s^{-1}) over the surface water, respectively; and F_{in} is the water flux from the upstream cells (m^3s^{-1}). For the case of small and no-Caspian Sea scenarios, where considerable areas were changed to land, we used a simplified Penman-Monteith equation (Allen et al., 1998; Peixoto and Oort, 1992) to estimate potential evaporation over areas that THMB simulates as water, rather than using the climate modelled actual evaporation (over land points). Therefore, we used potential evaporation for E_w (over water) in equation 3.1 rather than actual evaporation in order to simulate Caspian Sea level with THMB. This approach assumes that actual and potential evaporation over a water body are effectively equal, and it was chosen in order to account for the increases in evaporation that would be expected if the Caspian Sea area increases during the simulation. If this is not accounted for then the volume of water in the small-CS and no-Caspian Sea scenarios would keep increasing until overflowing into the neighbouring drainage basin (Black Sea, the sill height is 40 m above sea level) because the prescribed evaporation rate from the Caspian Sea is too small (as it would be taken from land grid cells). Potential evaporation provides a more realistic estimate of E_w over areas that convert from land to water during the course of the THMB simulation.

3.3 Results

3.3.1 The impact of Caspian Sea surface area on regional climate

Here we present the impacts of varying Caspian Sea area on surface water budget (evaporation and precipitation), Caspian Sea level, lower level vertically integrated water-vapour transport (IVT), and 2-m air temperature (T2m). All results presented below are based on monthly climatological model output.

Our findings show that the variation of Caspian Sea area has a strong influence on the regional climate. Across the four scenarios evaporation increases as the Caspian Sea surface area increases (Fig. 3.2a). The mean annual evaporation increases up to ~400% over Caspian Sea and ~50% over the Caspian Sea catchment (over land and lake surface) for the BC scenario compared to no-Caspian Sea (Fig. 3.2b). Increases in evaporation across the Caspian Sea

catchment area directly follow from the increase in surface area of the Caspian Sea itself. The annual mean evaporation anomaly over the wider Caspian Sea catchment area is predominantly higher when a Caspian Sea is present than with the no-Caspian Sea scenario (more than 3 mmday^{-1} in places) (Fig. 3.3a, e, i). Higher evaporation over the Caspian Sea is more pronounced during the autumn and winter seasons (Fig. S6.7). This is because of greater thermal inertia resulting from higher heat capacity plus lower albedo of the lake compared to bare land surface. More heat (energy) is stored during spring and summer, which is released later during autumn and winter, leading to a warmer surface, lower atmospheric stability, and higher evaporation.
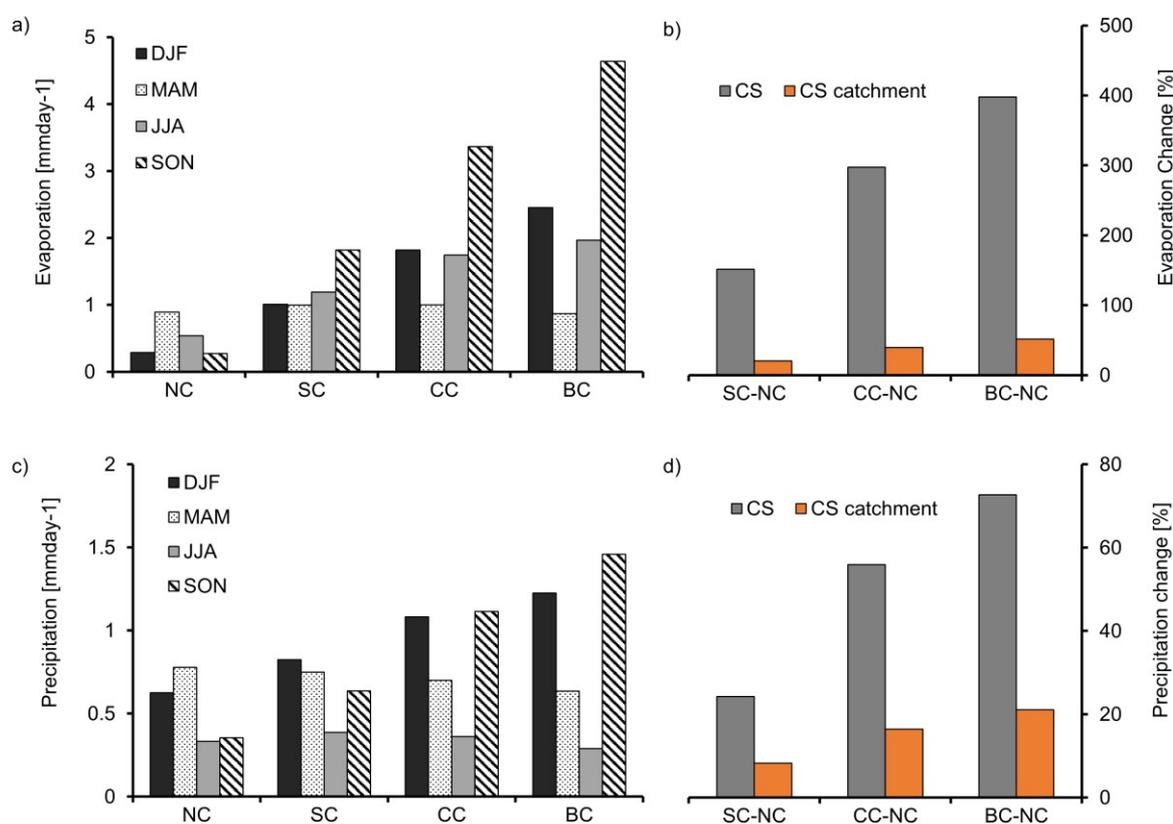
Figure 3.2. a) Mean seasonal evaporation over Caspian Sea surface area, b) mean annual percentage change of evaporation relative to no-Caspian Sea scenario over Caspian Sea surface area (in grey) and Caspian Sea catchment (in orange), c) same as 'a' but for precipitation, and d) same as 'b' but for precipitation. Area of interest considered for calculation: large Caspian Sea (referred in the figure as 'CS') and Caspian Sea drainage basin

including land and water surfaces (referred in the figure as 'CS catchment'). (Key: BC – Large Caspian Sea, CC – Present-day Caspian Sea, SC – small Caspian Sea, NC – No-Caspian Sea, DJF – December/January/February, MAM – March/April/May, JJA – June/July/August, SON – September/October/November).

The changes in Caspian Sea surface area contribute considerably to precipitation distribution and intensity (Fig. 3.2c, d; 3.3b, f, j; S6.8). The mean annual precipitation increases with a larger Caspian Sea area by up to ~70% over the Caspian Sea and ~20% over the Caspian Sea catchment (over land and lake surface) for BC compared to no-Caspian Sea scenario (Fig. 3.2d). The largest precipitation anomalies (greater than 1 mmday^{-1}) occur over the south-western part of Caspian Sea. The two possible primary reasons for higher precipitation in the south-western part of Caspian Sea are the amount of evaporation available over the sea (which depends on the size of the sea and the length of air flow over sea to pick up moisture, i.e. fetch) and lower level easterly winds driving vapour flux in south-western direction (Fig. 3.3d, h, l) towards the Caucasus and Elburz mountains (Arpe et al., 2019). Significant, though smaller, changes in the annual mean precipitation (< 0.5 mmday^{-1}) are observed over most parts of the Caspian Sea catchment area, which can be linked to the combined effect of lower level easterly wind driving the moisture flux and larger scale circulation processes. Seasonal changes of precipitation have a similar spatial pattern to changes in evaporation during autumn and winter (Fig. S6.8), partly compensating for the water loss from the Caspian Sea due to evaporation. The presence of a Caspian Sea produces more precipitation over the sea in autumn and winter (more than 2 mmday^{-1}), but less precipitation over sea in spring and summer when surface cooling tends to stabilize the atmosphere (Fig. 3.2c, S6.8). This indicates that winter and autumn precipitation changes dominate the annual mean anomalies. Although changes in precipitation tend to follow evaporation during autumn and winter, the changes are not linearly related throughout the year.

The enhanced evaporation over the Caspian Sea in autumn leads to increased moisture in the atmosphere. This not only increases the precipitation over the Caspian Sea itself but also the land around the Caspian Sea. This has a consequence for evaporation in these areas. Arpe et al. (2020) hypothesized that with strong westerlies the enhanced moisture in the atmosphere might be blown to the east and lost from the water budget of the Caspian Sea

leading to a drop of the Caspian Sea level and increase in the water levels of central Asian lakes.

The magnitude of the surface water budget (P-E) varies with Caspian Sea surface area, both over the sea itself and the wider catchment (over land). P-E anomalies are negative over the Caspian Sea since the evaporation increase greatly exceeds the precipitation increase over the sea surface (Fig. 3.3c, g, k, S6.9). P-E anomalies are positive over the land surface, where precipitation anomalies exceed the evaporation anomalies. These changes (greater than 3 mmday^{-1} over Caspian Sea) are more pronounced during autumn and winter seasons when the precipitation and evaporation changes are greater (Fig. S6.9). The mean P-E over the Caspian Sea catchment (land and lake surface) decreases as Caspian Sea surface area increases, which indicates negative lake surface-evaporation feedback domination (Fig. 3.4a). Changes in P-E would have direct impacts on Caspian Sea level. As a closed drainage basin, variation of Caspian Sea surface area strongly influences Caspian Sea level change, as the amount of evaporation is positively related to changes in sea surface area. Based on offline Caspian Sea level simulations with THMB using input boundary conditions from Caspian Sea climate scenarios, the simulated Caspian Sea levels were ~27.5 m and ~25.25 m below mean sea level for current and large Caspian Sea scenarios respectively. Prescribing the correct current Caspian Sea area in CESM produces a Caspian Sea level that is closer to the mean present-day observed sea level. The default representation of the Caspian Sea in CESM (BC scenario) produced a Caspian Sea level of ~2 m above the current observed state. The simulated Caspian Sea level for small and no-Caspian Sea scenarios were ~75 m and ~138 m below mean sea level.
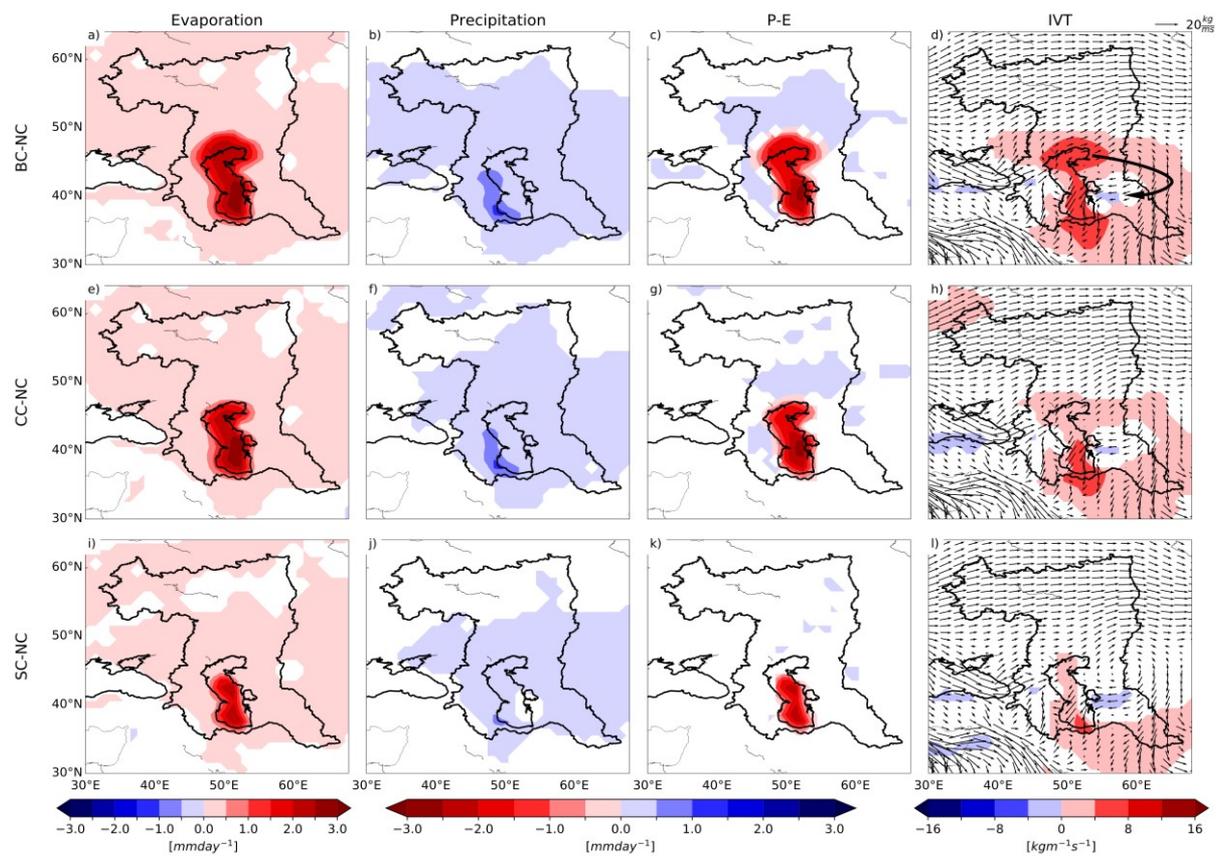
Figure 3.3. Annual mean changes for evaporation (a, e and i), precipitation (b, f and j), P-E (c, g and k) and lower level (1000 – 850 hPa) vertically integrated water vapour transport (IVT) (d, h and l) for large, current and small Caspian Sea with respect to no-Caspian Sea scenario. The shaded colours are areas where mean anomaly is different from zero at 95% confidence level. The IVT is calculated by integrating the zonal and meridional moisture fluxes. The vector field are not anomaly values, but actual values of IVT for BC (d), CC (h) and SC (l).

To understand the drivers of moisture transport that contribute to changes in water balance we investigate lower level IVT (> 850 hPa). The vector fields represent the actual amount of IVT, whereas the colour plot are the anomalies of IVT values with respect to no-Caspian Sea (Fig. 3.3d, h, l). The moisture flux increases with larger Caspian Sea area. Lower level wind patterns over the Caspian Sea and the eastern part of the Caspian Sea catchment form an anti-cyclonic pattern and this plays vital role in transporting moisture generated over the Caspian Sea, as well as from the eastern part of the catchment area (Fig. 3.3d). The easterly surface winds (from Kazakhstan and Turkmenistan) shift direction to the south-west around the western Caspian Sea catchment area and this contributes significantly to the

moisture flux directed towards the south-western parts of Caspian Sea. The effect of westerly winds on the north Caspian Sea is enhanced with larger Caspian Sea area, as more water is available for evaporation in the north Caspian Sea.

Changes in Caspian Sea area also play a significant role in air temperature change over the Caspian Sea and surrounding region. The results reveal strong responses in the regional annual mean T2m, where temperature significantly decreases (more than 3 °C) over Caspian Sea. Larger Caspian Sea areas induce increases (decreases) in T2m during autumn and winter (spring and summer) seasons (Fig. 3.4b and S6.10). Seasonal variation of T2m for larger Caspian Sea clearly show significant decrease over and around the Caspian Sea, predominately during spring and summer time (Fig. S6.10 b, c, f, g, j, k), when the amount of solar radiation received during this time is higher compared to other seasons. Coincidentally, the summer sea surface temperatures over the southern Caspian Sea basin drop from 23.37°C (SC) to 21.21°C (CC) to 20.96°C (BC). This is as previously found by Arpe et al. (2019), who indicate that the expansion of the shallow northern part of the lake enhances evaporation, which leads to an enhanced loss of energy within the Caspian Sea. This then causes a decrease of the sea surface temperature in summer for the Caspian Sea as a whole.
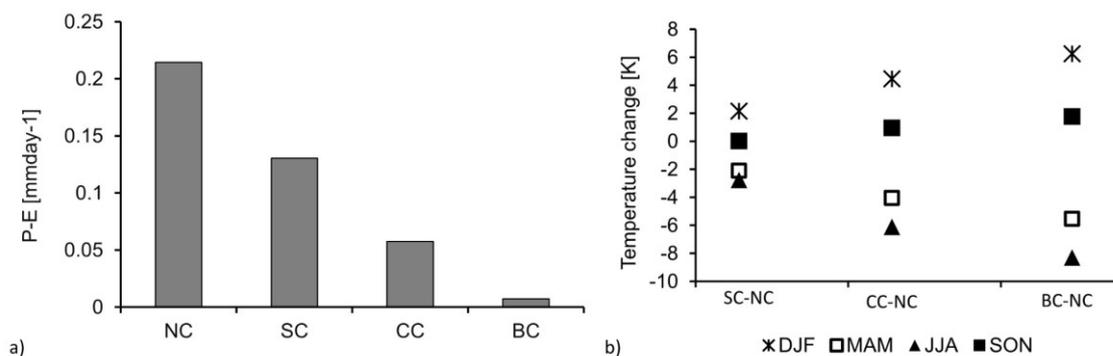
Figure 3.4. a) Mean P-E over Caspian Sea catchment, and b) mean seasonal 2-m temperature (T2m) changes with respect to the no Caspian scenario over Caspian Sea surface areas. Area of interest considered for calculation: drainage basin including land and water surfaces (for 'a') and large Caspian Sea (for 'b'). Abbreviations as in Fig. 3.2.

3.3.2 The impact of Caspian Sea area variation on large scale climate

The results of this study show that the presence of different Caspian Sea areas affect large-scale climate over the entire northern hemisphere. Annual changes show significant warming (>1 °C) in surface air temperatures extending in a north easterly band over the northern catchment area and as far as east Siberia and north-west Pacific (Fig. 3.5a, b, c). The warming over the north-west Pacific increases from the small to large Caspian Sea scenarios when compared with the no-Caspian Sea scenario (Fig. 3.5a, b, c). Also, it appears that temperature changes are restricted in southern Caspian Sea by the Elburz Mountains, which was also noted by Nicholls and Toumi (2014) and Arpe et al. (2019). The surface temperature anomaly patterns appear more spatially extensive when compared to precipitation where annual mean changes appear more focused on the regional surroundings of the Caspian Sea catchment area (Fig. 3.5d, e, f). Upon examining the large-scale changes in sea level pressure as Caspian Sea area increases, higher pressures are seen extending from the Mediterranean towards southern Caspian Sea (anomalies of up to 125 Pa) (Fig. 3.5g, h, i).

The zonal winds at 200 hPa show changes in the jet stream, which plays a key role in distributing moisture, heat, and pressure across this region (Fig. 3.5j, k, l). The results indicate a north-south dipole anomaly in the jet stream pattern with a decrease in speed over the northern and central Caspian Sea catchment area which extends in an easterly band across Asia and the north-west Pacific and decreases as Caspian Sea area increases. The jet speed increases as Caspian Sea area increases over the southern Caspian Sea catchment area. In order to understand the influence of different Caspian Sea areas on the mid tropospheric flow, we investigated changes in geopotential height and temperature at 500 hPa (Fig. 3.6). Results show that annual mean temperatures (at 500 hPa) are associated with corresponding changes in geopotential height resulting in a weakening of the 500 hPa troughs over the northern Pacific as Caspian Sea area increases (Fig. 3.6d, e, f). There is a significant link between decreases in temperature at 500 hPa and the reduction in geopotential height over the southern Caspian Sea catchment area.
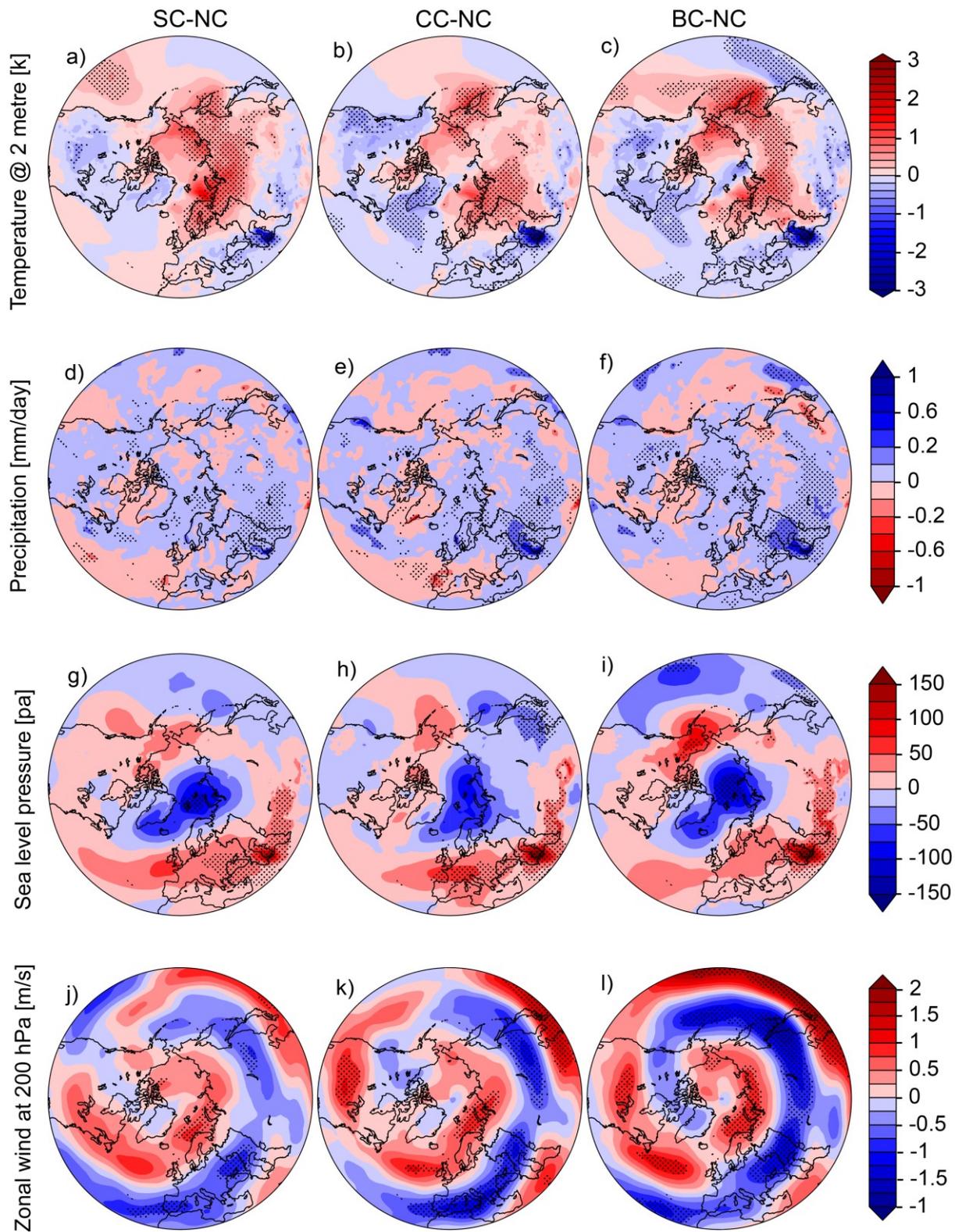
Figure 3.5. Annual mean changes of 2-m temperature (a, b and c), precipitation (d, e and f), sea level pressure (g, h and i) and zonal wind (j, k and l) at 200hPa showing changes in the jet stream for small Caspian (SC), current Caspian (CC) and big Caspian (BC) with respect to

no-Caspian (NC). Stippling indicates regions where the change is statistically significant at the 95% level based on a Student's t-test.
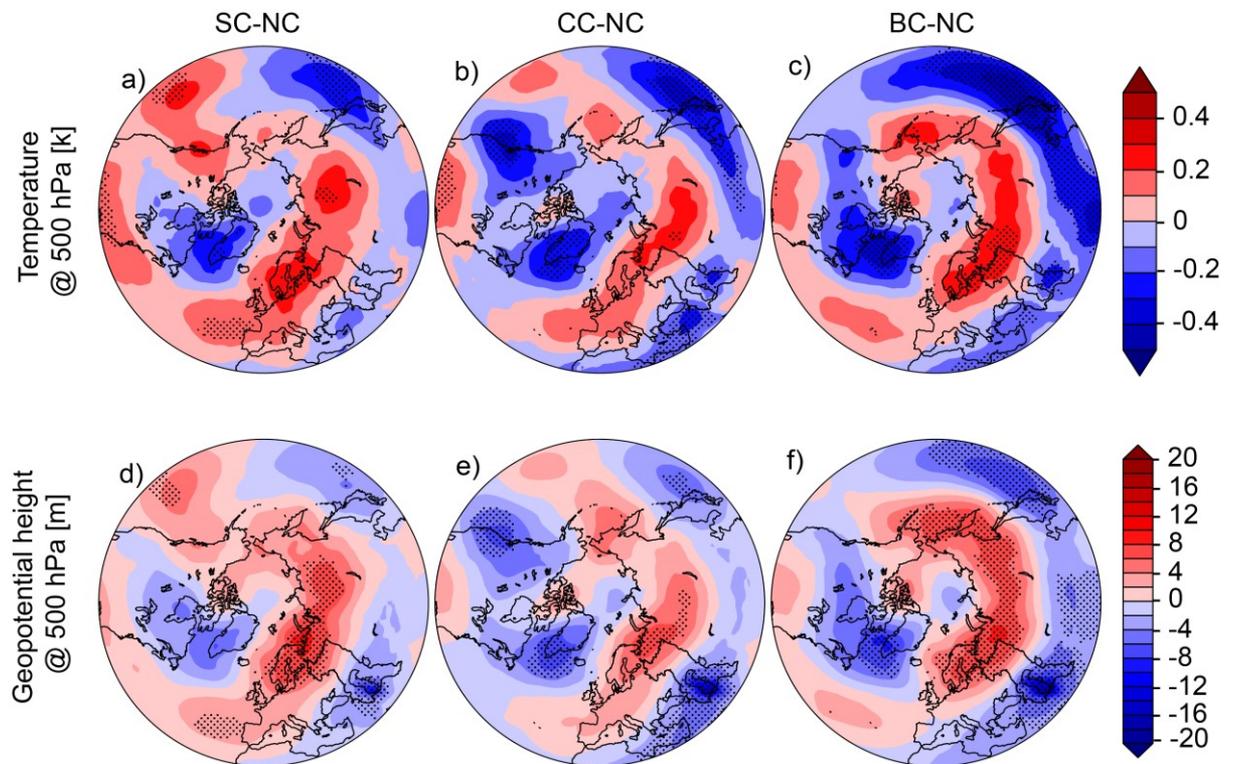
Figure 3.6. Same as Fig. 3.5 but for temperature (a, b and c) and geopotential height (d, e and f) at 500 hPa.
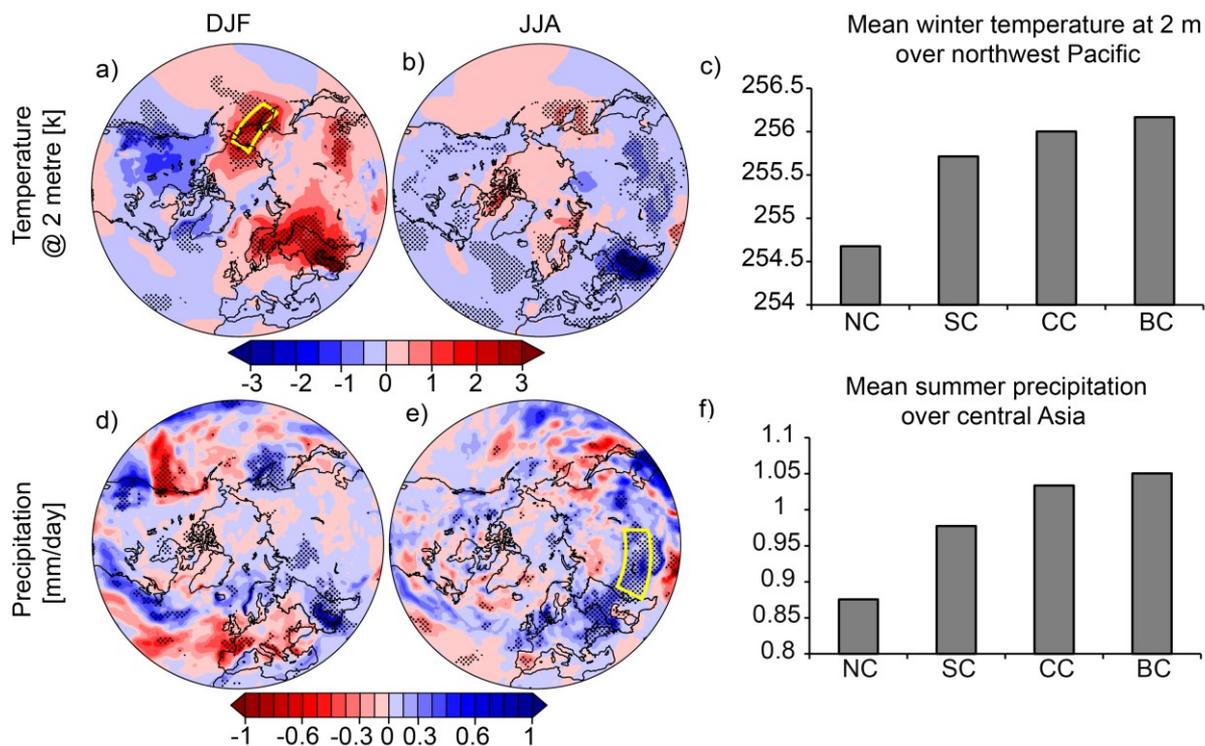
Figure 3.7. Winter and summer changes of 2-m air temperature (a and b respectively) and precipitation (d and e respectively) for current Caspian Sea minus no-Caspian Sea scenario. Mean winter 2-m temperature (c) averaged over north-west Pacific region [51-72°N and 155-187.5°E] (yellow box area), and mean summer precipitation (f) averaged over central Asia region [39-50.5N and 62.5-100E] (yellow box area) for the four Caspian Sea surface area change scenarios. Stippling indicates regions where the change is statistically significant at the 95% level based on a Student's t-test. Abbreviations as in Fig. 3.2.

The seasonal results provide further insight into the processes by which different Caspian Sea sizes influence large-scale climate over the entire northern hemisphere. Here, we only consider winter and summer changes and take the current Caspian Sea scenario (compared to no-Caspian Sea) as an example. For examining the seasonal changes for other Caspian Sea sizes, the reader is directed to the supplementary figures (Fig. S6.11 and Fig. S6.12), and these can be compared to the mean climatologies presented in Fig. S6.13 and Fig. S6.14. The most striking and significant seasonal feature is the intense warming during winter for air temperatures over the Caspian Sea and the northern catchment area, which extends as far afield as the north-west Pacific (Fig. 3.7a). By comparison, the summer reduction in temperatures is restricted to the Caspian Sea catchment area (Fig. 3.7b). The mean winter

temperature over the north-west Pacific region [51-72°N and 155-187.5°E] is calculated for all Caspian Sea scenarios (Fig. 3.7c). Generally, the warming increases from no-Caspian Sea to large Caspian Sea area. On the other hand, the winter increase in precipitation is mostly restricted to the Caspian Sea region (Fig. 3.7d; compare to Fig. S6.13 for the mean climatologies). However, the summer increases over central Asia are of interest (>0.6 mm/day). Arpe et al. (2020) discuss the possibility of enhanced evaporation to transport moisture to the central Asian lakes where it is enhancing the precipitation; a process suggested here also (Fig. 3.7e). When examined over the central Asia region [39-50.5°N and 62.5-100°E], precipitation tends to broadly increase for all simulations compared to the no-Caspian Sea scenario (Fig. 3.7f). This increase in summer precipitation over central Asia may be driven by the associated changes seen previously in surface winds, moisture flux, and the lake effects of the Caspian Sea which transports moisture afield. However, this merits further investigation.

The winter sea level pressure anomalies show an east-west dipole over the Caspian Sea catchment area and low pressure anomalies over the north-west Pacific (and Siberia), and high-pressure anomalies over Europe (and northeast Pacific) (Fig. 3.8a). However, during summer high-pressure anomalies are seen over the Caspian Sea, southern catchment area, and central Asia region (anomalies of up to 160 Pa) (Fig. 3.8b).

The presence of different Caspian Sea sizes affects the mid (500 hPa) and upper (200 hPa) tropospheric circulation patterns. We firstly examined winter and summer changes for the geopotential height and the location of the jet stream by investigating the zonal winds at 200 hPa (Fig. 3.8e,f; compare to Fig. S6.14 for the mean climatologies). The seasonal responses of both to the presence of different Caspian Sea areas during winter and summer illustrate high seasonal differences, especially in the structure of the subtropical jet stream (Fig. 3.8e, f). Reduced summer surface temperatures (Fig. 3.7b) trigger a reduction in the summer geopotential height (~28m) (Fig. 3.8d) and a large-scale southward shift of the jet stream (Fig. 3.8f) that was also observed in the annual mean anomalies. A possible explanation for this shift in the jet stream (also seen in Nicholls and Toumi, 2014) arises from changing horizontal temperature gradients between warm and cold regions that influence the westerlies. Signals from surface temperature may propagate up to higher atmospheric levels, affecting the

geopotential height. The above summer relationship is consistent at the 500 hPa level as well (Fig. 3.8g-l).

Finally, we find that teleconnections in the large-scale atmospheric circulation significantly influence sea-ice conditions in the remote North Pacific and Arctic. As Caspian Sea area increases, there is a reduction in sea-ice around the North Pacific (Okhotsk Sea, Fig. 3.9). This region has a particularly robust trend in sea-ice retreat as Caspian Sea area increases. The impact is primarily in the winter months (the area is not sea-ice covered in summer; see Fig. S6.14). With reduced sea-ice extent during winter as Caspian Sea area increases, the lower atmosphere is exposed to large upward sensible heat flux anomalies (not shown) from the relatively warm ocean, producing a positive feedback that amplifies the initial change. This highlights the importance of performing coupled ocean-atmosphere modelling in order to capture relevant feedbacks in the climate system. It also hints at potential implications that are pertinent for human activities around the Arctic if large changes in Caspian Sea area occur in the future (Nandini-Weiss et al., 2020).
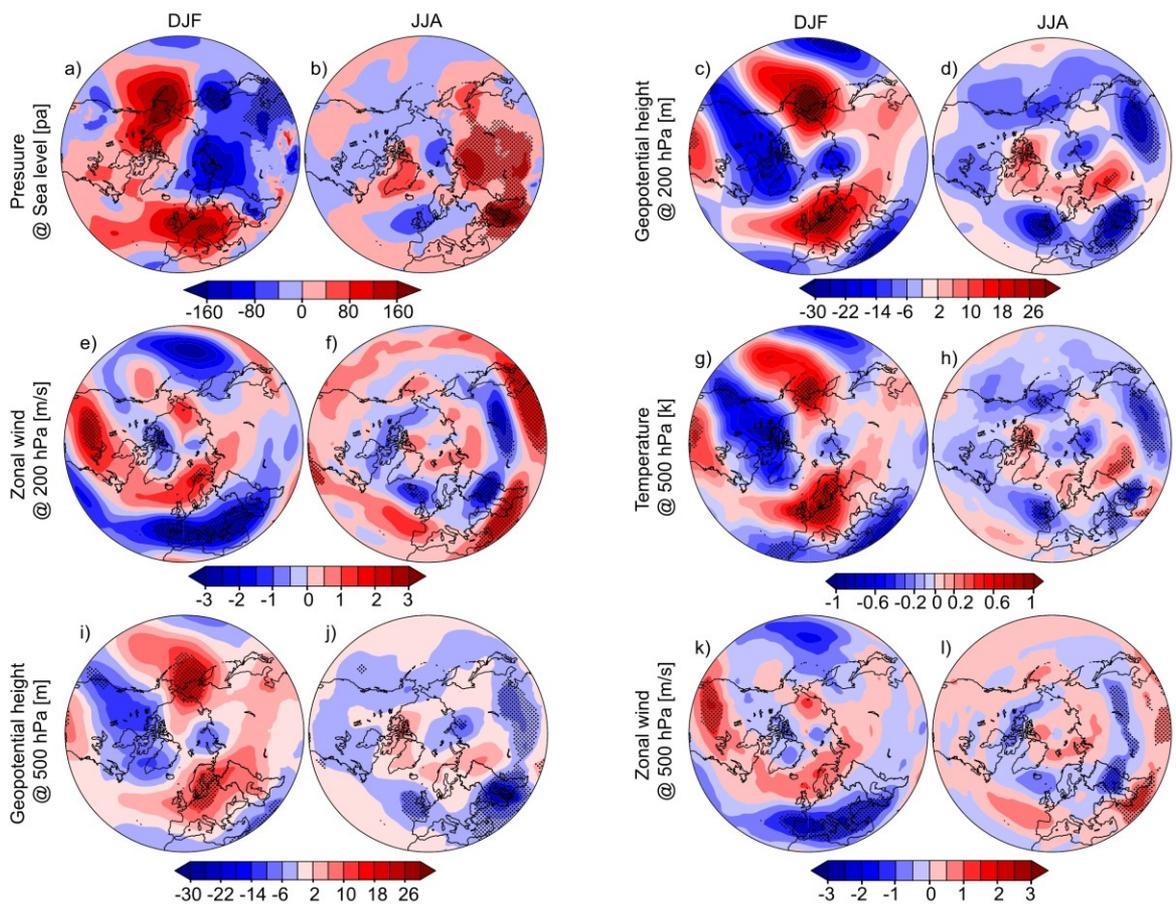
Figure 3.8. Winter and summer changes of sea level pressure (a and b), geopotential height at 200 hPa (c and d), zonal winds at 200 hPa showing changes in the jet stream (e and f), temperature at 500 hPa (g and h), geopotential height at 500 hPa (i and j), and zonal winds at 500 hPa (k and l) for current Caspian Sea minus no-Caspian Sea scenario. Stippling indicates regions where the change is statistically significant at the 95% level based on a Student's t-test. Abbreviations as in Fig. 3.2.
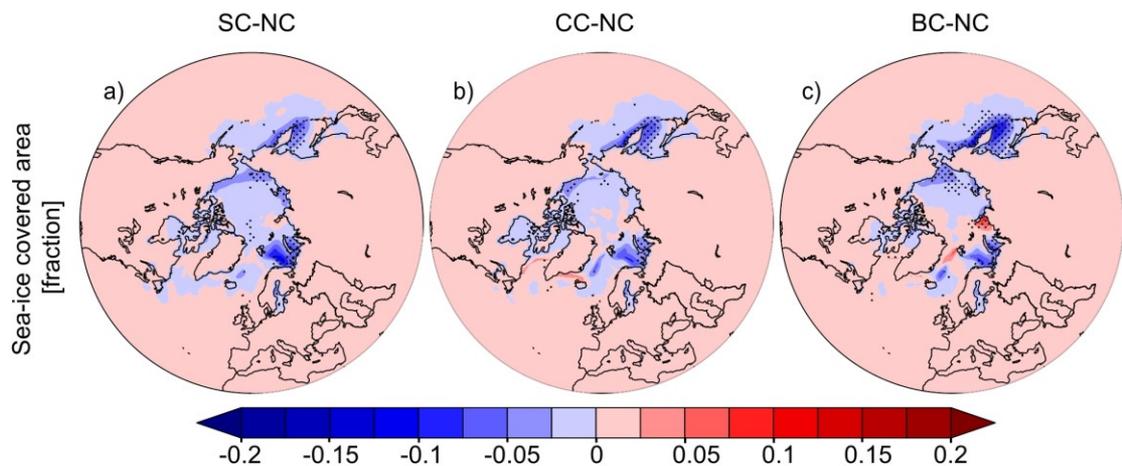
Figure 3.9. Annual mean changes in sea-ice covered area (%) for (a) small Caspian (SC), (b) current Caspian (CC) and (c) big Caspian (BC) with respect to no-Caspian (NC). Stippling indicates regions where the change is statistically significant at the 95% level, with significance levels estimated using a Student's t-test.

3.4 Discussion

The results seen in this study confirm that variations in the surface area of the Caspian Sea affect the climate in the regional catchment area and large-scale circulation patterns in the northern hemisphere. We note that both precipitation and evaporation increase (decrease) with a larger (smaller) Caspian Sea area, since a larger Caspian Sea produces and contributes more moisture to the atmosphere in this region compared to a smaller (no) Caspian Sea, particularly during late autumn–early winter, when cold, dry air masses pass over the relatively warm Caspian Sea, given the high heat capacity of the lake. Our study also confirms that evaporation plays a significant role on Caspian Sea level variability in a closed basin like

Caspian Sea. This is similar to findings by Chen et al. (2017a), although their study did not include the compensating effect of precipitation when considering the impact of a warmer climate on Caspian Sea level, and so they potentially overestimated a lowering of Caspian Sea level due to warming. Enhanced precipitation in the south-west of the Caspian Sea is clearly seen in our study. This contradicts a previous study by Arpe et al. (2019) possibly due to the lower horizontal resolution in their experiments and its influence on the representation of topography in that more mountainous area; but agrees with a regional climate modelling study by Nicholls and Toumi (2014) and a study by Tsuang et al. (2001).

The changes in precipitation during winter tend to follow evaporation. However, the changes are not linearly related throughout the year (similar to Nicholls and Toumi, 2014). Also, the magnitude of precipitation change is less than evaporation (~20% increase in precipitation over the Caspian Sea catchment compared to ~50% increase in evaporation for large Caspian Sea relative to no-Caspian Sea). Our study shows evaporation and precipitation are lowered during spring by the presence of the Caspian Sea (comparable to Lofgren, 1997; Nicholls and Toumi, 2014; Notaro et al., 2013). A partial explanation for this lies in the contrasting seasonal thermodynamics (and thermal inertia of the sea) and atmospheric moisture recycling. The summer atmospheric moisture recycling and distribution is known to play a key role in changing the regional climate (and convective instability). The amount of atmospheric moisture available is driven by the temperature difference between surface atmosphere and sea surface as well as surface easterly winds, and this relationship changes upon a given Caspian Sea area. However, quantifying this relationship is quite complex and merits future investigation, as it is not within the scope of this study.

The change in precipitation and evaporation plays a vital role in the variability of the Caspian Sea level as the area of the Caspian Sea changes. The cumulative change in P-E is significant over the Caspian Sea as the amount of evaporation exceeds precipitation for larger Caspian Sea, but over the whole Caspian Sea catchment area the change is not as significant. This has implications for the variability of Caspian Sea level. The relationship between the Caspian Sea level and P-E is complicated by the fact that changes in the Caspian Sea area is not directly proportional to the change in Caspian Sea level. A drop of Caspian Sea level reduces the Caspian Sea area and the total evaporation, which in turn affects the amount of

water vapour in the atmosphere. Based on Caspian Sea level offline simulations with THMB, we find significant Caspian Sea level change when the Caspian Sea area is very large or small compared to the current Caspian Sea. In both cases, the runoff contribution from the Caspian Sea catchment area and precipitation over the Caspian Sea fail to balance evaporation over the sea, which results in either an increase or decrease in the Caspian Sea level. More specifically, the resulting Caspian Sea level in the THMB simulations is always closer to the present-day Caspian Sea level than to the prescribed Caspian Sea level in the corresponding CESM simulation for large and small Caspian Sea. This points to a negative feedback between Caspian Sea surface area (or Caspian Sea level) and catchment-scale hydroclimate (i.e. water budget). Although precipitation in the south-western Caspian Sea increases with increasing Caspian Sea level (a positive feedback), the well-known negative lake surface-evaporation feedback still dominates. The feedbacks between the changes in Caspian Sea level and the atmospheric water budget could be further examined and quantified by incorporating an interactive lake component with variable Caspian Sea area within the climate model itself.

Another key interest in this study is the impact of the changing Caspian Sea areas on geographically remote regions in the northern hemisphere.

The enhanced impact of surface air temperatures extending as far as east Siberia and north-west Pacific during the winter. These temperatures increase based on larger area changes and vice versa and are relative to a no-Caspian Sea scenario. Enhanced warming over the north-western Pacific may be driven by changes in Caspian Sea area dependent air masses. During winter, a larger Caspian Sea area may lead to reduction in atmospheric stability due to Caspian Sea being warmer than the surrounding air temperatures (also seen from Nicholls and Toumi, 2014). Hence, the seasonal temperature anomalies may lead to atmospheric instability (implications on cyclogenesis), during winter and greater stability (anti-cyclogenesis) during summer (Arpe et al., 2019; Nicholls and Toumi, 2014). The temperature changes are linked to sea level pressure changes, which show similar patterns for the same region, highlighting surface temperatures as drivers of low-level atmospheric circulation. Typically, enhanced (warmer) surface temperatures initiate updrafts, with resultant effects on lowering sea level pressure. Moreover, the winter season around the Caspian Sea catchment area (relative to no-Caspian Sea scenario) is dominated by lower

pressure, stronger low-level winds, and increased moisture (enhanced temperature and evaporation changes).

A second relationship of interest focuses on the enhanced impact of precipitation in the central Asia region during summer. This increase (as Caspian Sea increases) in precipitation may be driven by enhanced moisture supply to the atmosphere from the evaporative lake surface, but also by the associated changes seen previously for surface winds and westerly winds, which transport moisture afield. The westerlies are stronger in winter but weakened westerlies during summer may pick up moisture over the sea and transport it towards the eastern dry plains near central Asia. Also, the generally westerly flow in winds is disturbed by the Caucasus Mountains and restricted by the Elburz Mountains in the south. During the summer, associated reduced surface temperatures and weaker westerlies are seen relative to the no-Caspian Sea scenario. Given this, it is particularly interesting that the summer precipitation increases as the Caspian Sea area increases.

A third key relationship focuses on the enhanced impact of temperature on tropospheric geopotential height and zonal winds resulting in a shift in the location of the jet stream, which influences circulation patterns. Here we discuss two aspects. Firstly, our results confirm the weakening of the 500hPa troughs (geopotential height) over the northern Pacific with increasing Caspian Sea area and vice versa. In the northern hemisphere, two frontal zones are well developed at the 500 hPa level, corresponding to strong thermal gradients. Heat sources can trigger stationary Rossby waves (Hoskins and Karoly, 1981) and a thermal response (changes in the temperatures at 500 hPa) may be the source for the wave pattern trigger seen for the geopotential height at 500 hPa. The second aspect relates to the southward shift in the location of the jet stream during summer. Different Caspian Sea surface area sizes influence the atmospheric circulation patterns high in the troposphere (up to 500 hPa and 200 hPa). Surface temperatures affect the geopotential height field in the upper atmosphere, which further impacts the zonal wind field due to the thermal wind relationship. Here, we note that the presence of different Caspian Sea areas affects the thermal gradient (under the geostrophic assumption), which drives the jet stream speed and location (also seen in Lofgren, 1997; Nicholls and Toumi, 2014). This summer relationship, where a surface thermal response triggers the reduction in geopotential height resulting in an enhanced dipole pattern

in zonal wind anomaly at 200 hPa, was seen in the regional modelling study by Nicholls and Toumi (2014). However, we have also tested this summer relationship at the 500 hPa level and confirm that the summer temperatures at 500 hPa indeed influence the reduction in geopotential height, which results in the same (but weaker) dipole pattern of the zonal wind anomaly seen previously at the 200 hPa level. It is also comparable with findings for the Great Lakes region (Lofgren, 1997), where a stronger meridional temperature gradient (intensified in the north and weakened in the south) leads to a poleward shift in the winter jet stream. This study agrees with the study of Nicholls and Toumi (2014), but here we expand on the understanding and inclusion of different realistic Caspian Sea areas, using a state-of-the art high-resolution coupled global climate model.

The large-scale impact of the Caspian Sea surface area, demonstrated in this study, has implications for global modelling of past and future climates. Paleoclimate simulations usually ignore changes in the Caspian Sea surface area in their boundary conditions. In such studies, either a present-day Caspian Sea surface area is assumed or the Caspian Sea surface area changes according to changes in the global sea level (a pragmatic but unrealistic approach since changes in the Caspian Sea level are independent of changes in the global sea level). Sometimes, paleoclimate modellers also simply remove the Caspian Sea from the boundary conditions. Since the Caspian Sea surface area has changed dramatically during Earth's history (Yanina, 2014), the wrong implementation of the Caspian Sea in paleoclimate simulations may introduce additional biases, in particular in the Caspian Sea catchment region, central Asia and the northern Pacific. The same holds for simulations of future climate change, since large changes of the Caspian Sea water budget and, hence, Caspian Sea level and Caspian Sea surface area have been projected. A recent study by Nandini-Weiss et al. (2020) suggested a Caspian Sea level decrease of 9 m (18 m) by the end of the 21st century for the RCP4.5 (RCP8.5) scenario.

Results shown here are from only one climate model and further multi-model studies could give different insights and possibly strengthen our findings. Furthermore, in the default version of the CESM a prescribed Caspian Sea area is used, in common with all other similar climate models. This affects realistic Caspian Sea moisture transports, which affects the atmospheric water budget, and reduces the potential for feedbacks between the climate and

Caspian Sea level. By performing idealized simulations of four Caspian Sea area changes, our findings aid in recognizing regional and large-scale climate impacts of the Caspian Sea and strongly support the inclusion of more realistic Caspian Sea area representation in future climate model developments.

3.5 Conclusions

Our choice of four Caspian Sea sizes that have not been used in previous studies, allows us identifying further impacts on regional climate over the Caspian Sea catchment area as well as large-scale climate over the entire northern hemisphere. When compared to a no-Caspian Sea scenario, evaporation over the sea increases with increasing area, while precipitation increases over the south-west Caspian Sea with increasing area. While the latter process represents an interesting positive feedback on Caspian Sea surface area, the well-known negative lake surface-evaporation feedback still dominates overall. The presence of the Caspian Sea when compared with no-Caspian Sea leads to enhanced precipitation over central Asia and increased warming over the north-western Pacific during winter involving significant changes in sea ice. Also, our results demonstrate a weakening of the 500 hPa troughs over the northern Pacific with larger Caspian Sea area. Lastly, we confirm a summer relationship of thermal response triggering mid and upper tropospheric geopotential height anomalies which results in a southward shift in the jet stream.

Our results indicate that an accurate representation of the Caspian Sea in climate models is important to avoid additional biases when evaluating the climate processes over the Caspian Sea catchment, central Asia, and the northern Pacific. This study allows for an accurate estimate of the change of the Caspian Sea level from the change of the Caspian Sea surface area when compared to a simulation carried out with an inaccurate Caspian Sea area. Evidence from the palaeorecord demonstrates that the Caspian Sea level has varied by >100 m over the Quaternary, with large attendant variations in Caspian Sea area. Our study indicates that consideration of potential changes in Caspian Sea area is likely important when modelling palaeoclimate scenarios, as well as for 21st century projections, but has so far not been given significant attention by the modelling community.

Acknowledgments

Data Availability Statement

For all of the described experiments, the climate variables used in this study are available as netcdf-file at PANGAEA (https://doi.pangaea.de/10.1594/PANGAEA.923110).

4. CHAPTER FOUR: The fate of the Caspian Sea under projected climate change and water extraction during the 21st century

Sifan A. Koriche, Joy S. Singarayer, Hannah L. Cloke

Key points

- Many climate models either ignore or do not properly prescribe Caspian Sea area with considerable variations, and this is a primary determinant in the modelled water budgets for both historical and future projections

- CMIP6 models have a tendency for drier projections than CMIP5

- This is the first study to combine latest state-of-the-art projections with extraction scenarios based on historical water use and projected population for 21st century

- Water extraction rates are equally as important as climate change in controlling future Caspian Sea level

- As result of the combined impacts of future water extractions and climate change, the shallow (6 m average depth) northern part of the Caspian Sea is at clear risk of desiccation occurring at some point before the end of the century

Abstract

The Caspian Sea delivers considerable ecosystem services to millions of people. It experienced water level variations of 3 m during the 20th century alone. Robust scenarios of future Caspian Sea level are vital to inform environmental risk management and water-use planning. In this study we investigated the water budget variation in the Caspian Sea drainage basin and its potential impact on Caspian Sea level during the 21st century using projected climate from selected climate change scenarios of shared socioeconomic pathways (SSPs) and representative concentration pathways (RCPs) and explored the impact of human extractions. We show that the size of the Caspian Sea prescribed in climate models determines the modelled water budgets for both historical and future projections. Most future projections show drying over the 21st century. The moisture deficits are more pronounced for the

extreme radiative forcing scenarios (RCP8.5/SSP585) and for models where larger Caspian Sea is prescribed. By 2100, up to 8 (10) m decrease in Caspian Sea level is found using CMIP5 RCP45 (85) models, and up to 20 (30) m for SSP245 (SSP585) scenario for CMIP6 models. Water extraction rates are as important as climate change in controlling future Caspian Sea level, with potentially up to 7 m further decline in Caspian Sea level, leading to desiccation of the shallow northern Caspian Sea. This will have wide-ranging implications for the livelihoods of the surrounding communities; increasing vulnerability to freshwater scarcity, transforming ecosystems, as well as impacting the climate system. Caution should be exercised when using individual models to inform policy as projected Caspian Sea level is so variable between models. We identify that many climate models either ignore or do not properly prescribe Caspian Sea area. No future climate projections include any changes in Caspian Sea surface area, even when the catchment is projected to be considerably drier. Hence, coupling between modelled atmosphere and lakes within climate models would be a significant advance to capture crucial two-way feedbacks.

Keywords: Caspian Sea level, CMIP5, CMIP6, water extraction, future climate change, water budget

4.1 Introduction

The Caspian Sea is the largest land-locked lake in the world, with a surface area currently larger than Japan. Over a hundred rivers contribute to its water balance over a vast catchment (3.6 Mkm^2; Fig. 4.1), covering six climatic zones (Chen and Chen, 2013). In the past, Caspian Sea has experienced large variations in water level, from tens to hundreds of meters on various time scales (Koriche et al., 2020a; Krijgsman et al., 2019), and its water level variability through time does not track that of the global ocean. Caspian Sea level variations during the last century were also much faster (up to 100 times) than global ocean level variations (Arpe et al., 2014). As the water level changes it substantially alters Caspian Sea surface area. For example, $\pm$>70% change from its current size occurred during various palaeo-time periods in the late Quaternary. Such changes in surface area impact the climate in the regional catchment due to feedbacks with evaporation, precipitation, and wind patterns, as well as the large-scale atmospheric circulation in the northern hemisphere (Arpe et al., 2019;

Koriche, Nandini-Weiss et al., 2020b). Caspian Sea climate impacts extend eastward, modifying summer precipitation over central Asia and even influencing sea-ice concentrations over the north-western Pacific (Koriche, Nandini-Weiss et al.,2020b).

Several previous studies have investigated historical changes in the Caspian Sea level (e.g., Arpe et al., 1999; Arpe et al., 2000; Arpe and Leroy, 2007; Chen et al., 2017a; Chen et al., 2017b; Golitsyn, 1995; Rodionov, 1994). Multiple natural and anthropogenic factors have combined to produce historical sea level variations. There was a dramatic decrease of 3 m in Caspian Sea level from the 1930s to 1977 (Fig. 4.2a), which has been attributed partly to precipitation decrease along the Volga catchment (Leroy et al., 2020 and references therein) and partly to the construction of dams that enabled the storage of increasing amounts of catchment water outside the Caspian Sea. The subsequent two decades saw a rise of 2.5 m in Caspian Sea, which has been linked to teleconnections between Caspian Sea and ENSO (Arpe et al., 2000). This was followed by a 1.5 m decrease over the last three decades, even as human extraction has decreased, which has been dominated by enhanced evaporation over the Caspian Sea itself during that time period, as regional temperatures increased (Chen et al., 2017a).

A few previous studies have addressed the implications for Caspian Sea level of future human-induced climate change. These have been performed using either Climate Model Intercomparison Project 3 (CMIP3) simulated projections from multiple models (Elguindi and Giorgi, 2006a, 2007) or individual model simulations (Arpe and Leroy, 2007; Renssen et al., 2007; Roshan et al., 2012). The results of these studies vary considerably, from predicting increasing Caspian Sea level over the 21st Century (Arpe and Leroy, 2007; Roshan et al., 2012) to substantial declines in Caspian Sea level (Elguindi and Giorgi, 2006a, 2007) of up to 9-18m (Nandini-Weiss et al., 2020). Elguindi et al. (2011) point to model spatial resolution as an important factor in estimating hydrologic balance over the Caspian Sea, especially in regions with mountainous terrain. Model structural differences also contribute to larger uncertainties in dynamical responses to climate change than in the thermodynamic response (Shepherd, 2014). This produces a broader range of regional outcomes for circulation-controlled climate fields such as precipitation, which results in challenges for assessing climate change impacts on the regional hydrological budget (Woldemeskel et al., 2016). The spatial representation of the Caspian Sea within climate models influences local and remote climate (Koriche, Nandini-

Weiss et al., 2020b), and in many models the rendering of the Caspian Sea is poor. Equally, as Caspian Sea area decreases, the area available for evaporation decreases, creating a negative feedback that is not accounted for in these studies (except in Renssen et al., 2007). However, their result is constrained by only using a single model of low spatial resolution and a simplified physics compared to General Circulation Models (GCMs).

In addition to climatic factors, artificial water extraction has increased the vulnerability of the Caspian Sea to desiccation. Discharge along the rivers of the Caspian Sea catchment is regulated by over 14,000 dams built for agricultural irrigation, domestic, and industrial purposes over the last 50-70 years, which together have the capacity to store more than 75% of the total discharge to the Caspian Sea (Akbari et al., 2020). Roughly 25000 km^2 (6-7%) of the Caspian Sea is now vulnerable to desiccation as Caspian Sea levels fluctuate (Akbari et al., 2020), primarily at the northern part of the Caspian Sea. Part of the rate of decrease can be attributed to water extractions and river diversions (Rodell et al., 2018). Hence, evaporation from the dams together with climate change and increased water extraction driven by population growth and change in lifestyle could amplify the decline of Caspian Sea, leading to accelerated desiccation, especially the northern shallowest part of the lake. Consequently, the bio-ecosystem, economies and livelihoods of many millions in the surrounding nations of the Caspian Sea could be severely affected in the future. One study (Kudekov, 2006) found that even with a constant rate of water consumption of 40km^3 per year (based on State Hydrological Institute of the Russian Federation estimates) three climate model projections still produced a rise in Caspian Sea level over the coming century. However, modelled projections of future Caspian Sea level have so far mostly not incorporated the important element of human water extraction.

The impacts of lake desiccation are serious, as exemplified by the Aral Sea (Micklin, 1988; Small et al., 2001; Zavialov et al., 2003). Hence, robust scenarios of future Caspian Sea level are vital to inform future planning of industrial, agricultural, and domestic water extraction as well as other activities including fisheries, shipping, and oil/gas production. In this study, we investigate the hydrologic budget changes and the water level variation of the Caspian Sea under 21st century climate change projections and idealized water extraction scenarios. The research addresses the following questions:

- How does the Caspian Sea water budget change in the CMIP5 and CMIP6 models in the 21st Century?

- How well the Caspian Sea is represented in the CMIP models and how does this influence their future climate projections?

- What are the implications for Caspian Sea level given 21st Century climate change and future water extraction scenarios?

We selected a number of climate models from CMIP5 and CMIP6 for analysis of their water budgets, based on their representation of the Caspian Sea. We collated available water extraction information and extrapolated 21st Century scenarios. Climate-change driven water budgets and human extraction scenarios were then combined to estimate the impacts on Caspian Sea level using a hydrologic model that accounts for the impacts of changes in Caspian Sea area on evaporation from the sea.

4.2 Methods

4.2.1 Model selection and data preparation

Close to 60 global climate models were included in CMIP5 (Taylor et al., 2012) and about 120 models in CMIP6 (Eyring et al., 2016). Analysis of their associated land-sea masks indicates that a considerable number of the CMIP5 and CMIP6 climate models either completely ignore, or do not accurately prescribe, Caspian Sea area. Therefore, we set selection criteria based on (1) how well Caspian Sea area is represented in the models, and (2) the availability of precipitation, and evaporation fields for both Representative Concentration Pathways RCP4.5 and RCP8.5 (Meinshausen et al., 2011) for CMIP5 and Shared Socioeconomic Pathways (SSP245 and SSP585) (Riahi et al., 2017) for CMIP6. RCP4.5 is an intermediate scenario, with 4.5 Wm^{-2} radiative forcing by 2100, and RCP8.5 is an extreme climate change scenario, with 8.5 Wm^{-2} radiative forcing by 2100. SSP245 and SSP585 represent similar (although not identical) intermediate and extreme scenarios, respectively, in CMIP6.

At the time this investigation was performed (September 2020), based on the above criteria, we selected in total 18 climate models, of which eleven are from CMIP5 and seven

are from CMIP6. We only considered the first ensemble simulation (CMIP5: "r1i1p1" and CMIP6: "r1i1p1f1") if a model had multiple ensemble simulations. The list of the models used in this study and their land-sea masks are presented in Fig. 4.1. See also supplementary information Fig. S6.15 and S6.16 for land-sea masks of models that were rejected from the main study due to poor CS representation and/or missing climate model fields (for model details see Table S6.2 for CMIP6 models and Table S6.3 for CMIP5 models). For comparison purposes, the model precipitation and evaporation fields were interpolated to the same resolution (6 arcminutes) by a first-order conservative interpolation method (remapcon), which works well for flux conservation (Jones, 1999), using the Climate-Data-Operator (CDO) software.

(a)

(b)
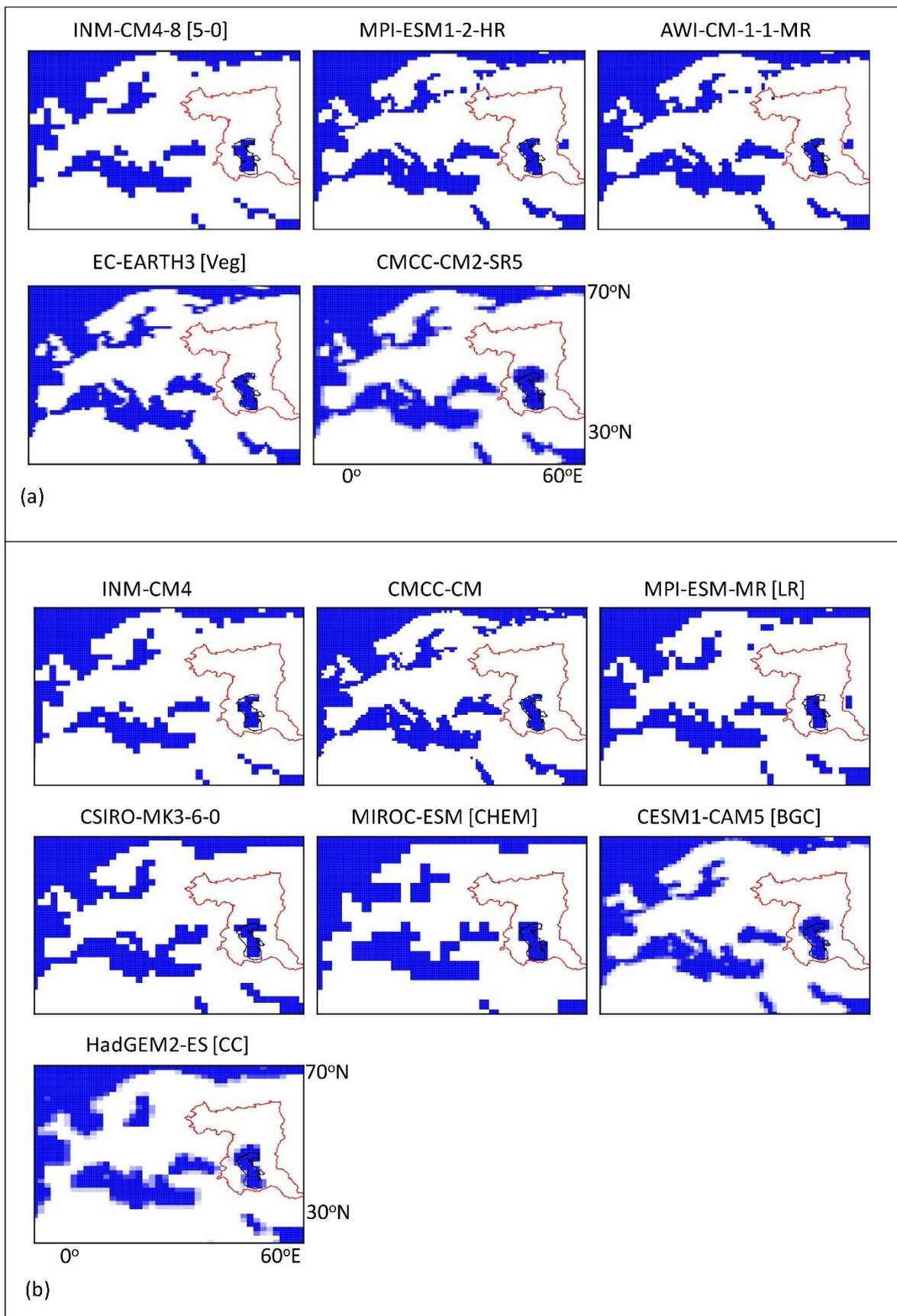
Figure 4.1. Land-sea mask maps of models used in this study from (a) CMIP6 and (b) CMIP5. The black line represents the current Caspian Sea extent, and the red line represents the extent of the Caspian Sea catchment. Some of the models share the same land-sea mask. Therefore, the number of land-sea mask map shown in this figure is less than the total selected climate models (i.e. 18).

4.2.2 Hydrologic budget assessment and Caspian Sea level modelling

The hydrologic budget variation was assessed by comparing the mean 'precipitation minus evaporation' (P-E) field between the start and end of the 21st century from the selected CMIP5 (running between years 2006 and 2098) and CMIP6 (over years 2015 to 2100) models for RCP4.5 (8.5) and SSP245 (585) scenarios. To compare the historical mean P-E from the climate model with year to year change in the Caspian Sea level record, averaged value over a much longer time period 1860-1995 was considered. To estimate the Caspian Sea level variation during the 21st century, we used a hydrologic model constructed for the Caspian Sea by (Koriche et al., 2020a). The model is based on fluxes of runoff over the Caspian Sea catchment, P-E over the Caspian Sea, and water extraction for human use (Eq. 4.1). Simulations of lake water level variation in a closed basin like Caspian Sea can be substantially affected by the variation of its water level, as this leads to changes in surface area, which would significantly impact the P-E over sea at each time step. Therefore, for every time step, the Caspian Sea surface area is updated based on the volume of previous time step to be considered for the current time step water balance (*P-E*) estimation (Eq. 4.1).

$$\Delta CSV^t = [(P_{land}^t - E_{land}^t)A_{land}^{t-1} + (P_{sea}^t - E_{sea}^t)A_{sea}^{t-1} - \Delta WE^t]\Delta t \qquad [4.1]$$

where: *CSV* is Caspian Sea volume, *P* is precipitation, *E* is evaporation/evapotranspiration, and *A* is surface area, all over the land or sea part of the basin as denoted by their subscript, ΔWE is the increment in human extraction of water, Δt is the time step (in this case one month). We assume that groundwater contributions are small, based on previous studies (Golovanova, 2015; Zekster, 1995), and so we have not included a groundwater component.

4.2.3   Analysis of water extraction

Currently, the Caspian Sea is fed by rivers from nine different countries whereas water extraction information is based on national-level data rather than on the Caspian Sea catchment boundary. This makes it difficult to get appropriate estimations of water withdrawals solely from the rivers flowing to the Caspian Sea. We have used records covering the period from 1940 up to 1995 (Golitsyn, 1995; Rodionov, 1994; Shiklomanov, 1981), which are derived estimates of what the Caspian Sea level would be with zero human water extraction (see Fig. 4.2a, solid colour lines), based primarily on State Hydrological Institute of the Russian Federation information that is not readily available. These are indirect measurements that can then be used to infer the amount of water withdrawn from the rivers contributing to the Caspian Sea when compared with the measured Caspian Sea level observational record (Fig. 4.2a, black dotted line). Following calculation of the yearly withdrawal volume, the estimated annual water extractions demonstrate a roughly threefold increase between 1940 and 1990 (Fig. 4.2b). We note that we are referring to net water extraction (consumptive water use), which is the amount of water leaving the basin after accounting for the return of a proportion of the water extraction that returns to the Caspian. Net water extraction can occur through several mechanisms, including evaporated water that precipitates outside the basin boundary or through export of water in irrigated crops, livestock, and other goods.

An alternative source of information relating to water withdrawal from the Caspian catchment was compiled by Demin (2007) from various economic and government sector reports for the years 1970-2003 (Fig. 4.2b). These data show a peak in water withdrawals around 1985-1990 before annual consumption decreases again, until it declines to 43km^2 in 2003. These figures include consumption, as well as evaporation from reservoirs within the catchment. The reasons for the decline in water extraction include more efficient water consumption in domestic and industrial processes, changes to land-use, and changes to regional population (Demin, 2007). However, this decline in water extraction was not sufficient to balance out the enhanced evaporation over the CS that occurred due to increased regional temperatures (Chen et al., 2017a), and so CS level declined over the last few decades.

For this study, we created future water extraction (WE) values for idealised future projections between 2015 and 2100 in the Caspian Sea basin based on these estimates (Fig. 4.2b). The first scenario (FWE1) is a constant extraction rate of 40 km^3 per year, based on Demin (2007), and previously used in Kudekov (2006). A second scenario (FWE2) for comparison had constant annual withdrawal at 20 km^3 per year (Fig. 4.2b green dashed line). In a third scenario (FWE3) we used new country level population projections for nations within the catchment (Vollset et al., 2020) to scale water withdrawal values. The regional population is projected to increase slightly up to mid-21st century before declining to below present-day levels by 2100 (Fig. 4.2b; see also supplementary information Table S6.4). In our simple translation we assume that the 2015 extraction rate is 40 km^3 per year and that projected changes in population can be linearly transformed to changes in water withdrawals (through domestic water use, agricultural activity, and industrial sector activity). These three water extraction scenarios bracket the large uncertainties in the compiled historical literature due to the difficulties in sourcing primary catchment level information (described above and shown in Fig. 4.2), as the modelled projections will likely be sensitive to the choice of extraction values.
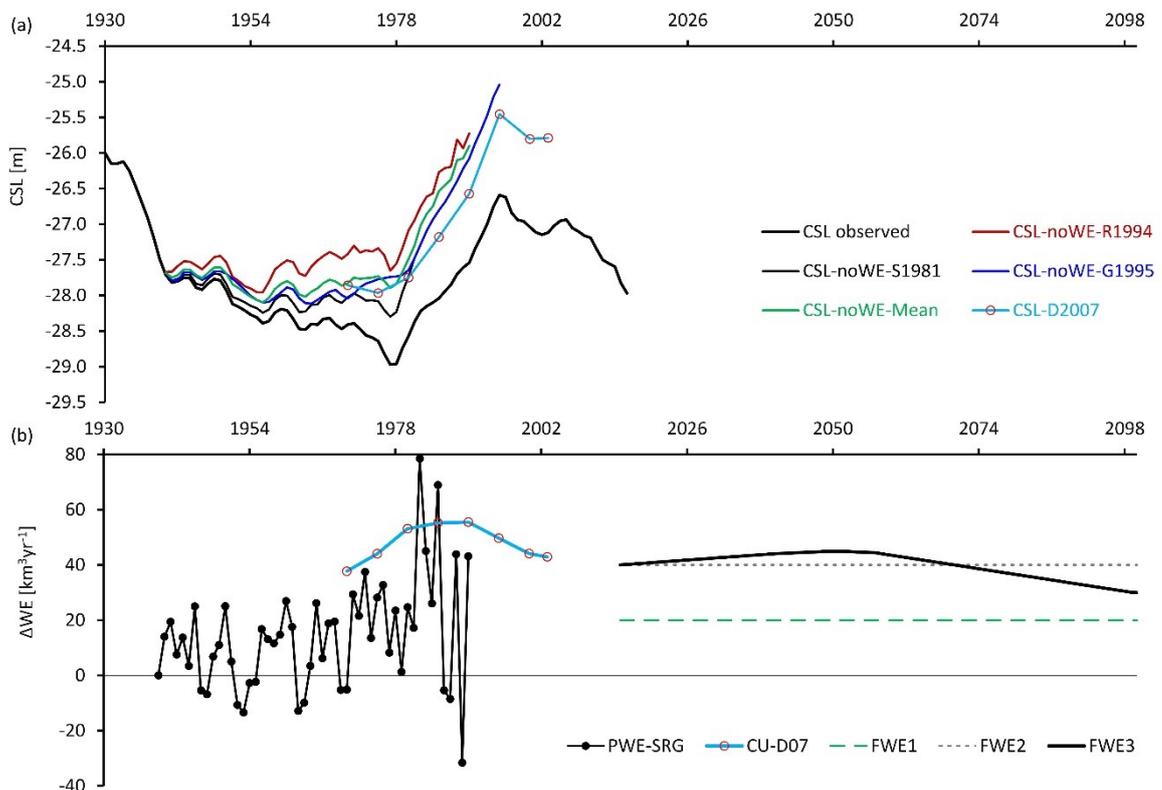
Figure 4.2. Water extraction information in relation to the Caspian Sea level: (a) shows the observed (black broken line) and literature-based Caspian Sea levels (solid lines), (b) volume of water extracted from the Caspian Sea based on difference between observed and mean estimated (no water extraction) Caspian Sea level by Rodionov (1994), Shiklomanov (1981) and Golitsyn (1995) (solid black line with dot marker). This was calculated by converting 'Caspian Sea level noWE-Mean' and 'Caspian Sea level observed' to volumes at each time point, and then subtracting to give the accumulated water extraction. We then subtracted the previous year's volume to give the water withdrawal for each year. The light blue line with circle marker (CU-D07) is estimated consumptive water use according to Demin (2007). The other three lines (broken grey and green, and solid black) represent the proposed future water extraction used in this study to evaluate the projected Caspian Sea level during the 21st century. The broken grey and green line represent 20 and 40 km^3 per year of future water extractions (FWE1 and FWE2) per year respectively, and the solid black line is estimated future water extraction based on population growth (FWE3). (Key: CSL – Caspian Sea level, WE – water extraction, R1994 – Rodionov 1994, S1981 – Shiklomanov 1981, G1995 – Golitsyn 1995, PWE-SRG – past water extraction based on Shiklomanov (1981), Rodionov (1994) and Golitsyn (1995), FWE – future water extraction).

4.3 Results

4.3.1 Water budget of the Caspian Sea basin and its relation to the Caspian Sea area representation in CMIP models

In this section we first calculate the present-day (20th century) modelled water budgets from CMIP5 and CMIP6 and compare them with observational water budget data derived from the Caspian Sea level record. Secondly, we examine the projected water budgets for the 21st century. We explore whether there is a relationship between the modelled present and future water budgets and the prescribed Caspian Sea area in the models.

We find a considerable spread in the annual mean water budget of the Caspian Sea catchment (P-E) between models in both CMIP5 (Fig. 4.3, red symbols) and CMIP6 (Fig. 4.3, blue symbols), with some models displaying a net positive water balance and some a negative

balance. When P-E is plotted against the prescribed Caspian Sea lake area (Fig. 4.3) we find a trend that models with larger Caspian Sea surface area are drier, whereas models with smaller lake area are wetter (more positive P-E). The correlation of the modelled catchment water budget on the size of the prescribed Caspian Sea is indicative of the importance of the magnitude of evaporation from the sea itself in controlling the overall balance. The larger the prescribed Caspian Sea the larger the amount of evaporation, which tends to outweigh any resulting increase in precipitation and so produces a smaller overall P-E. It is also clear here that even though we have selected models that better represent Caspian Sea surface area, some of the models (particularly in CMIP5) are up to 75% larger than the observed Caspian Sea over the last century (Fig. 4.3, black symbol).
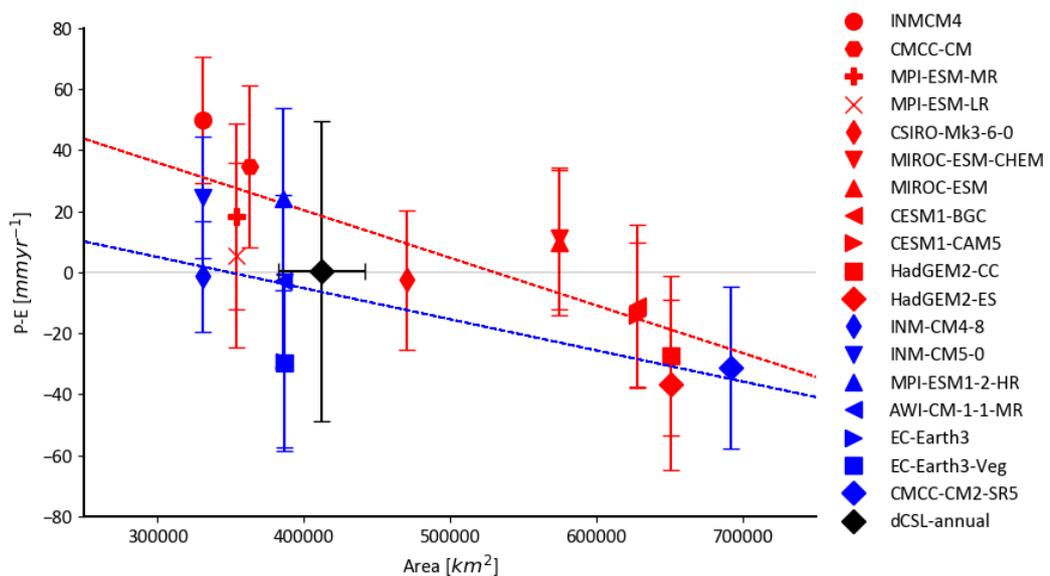
Figure 4.3. Mean P-E over the CS basin for CMIP6 (blue) and CMIP5 (red) models for 1860-1995 plotted against the prescribed CS area in the respective CMIP models. The black symbol represents mean year to another year variation of the CS level, also from 1860 to 1995. The error bars represent one standard deviation (inter-annual) of the mean for the period considered. The linear fits are significant at the 99% level for CMIP5 (r = 0.82) and 90% level for CMIP6 (r = 0.61).

One difficulty faced when attempting to compare and evaluate the modelled P-E with observational data is that the Caspian Sea level has been increasingly influenced by human

water withdrawals, which are not included in the model boundary conditions, making the recorded water balance appear more negative than it would be otherwise. A second potential issue is that there is large interannual to decadal-scale variability in the water budget due to modes of internal climate variability such as ENSO (e.g., Arpe et al., 2000), and, due to the set-up of the models, they do not necessarily reproduce the state of those modes at the correct historic time (nor would we expect them to do so). Therefore, comparison of the water balance to a short record or short reanalysis dataset (e.g., ECMWF reanalysis version-5 (ERA5), which overlaps with CMIP5 between 1979 and 2005) will not be appropriate. Instead we compare the model output with the Caspian Sea level record, corrected to exclude any human water withdrawals (see Fig. 4.2a), and averaged over a much longer time period 1860-1995 (Fig. 4.3, black symbol). The observational data show that the Caspian Sea has been precariously balanced, fluctuating between positive and negative over the last century. Models with a prescribed Caspian Sea surface area closer to historical observations generally also produce a water budget closer to our observationally-derived estimate.
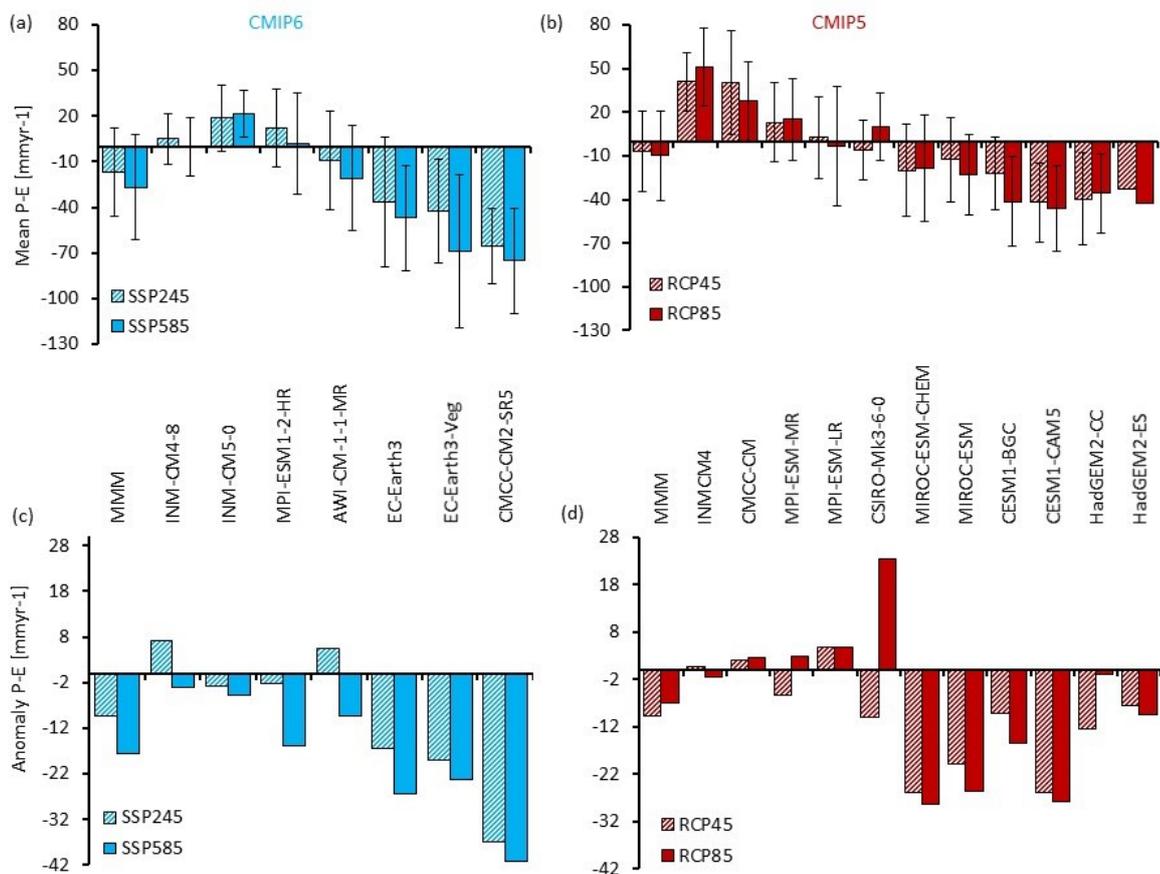
Figure 4.4. (a) and (b) show mean P-E by the end of 21st century [2070-2100] for CMIP6 and CMIP5 respectively, and (c) and (d) show anomalies of P-E between the end and start of 21st century for CMIP6 and CMIP5 respectively. For CMIP6, the P-E anomalies are based on between the mean P-E during 2070-2100 and 2015-2030, and whereas, for CMIP5 between the mean P-E during 2070-209 and 82006-2020. The Caspian Sea area increases from left to right. MMM refers to the multi-model mean. The error bars represent one standard deviation (inter-annual) of the mean for the period considered.

Fig. 4.4a-b show the mean water budgets (P-E) of the Caspian Sea basin by the end of the 21st century (2070-2100) as projected by CMIP6 and CMIP5 models for medium (SSP245/RCP45) and high (SSP585/RCP85) radiative forcing scenarios. Models that represent Caspian Sea area more accurately in CMIP5 (CMCC, MPI, CSIRO) tend to still have a neutral or positive P-E by 2100 (Fig. 4.4b). In CMIP6, models with better prescribed Caspian Sea area (MPI, AWI, EC-Earth3) tend to have a neutral or negative P-E by the end of the century (Fig. 4.4a). To evaluate the direction of future water budget change in the Caspian Sea basin, we use the anomalies between the start and end of the 21st century for both modelling groups as presented in Fig. 4.4c-d. In both scenarios the model P-E anomalies almost all show conditions getting drier (up to 40 mmyr^{-1}) by the end of the 21st century (Fig. 4.4c-d). The drying is generally more pronounced in the high radiative forcing scenario (SSP585/RCP85) than the medium scenario (SSP245/RCP45). This is the case for all CMIP6 models, and six out eleven CMIP5 models. The CMIP5 multi-model mean doesn't show this trend as it is heavily weighted by the CSIRO-Mk3-6-0 model. This model displays considerable multi-decadal variability and a neutral long-term trend, and so the averaging periods are more affected by 'noise'. It is only the last two decades of the simulation that RCP8.5 anomalies become much wetter than RCP4.5, due to multi-decadal variability.

The CMIP6 models tend to have a more negative (drier) water budget than the CMIP5 models, both historically and in the future projections. These models generally have higher spatial resolutions, better physics parameterizations, and more Earth system components (Eyring et al 2016) than CMIP5 models. Recent studies have also found that this generation of models also have higher equilibrium climate sensitivities (ECS) and warmer 21st century projections (Hausfather, 2019; Tokarska et al., 2020; Wyser et al., 2020), which may play an

important role here, given the importance of evaporation over the sea for the overall water budget of the Caspian Sea. The treatment of the lake in the models (e.g. parameters relating to lake heat absorption and mixing) and coupling of the lake surface to the atmosphere will likewise be important in the variation between model water budgets. The magnitudes and patterns of the seasonal cycle of precipitation and evaporation over land are relatively consistent over land (see supplementary information Figs. S6.17a-b for CMIP6 and Fig. S6.18a-b for CMIP5) but highly variable between models over the sea (Fig. S6.17c-d and Fig. S6.18c-d). The timing of maximum evaporation varies between August and November and the minimum between February and May. Two CMIP6 models (EC-Earth3 and EC-Earth3-veg), which display highly negative water budgets, despite their Caspian Sea areas being close to observed, have Caspian Sea evaporation that remains relatively high even in winter compared to other models (close to 70% higher evaporation, Fig. S6.17c). These models have an ECS that is relatively high (> 4 °C; Tokarska et al., 2020). Conversely, the INM-CM5-0 CMIP6 model, which has a highly positive water budget, has a much lower maximum evaporation than other models and low ECS (< 2 °C; Tokarska et al 2020). The same model seasonality characteristics are maintained through the future projections (Fig. S6.19-S6.22).

4.3.2   Simulation of 21st century Caspian Sea level

In the future the drivers of Caspian Sea level variation are expected to intensify due to the pressures from the intensive utilization of natural resources. In this section, we explore the question of how increasing anthropogenic climate change and human water withdrawals will impact Caspian Sea level using a water balance model driven by modelled climate projections and idealised extraction scenarios.

The first set of Caspian Sea level simulations are driven by both medium (SSP245/RCP45) and extreme (SSP585/RCP85) radiative forcing scenario climate outputs from CMIP6 and CMIP5 models without considering water extraction. By the end of the 21st century, up to 8 (10) m decrease in the projected Caspian Sea level is found using CMIP5 RCP45 (85) models (Fig. 4.5a). In CMIP6 based simulations, our results show a decrease in Caspian Sea level up to 20 m and 30 m for SSP245 and SSP585 scenarios respectively (Fig. 4.5b). The reasons for the larger decreases in CMIP6 Caspian Sea level than CMIP5 Caspian Sea level are partly

explained below (in particular, higher ECS). The declines in the Caspian Sea level are larger with models where larger Caspian Sea is prescribed in the climate model, and those with higher projected evaporation (e.g. EC-Earth3 and EC-Earth3-Veg). The largest decline of the Caspian Sea level seen in EC-Earth3 and EC-Earth3-Veg models based simulations are because of the higher projected evaporation in these models (close to 70% higher evaporation compared to the other models). On the other hand, models where the prescribed Caspian Sea is smaller tend to display increase in the projected Caspian Sea level (four CMIP5 models but only one CMIP6), since the P-E over the Caspian Sea basin is positive (Fig. 4.5a-b). In both modelling groups (CMIP6 and CMIP5), we observed that the projected Caspian Sea level increases in models with cold bias and smaller ECS (e.g. INM-CM model families). We also find that the Caspian Sea level projections for CESM-CAM5 (5-6 m) from CMIP5 are smaller than found by Nandini-Weiss et al. (2020) of 9-18m using the same model. Our water balance modelling results in a negative lake-level-evaporation feedback that is not represented in the other study. Here, as Caspian Sea level declines the surface area shrinks, which reduces the evaporation component, slowing down the rate of desiccation. As a result, Caspian Sea level decline is not as pronounced as in Nandini-Weiss et al. (2020).
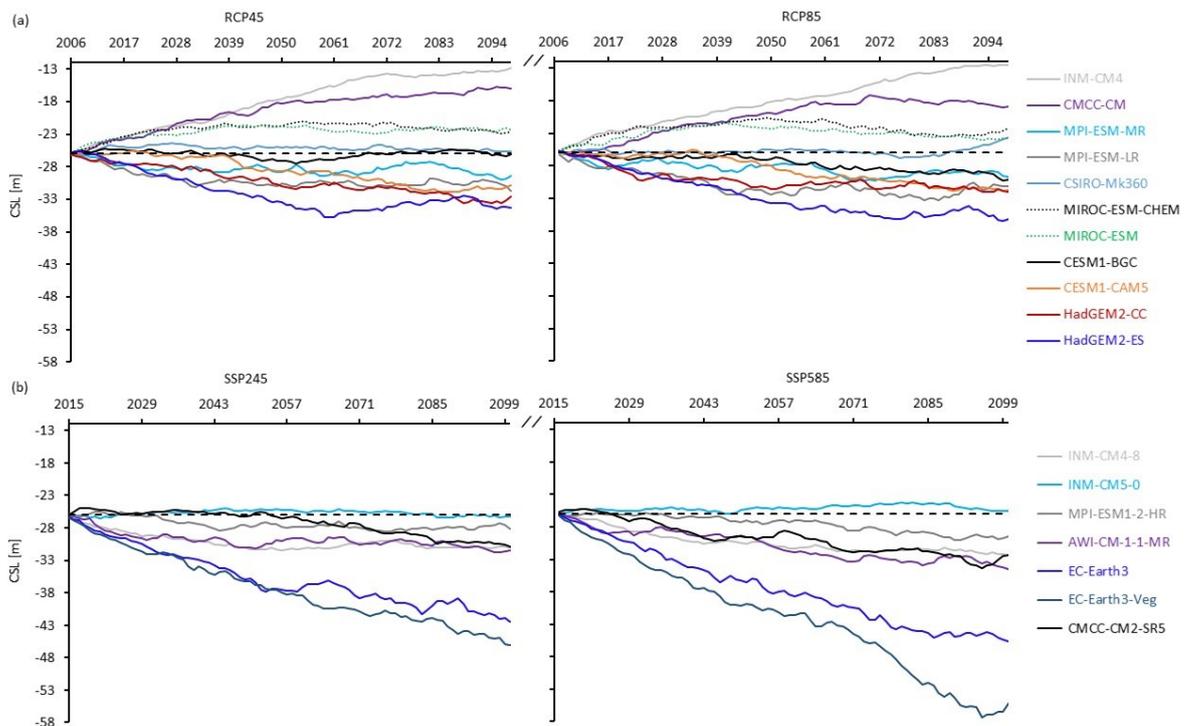
Figure 4.5. Simulated Caspian Sea level projections without considering extraction and based on (a) CMIP5 models for RCP45 and RCP85 scenarios and (b) CMIP6 models for SSP245 and SSP585 scenarios. The models are listed in the order of increasing Caspian Sea area from top (smallest) to bottom (largest).

Next, we incorporate the three idealised water extraction scenarios, as described in §4.2.3. In our analysis of water extraction impacts we only consider the results from CMIP6 radiative forcing scenarios (SSP245 and SSP585) as they are based on latest versions of climate models with improved process representations. In all scenarios, all models display a decline in Caspian Sea level but there is variation in the magnitude of this decline. Up to 7 m decline in Caspian Sea level is observed due to water extraction. Under SSP245 scenario the decline in the Caspian Sea level ranges from 0.7 to 3.6 m for FWE1, 1.4 to 7.6 m for FWE2, and 1.2 to 7.3 m for FWE3 (Fig. S6.23b-d). Under SSP585 CS level ranges from 0.9 m to 4.4 m in FWE1, 2.2 to 9 m in FW2, and 1.9 to 7.2 m in FWE3 (Fig. S6.23b-d).

We note that the Caspian Sea level-Surface area relationship becomes more complicated when Caspian Sea level varies between -27 m and -34 m the Caspian Sea area changes are proportionately large compared with when Caspian Sea level is below this. This occurs when the shallow northern part of the Caspian Sea (average depth ~ 6m) comes into play. As a result, even when the trend in Caspian Sea level is seemingly relatively smooth, there is large interannual variability in the modelled Caspian Sea surface area of up to 10% (Fig. 4.6a-b, S6.24), particularly in those models that have a slower decline in Caspian Sea level. It will result in larger seasonal variation in flooding of surrounding wetlands. This variability in Caspian Sea area, particularly in the shallow northern Caspian Sea has implications for coastal communities and conservation of marginal environments at the edge of the lake.

We considered a key indicator, or threshold, in the future of the Caspian Sea to be the point when the shallowest northern section becomes completely desiccated. We used the multi-model mean (MMM) projections of the Caspian Sea level under the two climate change scenarios and four idealised water extraction cases to calculate at what point in the 21st century this threshold occurs (if at all). In all scenarios except for SSP245 with no water extraction this level of desiccation occurs at some point before the end of the century (Fig.

4.6). For the extreme SSP585 scenario MMM and the population based FWE3 extractions the northern Caspian Sea is desiccated by 2050 (and is a point crossed by 5 out of the 7 individual models). When considering this indicator of Caspian Sea decline, the rate of water extraction is effectively as important as the climate change scenario in terms of the timing. The higher the extraction rate the less difference the climate change scenario makes, and vice versa. With FWE3 there is only ~ 12 years difference between SWSP245 and SSP585, whereas with FWE1 there is ~ 45 years difference (Fig. 4.6c). The timing of the desiccation among individual models are different (Fig. 4.6a-b, S6.24).
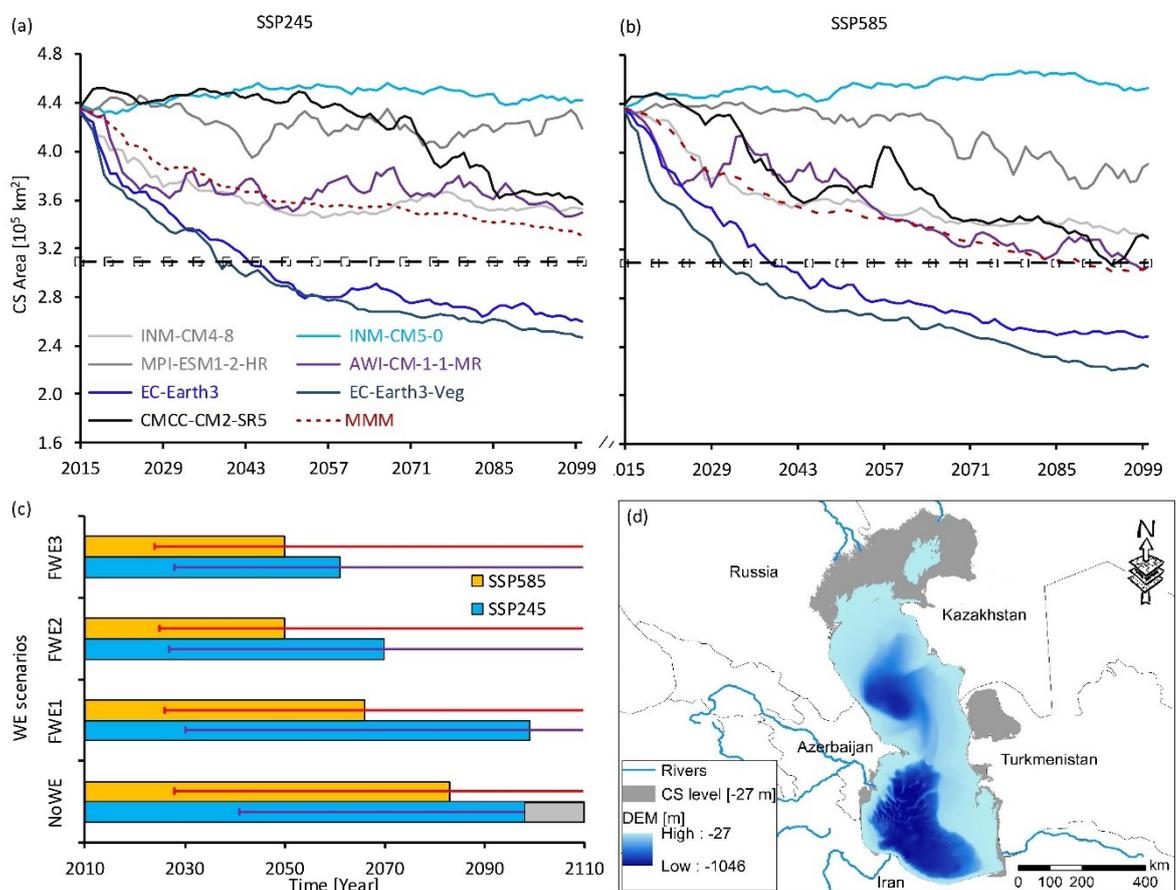
Figure 4.6. Projected Caspian Sea area of the 21st century based on CMIP6 (a) medium and (b) extreme emission scenarios and without water extraction. Broken line with box marker is the magnitude of area vulnerable to desiccation for a 6 m CS level decline. (c) The time at which the northern part of the Caspian Sea area with average depth of 6 metres will be desiccated for four experiments with three water extraction and a no-water extraction (NoWE) scenarios using multi-model-mean climate output from CMIP6 extreme and medium

emission scenarios (for individual models, refer to Table 4.1). The error bar represent the minimum (EC-Earth3-Veg for both scenarios) and maximum time to desiccation. The grey part of the bar-chart of the NoWE scenario indicates that the northern part of Caspian Sea area will not be affected until the end of 21st century. (d) Map showing area vulnerable to desiccation for a 6 m Caspian Sea level decline shown in grey. Abbreviations as in Fig. 4.2.

Table 4.1. The time at which the northern part of the Caspian Sea area with average depth of 6 metres will be desiccated for four experiments with three water extraction and a no-water extraction (NoWE) scenarios for individual CMIP6 models.

	SSP585				SSP245			
	NoWE	**FWE1**	**FWE2**	**FWE3**	**NoWE**	**20km3**	**40km3**	**Pop**
INM-CM4-8		2093	2055	2050			2047	2045
INM-CM5-0								
MPI-ESM1-2-HR								
AWI-CM-1-1-MR	2096	2074	2056	2056			2096	2096
EC-Earth3	2035	2034	2032	2030	2041	2033	2031	2031
EC-Earth3-Veg	2028	2026	2025	2024	2037	2030	2027	2028
CMCC-CM2-SR5	2093	2088	2065	2065				
MMM	2083	2066	2050	2050	2110	2099	2070	2061

4.4 Discussion and Conclusions

In this study we have investigated the water budget variations in the Caspian Sea basin and its potential impact on the Caspian Sea level during the 21st century using projected climate change from selected CMIP6 and CMIP5 models (Eyring et al., 2016; Taylor et al., 2012). Furthermore, we have explored the impact of idealised human water extractions on the future Caspian Sea level variations. We find that the size of the Caspian Sea prescribed in the climate models is an important determinant in the modelled water budget (P-E), which previous studies fail to illustrate. The P-E is negative for models with larger prescribed Caspian Sea and positive for the smaller Caspian Sea. Models that are closer to the observed size of the Caspian Sea tend to be closer to the observed water budget.

Most of the future water budget projections by CMIP6 and CMIP5 models show a drying over the 21st century compared to present. CMIP6 models are generally drier than CMIP5

projections in the Caspian Sea catchment, which could be related the addition of more sophisticated earth system processes and higher resolution. The moisture deficits (leading to declining Caspian Sea levels) are more pronounced for the extreme radiative forcing scenario (RCP85/SSP585), and with models where larger Caspian Sea is prescribed. This is due to a noticeable increase in over-sea evaporation that is larger than the precipitation both over land and over the Caspian Sea as result of increased warming in the case of the extreme radiative forcing scenario that attributed to decline in the Caspian Sea level during the 21st century. Previous studies have also shown decline in Caspian Sea level (Elguindi and Giorgi, 2007; Renssen et al., 2007) over the same period without considering water extraction. However, based on our results, the projected Caspian Sea level is variable between models, with some models projecting increased Caspian Sea level, related to larger prescribed Caspian Sea area and differences in climate sensitivity. Therefore, caution should be exercised when using individual CMIP models or ensemble means to inform policy for mitigation measures.

During the historical period, human extractions from the Caspian Sea basin has played considerable impact on Caspian Sea level variations. This is because many artificial reservoirs have been built to address the societal demands of the communities residing in the Caspian Sea basin. Therefore, a considerable amount of water is now stored in those reservoirs, and this has hindered natural hydrological processes. The ongoing annual withdrawals put added pressure on the Caspian Sea level, even as water-use efficiency is improved and population stabilises. We find that impacts from water extraction rates are as equally important as climate change for projected future declines in Caspian Sea level. The shallow (6 m average depth) northern part of the Caspian Sea is at clear risk of desiccation by the end of the 21st century, as occurred in all but one of our modelled scenarios. This would lead to severe impacts on biodiversity, ecosystems, economies, and geo-political situations of the surrounding countries. Some of the major impacts that would be anticipated include reduction in major food-source habitats, degradation of river-deltas, increased pollution in the central basin, disruption of ecosystems and unique biotas, reduction in income generating services (Prange et al., 2020).

Coupling between modelled atmosphere and lake area within GCMs would be a significant advance to enable incorporation of the two-way feedbacks. As we have found, many climate

models either ignore or do not properly prescribe Caspian Sea area, and no future projections include any changes in Caspian Sea surface area, even when the catchment is projected to be considerably drier, with potential for considerable decrease in lake area. Changes in Caspian Sea surface area influence the regional atmospheric water budget and have large remote impacts (Koriche, Nandini-Weiss et al., 2020b).

Water mass circulation is one further component that is neglected in these simulations. One recent study by Huang et al. (2021) simulated the response of Caspian Sea circulation to doubling of CO_2 in an ultra-high-resolution global model, which included Caspian Sea circulation. Their model displayed a slowdown of northern and southern Caspian Sea gyres but an increase in intensity of the central gyre. Resulting impacts on mixing of heat could influence evaporation rates and seasonal cycles. However, the first order Caspian Sea level decrease found in this model was a similar magnitude to other studies (e.g., Renssen et al., 2007), although the modelled Caspian Sea in Huang et al (2021) still had a fixed prescribed volume and surface area, and no account was made for changes in surface area in the calculation of Caspian Sea level.

Considerable uncertainty in the historical drivers of Caspian Sea variation has arisen due to the lack of coordinated water monitoring systems at catchment level. This has made it difficult to pin down the relative impacts of climate change and human water extraction, and to assess which models are better at reproducing the Caspian Sea water balance. Therefore, a coordinated effort among the countries in the Caspian Sea basin is vital for the implementation of integrated watershed management approach to better understand hydroclimatic changes in the Caspian Sea basin, so that improvements could be made to models for better projections of the Caspian Sea level and area.

Acknowledgements

in Table S6.2 and Table S6.3 of this paper) for producing and making available their model output. For CMIP the U.S. Department of Energy's Program for Climate Model Diagnosis and Intercomparison provides coordinating support and led development of software infrastructure in partnership with the Global Organization for Earth System Science Portals.

5. CHAPTER FIVE: Summary and future work

5.1 Summary

The Caspian Sea plays a key role in the Ponto-Caspian region. Its ecosystem is of a unique nature that is home to many endemic species and provides various ecosystem services such as food resources (e.g., Caspian kutum, Caspian zander, sturgeon), income generation (e.g., fisheries, tourism), and other benefits to many millions of people in the surrounding nations and beyond (Grigorovich et al., 2003; Interim Secretariat of the Framework Convention for the Protection of the Marine Environment of the Caspian Sea, 2012, 2020; Marret et al., 2004). Over many decades during the historical period, these species have increasingly suffered from environmental (e.g., water-level fluctuations) and anthropogenic pressures such as water extraction, oil exploration, and global shipping, leading to habitat degradation, pollution, and invasive species introduced either accidentally via shipping or intentionally for fisheries (Grigorovich et al., 2003; Lattuada et al., 2019; Latypov, 2015).

The Caspian Sea has been dominated by major changes in water level, resulting in episodic connection to the Black Sea during the Quaternary (Krijgsman et al., 2019 and references therein). This had implications on the biodiversity of the region during its geological and recent past periods. Therefore, understanding the hydroclimatic changes of the Caspian Sea is crucial, as this can help to understand the driving mechanisms that contributed to the water level variation and the role it played in the biodiversity change during the past. This enhanced understanding will help in the planning of conservation measures in sustaining the present-day ecosystem, understanding the extent of the current biodiversity crisis, and enhancing ecosystem services.

To address these issues, the primary aim of this thesis was to improve our understanding of drivers and feedbacks impacting the Caspian Sea hydroclimate, for which the effects of climate on the Caspian Sea level through the changing balances of evaporation, precipitation and drainage patterns from the late Quaternary to the end of the 21st century are investigated. Consequently, this aim has resulted in the following research questions:

1. *What are the drivers of the Caspian Sea level during the late Quaternary?*

2. *How significant is the effect of Caspian Sea surface area changes on the regional and large-scale hydroclimate?*

3. *What is the fate of the Caspian Sea under projected climate change and human interventions?*

The key conclusions and answers to each of these questions are summarised in Fig. 5.1 and as below.
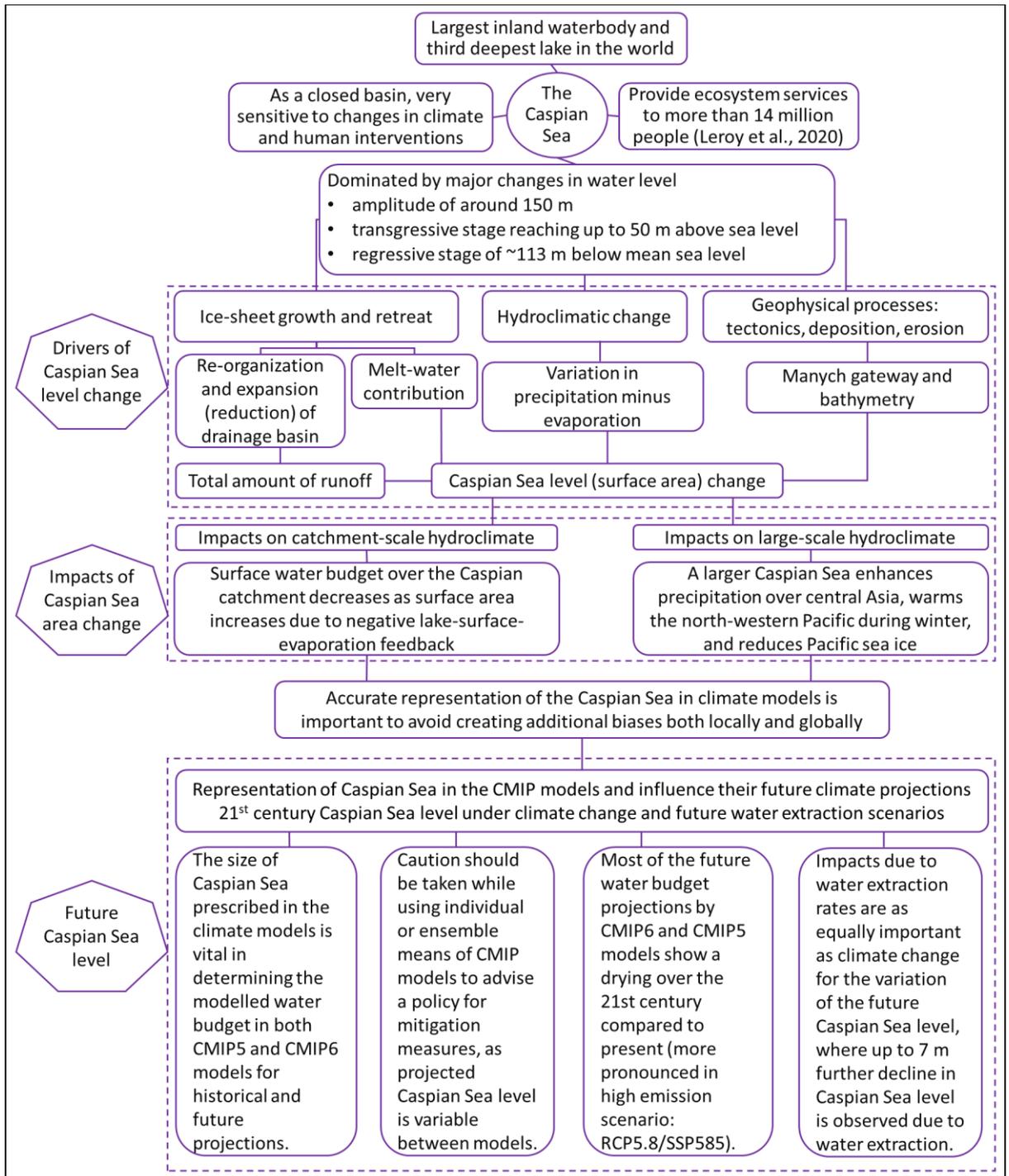
Figure 5.1. The overall summary of the background and motivations, and the key points and the links between the results presented in chapter 2, 3, and 4.

5.1.1   What are the drivers of the Caspian Sea level during the late Quaternary?

The Caspian Sea water level variation is complex, resulting from different processes and settings. There are ongoing debates about the timing, mechanisms, and the source of runoff. Consequently, diverse thoughts exist on the importance of particular drivers of Caspian Sea level change (Krijgsman et al., 2019 and references therein). Chapter 2 studied this further by evaluating the relative impacts of hydroclimatic change, ice-sheet accumulation and melt, and isostatic adjustment on the Caspian Sea level during the late Quaternary. Modelled Caspian Sea level variation, driven by the aforementioned forcings, was compared with newly collated palaeo lake level data covering the last glacial cycle. Overall, the results showed that the topographic change and the reorganization of the river drainage systems due to the Fennoscandian ice-sheet growth and retreat played the dominant role in the variation of the Caspian Sea level (especially the transgressive stages), although impacts related to pro-glacial lakes outburst and glacial melting from the Himalayan region may not be ruled out.

There are different ice-sheets datasets available (Wickert, 2016 and references therein) with slightly different reconstructions and with some uncertainty due to course spatiotemporal resolutions. The reconstruction of the river basin evolution during the late Quaternary is based on the most recent local ice-sheet and GIA model (ICE-6G), which has shown better performance compared to its predecessors (ICE-3G and ICE-5G) and closer to glacial geological data (Wickert, 2016). The restructuring of river drainage systems due to topographic changes in the last glacial resulted in 60-70% increase in the Caspian Sea drainage basin area that led to increased runoff contributions. This was crucial especially at the start of deglaciation period (between 20 and 15 kyr) when the climate gets warmer, as a result the combined impact of meltwater and increased runoff from the expanded area caused the highest transgression during the last deglaciation period (19 – 12 kyr BP). However, the magnitude of runoff contribution over the basin area out-weighs the melt-water contributions. The other important issue to note here is that the presence of pro-glacial lakes may have changed the timing of ice-sheet meltwater routing by temporarily storing meltwater and/or redirecting its release due to reaching overspill level, ice-damming collapse,

or impact of isostatic adjustment (Carrivick and Tweed, 2013) , and this is a factor unable to be incorporated in the current modelling framework used in this study.

The impact of the Younger Dryas millennial-scale event was also a determinant for the regressive stage of the early Holocene Caspian Sea level (e.g., the Mangyshlak regression). This can be associated with decrease in the water budget (i.e., drier conditions over the basin) related to the collapse of the Atlantic Meridional Overturning Circulation (AMOC) due freshwater input. Even though different palaeo-environmental records show different timing, the modelling result suggests that the early Holocene deepest low-stand of the Caspian Sea resulted from Younger Dryas conditions overlaps in time with the uncertainties in the chronology of the Mangyshlak regression, agreeing with some of the previous findings in the literature (e.g. Bezrodnykh and Sorokin, 2016; Kislov, 2018).

In conclusion the dominant forcing that controlled the Caspian Sea level during the deglaciation period (between 19- 12 kyr) were the hydroclimate and ice-sheet accumulation/melting that resulted in the change in topography and glacial isostatic adjustment. However, during the Holocene the variations in Caspian Sea level were dominated by hydroclimate change. These results stress that source of the palaeo Caspian Sea level variations is complicated. Therefore, care should be taken when identifying the potential connections between the past and future sensitivities of the Caspian to climate change, as the glacial Caspian Sea level was partly influenced by activities that happened beyond its current catchment boundary and so are not relevant for the present-day and future. The interglacial periods are potentially more relevant than glacial periods for understanding the sensitivity of present and future Caspian Sea level variations. For example, the last interglacial period (130–115 kyr) climate (close to 4.0 °C warmer than present with reduced ice-sheet extent globally) could be the best candidate to help understand the impacts of future climate change on the Caspian Sea. However, there are limited palaeo-environmental records for validation and model initial (boundary) conditions for this time period. Putting aside those limitations, these results objectively identified the relative importance of different driving factors and their associated impacts on the extreme Caspian Sea level variations during the late Quaternary.

5.1.2 How significant is the effect of Caspian Sea surface area changes on the regional and large scale hydroclimate?

The change in Caspian Sea surface area is highly influenced by the variation in its water level, due to the shape of the lake bathymetry (see Fig. 1.4). Therefore, to understand the feedbacks of Caspian Sea surface area changes and the potential impacts on the climate in the regional catchment and large-scale hydroclimate, CESM1.2.2 (fully coupled global climate model) was used to perform sensitivity experiments for three realistic representations of the Caspian Sea sizes and one experiment without considering the Caspian Sea (Chapter 3), all under pre-industrial boundary conditions. The Caspian Sea surface area affects regional climate over the catchment as well as large-scale climate over the entire northern hemisphere. The strongest influence objectively identified is on the regional atmospheric water budget as well as on the near surface temperature. The water budget (precipitation minus evaporation) increases as the Caspian Sea surface area increases. Presence of larger Caspian Sea has a potential to increase the mean annual precipitation up to 75% over the Caspian Sea and 20% over the Caspian Sea basin, and also a fourfold increase in the mean annual evaporation over the Caspian Sea is observed. Since a larger surface area enhances evaporation from the lake surface, adding more moisture to the atmosphere, this affects both the water budget of the region as well as large-scale hydroclimate and global atmospheric circulation.

The impacts of the Caspian Sea surface area change are not limited to the influence on the catchment climate, but its impacts extend eastward, as far as the north-western Pacific. Larger Caspian Sea impacts include enhanced precipitation over central Asia and increased warming further as far as east Siberia and North-western Pacific, accompanied by reduced Pacific sea ice. These results suggest that the Caspian Sea Surface area change plays a key role in the large scale processes. Therefore, if the Caspian Sea is ignored in a model's boundary conditions or an inaccurate size of Caspian Sea is prescribed, this could lead to climate biases in the catchment as well as over the broader northern hemisphere.

In global climate models in general large lakes (e.g., the Caspian Sea) are either completely overlooked or included as a large shallow pool of surface water (e.g., MIROC-ESM, CESM1-CAM5) , and this affects heat capacity and storage. One recent study examined the Great

lakes representation in CMIP5 models, and found that most models do not correctly simulate the Great Lakes impact on the regional climate due to the way they are prescribed (Briley et al., 2021). Likewise, this thesis has found that realistic representation of the Caspian Sea area is necessary for robust modelling of paleo climate states, and climate projections for the 21st century. Given the rapid and large variations in area that the Caspian Sea has potential for, and the size of the climatic impacts, climate models should consider developments to better prescribe or interactively model the Caspian Sea. For example, a study by Xue et al. (2017) investigated a two-way coupled 3D lake-climate regional modelling system for the Great Lakes, which significantly improved the thermal structure, surface fluxes, and ice compared to previous studies.

Such a modelling methodology as described above could be implemented for the Caspian Sea using global circulation or earth system models to improve lake-atmosphere feedbacks. On the other hand, perhaps the more important factor for the Caspian is the feedback with the rapidly changing surface area of the lake, and in this case the introduction of a computationally expensive 3D lake model may not be needed and would possibly even be prohibitive to the incorporation of changing land-sea mask boundary conditions. A previous study explored this aspect using an offline lake hydrology model for Lake Chad to asynchronously couple the changing lake area boundary condition to a low-resolution climate model (Farrow, 2012), although biases in the climate model (particularly precipitation distribution) were still evident and negatively impacted the coupling process. A first step for the Caspian could involve offline coupling of a 2D lake circulation model (latitude-depth, to capitalise on the lake's long north-south orientation) to improve temperatures and surface fluxes over the lake with a water balance hydrology model to calculate the surface water area.

There are also ongoing and future research initiatives to advance the modelled processes in terrestrial water cycle models that will eventually consider incorporating these sorts of lake processes (e.g., Hydro-JULES; Dadson et al., 2019) Other major international initiatives are aiming to create cloud-based exa-scale high-resolution (1km) 'digital-twin' models that will take in real-time data to radically advance our ability to make predictions and model the societal implications (e.g., Destination Earth; Nativi and Craglia, 2020), although it will be several years before such models are available. This study demonstrates the importance of

considering the interactive modelling of Caspian Sea processes that should be taken into consideration in these huge modelling initiatives.

5.1.3 What is the fate of the Caspian Sea under projected climate change and human interventions?

In contrast to the global ocean, the land-locked Caspian Sea has declined over the last two decades and currently its level is at 28 m below mean sea level. It is vital to explore its future fate under anthropogenic climate change and pressures from population growth/decline and change in lifestyle. Therefore, it is necessary to assess the representation of Caspian Sea in the CMIP models as well as the impacts from future water extractions and anthropogenic climate change. The change in Caspian Sea surface area is a determining factor of hydroclimate over the Caspian Sea basin, as well as large part of the northern hemisphere (Chapter 3). Chapter 4 examined future hydroclimate projections using selected global climate models from CMIP5 and CMIP6 and considered idealized water extraction scenarios.

The representation of the Caspian Sea in CMIP models varies considerably, with many of the climate models either ignoring or poorly prescribing the Caspian Sea surface area. Consequently, models with a larger prescribed Caspian Sea experience decreased water budgets over the Caspian Sea basin during the historical period as well as the 21st century. Drying of the water budget during the 21st century is observed in both CMIP5 and CMIP6 climate models. The drying is more pronounced for the high emissions scenario and with larger Caspian Sea size, owing to increased lake evaporation that is not balanced by increasing river discharge or precipitation. These results reiterate how significant the impact of the Caspian Sea size is on the regional hydroclimatic changes, as also shown in Chapter 3. Care needs to be taken when interpreting the future water budget variations over the Caspian Sea basin from CMIP climate models, as the change in water budget (and the Caspian Sea level) is highly dependent on the size of the Caspian Sea prescribed in the climate model.

Though human interventions are an integral part of the future climate change, not all aspects of anthropogenic impacts are considered in climate models. Human water extraction is one such impact with relevance to Caspian Sea level variations, explored in Chapter 4. During the historical period, human interventions in the Caspian Sea basin has played

considerable impact on Caspian Sea level variations. This is because many artificial reservoirs have been built to address the societal demands of the communities residing in the Caspian Sea drainage basin. As a result, a considerable amount of water is currently stored in those reservoirs, and this has hindered natural hydrological processes. This study has found that water extraction rates are likely to be as important as climate change in controlling future Caspian Sea level. The result shows that up to 7 m additional decline in the Caspian Sea level is projected considering water extraction scenarios, and combined with the projected decline due to climate change, this could be up to 37 m decline in Caspian Sea level by the end of the 21st century. A decline in the Caspian Sea translates to a large decrease in surface area and this will have an enormous implications (e.g., on the availability of fresh water, vulnerability to loss of livelihood; Prange et al., 2020) for the many millions of inhabitants that are dependent on the Caspian Sea, especially for the coastal communities and the surrounding nations, as well as on the bio-ecosystems.

This research work has shown that the Caspian Sea plays a vital role in the variability of the regional and large-scale climate systems on the northern hemisphere. This can help understand the sensitivity of the biodiversity of the Pontocaspian basin (e.g. endemic fauna) to previous climate (and connectivity between Black Sea and Caspian Sea) changes. However, due to limitations of data and time constraints, the new palaeo-records generated by other projects in the PRIDE project were not of the right timing to compare with the existing climate simulations. As such, the integration of the various PRIDE work packages was not as expected at the outset of the project. Given the future projections for the CS based on CMIP6, it does seem increasingly likely that the connections between the lakes of the Pontocaspian region are unlikely to occur in a future warming climate, but that desiccation of the large northern shallow region may impact the niche distribution of fauna, which is a factor that future biodiversity studies should urgently examine.

5.2 Future work

This thesis has highlighted that the Caspian Sea is an important component of the regional and large-scale hydroclimate cycle, where changes in its water level and area significantly affect the hydroclimate and bio-ecosystem of the Ponto-Caspian region. As presented in Chapter 2, the Caspian Sea has experienced large variations in water level from tens to

hundreds of meters on various time scales leading to substantial changes in its surface area. This can potentially be reflected in the hydroclimate changes of the regional catchment and large-scale circulation patterns in the northern hemisphere (Chapter 3). Chapter 3 (and several other studies, e.g., Arpe et al., 2019) only examined at the impact of prescribed lake area on the atmosphere, but the whole feedback loop was not examined. As also shown in Chapter 4, many climate models either ignore or do not properly prescribe Caspian Sea area, and no future projections include any changes in Caspian Sea, even though the catchment is projected to be drier, with potential for considerable decrease in lake area. On the other hand, other studies (e.g. Turuncoglu et al., 2013a; Turuncoglu et al., 2013b; Xue et al., 2017) have used regional climate modelling schemes, since regional climate modelling is better for resolving large-lake hydrodynamics and interactions with the overlying atmosphere. However, regional climate modelling suffers from limitations related to lateral boundary conditions (no large-scale atmospheric feedbacks) and this has implications for Caspian Sea feedbacks as its impacts reach far afield to the northwest Pacific. Therefore, coupling between modelled climate and lake using a fully coupled global model is necessary, where the feedbacks are dealt both ways, from lake to the atmosphere and vice versa for the changing Caspian Sea surface area. Climate projections that include feedbacks from the Caspian Sea would better inform environmental risk management and future planning for the region of industrial, agricultural, and domestic water extraction as well as other activities including fisheries and shipping.

Lakes in general can influence local and regional as well as large-scale climate by the effects they have on the different radiative and thermal properties (Lofgren, 1997; Long et al., 2007; MacKay et al., 2009; Samuelsson et al., 2010). Therefore, how lakes are modelled in various models could affect their feedbacks and climate impacts. The circulation patterns of the Caspian Sea itself have not been considered in this study. However, the Caspian Sea has three zones of circulation due to the slightly saline water, the shape of the lake (bathymetry and elongated surface area in the north-south direction) and locations of riverine input (Dyakonov and Ibrayev, 2019; Leroy et al., 2020). Circulation in the sea is both wind-driven and thermohaline (density-driven) in nature. Potential future climate changes that may impact the distribution of the heat structure and the salinity regime may have implications for the variability of the sea surface temperature and evaporation rate over the sea (Diansky

et al., 2018; Jamshidi, 2017; Komijani et al., 2019). However, such processes require high spatiotemporal resolutions which would be prohibitively expensive computationally to set-up. However, information from such a high resolution regional modelling scheme or observations could be used to parameterize simpler lake models or to prescribe lake fields in global models.

Another aspect of Caspian Sea studies that needs greater attention is the limitation of data for various geophysical characteristics during palaeo and recent past periods, which makes it difficult to evaluate model outputs. For example, two late-glacial sources of runoff to the palaeo-Caspian Sea have been proposed in the literature: (1) Siberian region meltwater complemented by proglacial lakes outburst via Aral Sea (Mangerud et al., 2004), or (2) glacial melt from the Himalayan plateaus via Amu-Syr-Darya river basin (Leroy et al., 2013). However, reconstruction of the geophysical evidence of this route was limited, with only low spatiotemporal resolution of topographic records currently available from which to reconstruct the late Quaternary period. Therefore, collection of additional palaeotopography and palaeoriver channel flows are essential to better evaluate the model.

Similarly, the hydroclimatic model results used to understand water budget changes during the late Quaternary are based on HadCM3, and the results could be sensitive to this choice of model and the way the model experiment was set up. In addition to being a relatively low spatial resolution model, 'snap-shot' simulations at regular 1ka intervals were used, assuming that the climate is in equilibrium at each time slice. While previous model-data comparisons suggest that this is a reasonable assumption (e.g., Singarayer et al., 2017; Singarayer and Valdes, 2010), it would be interesting to compare this with transient simulations, especially considering the importance of millennial-scale events (such as the Younger Dryas) to the Caspian Sea. Consideration of a spatially distributed hydrological routing model based on better representation of palaeo-topographic information and with climate models of higher temporal and spatial resolution would be needed to explore remaining questions concerning palaeo-runoff sources and timings.

Currently, the Caspian Sea is fed by hundreds of rivers from 9 different countries where most water resource uses are based on political boundaries of every nations. Therefore, there are differences in water use policy and lack of co-ordination at the regional level.

Furthermore, as shown in this study and many others (e.g. Akbari et al., 2020; Prange et al., 2020) the northern shallow part of the Caspian Sea is susceptible to desiccation, and consequently, most of the bio-environments, with many millions of inhabitants, in the Caspian Sea basin are at great risk to loss of livelihoods due to loss of industries based near water (e.g. fisheries, oil) and agriculture. Despite the potential impact of Caspian Sea on the regional and large scale climate as well as its vulnerability to human interventions due to various activities (e.g., water extraction, oil exploration), less attention has been given to the Caspian Sea from international organizations (e.g., IPCC) compared to global ocean (Prange et al., 2020). Therefore, development of environmental risk assessments for future water use scenarios, coastal development, and coordination of transboundary mitigation and adaptation strategies, which incorporates the participation of various stakeholders involved in the region are vital to implement. Mitigation and conservation measures should take into consideration the issues concerning uncertainties due to inter model differences in projected climate (as some models show decline and some an increase in sea level) as well as for large interannual variability of Caspian Sea level (as observed in the historical sea level record). In order to take into account the uncertainties in projections, risk management could be achieved by employing event-based storyline approach where emphasis are put on plausibility rather than probability and by prioritising based on the severity of the risk anticipated (Arnell et al., 2021; Sillmann et al., 2021).

6. Appendices

6.1 Appendix 1: Supplementary information for 'What are the drivers of Caspian Sea level variation during the late Quaternary?'

Table S6.1. Caspian Sea palaeo transgressive and regressive stages from start of late Pleistocene until early Holocene.

High-(low)stand	Age (kyr BP)	Caspian Sea level (m a.s.l.)	Reference
Late Khazarian transgression	143–76	20	Sorokin (2011)
	130 - 76	-10 to 20	Mamedov (1997)
	?	-10	Yanina (2014); Yanina et al. (2018)
	127(130)–122	?	Shkatova (2010)
	130–80	5-10	Levchenko and Roslyakov (2010)
Atelian regression	85-75	-120 to -140	Krijgsman et al. (2019) and references therein
	70–50	-100	Sorokin (2011)
	?	-140	Yanina (2014)
Early Khvalynian transgression	32-25 ka	- 5 to 0	Mamedov (1997)
	?	+50	Tudryn et al. (2013)
	30 – 17	?	Shkatova (2010)
	30-21	?	Bezrodnykh et al. (2004)
	>40–25	50	Sorokin (2011)
	?	50	kroonenberg et al. (1997); Kroonenberg et al. (2005)

High-(low)stand	Age (kyr BP)	Caspian Sea level (m a.s.l.)	Reference
Enotaevkan regression	24-17	-50	Mamedov (1997)
	?	-80 to -100	Tudryn et al. (2013)
	?	-105	Krijgsman et al. (2019) and references therein
	~17	-70	Sorokin (2011)
Mangyshlak regression	?	-75	Tudryn et al. (2013)
	9-7	-73 to -75	Bezrodnykh et al. (2004)
	12.4-9.5	-80	Bezrodnykh and Sorokin (2016)
	9.8-7.5	-70 to -75	Sorokin (2011)
	~9	-80 to -113	Kroonenberg at al. (2008) and references therein
	10-8.5	-110	Mayev (2010)
	~11.6-8	-90	Bezrodnykh et al. (2020)
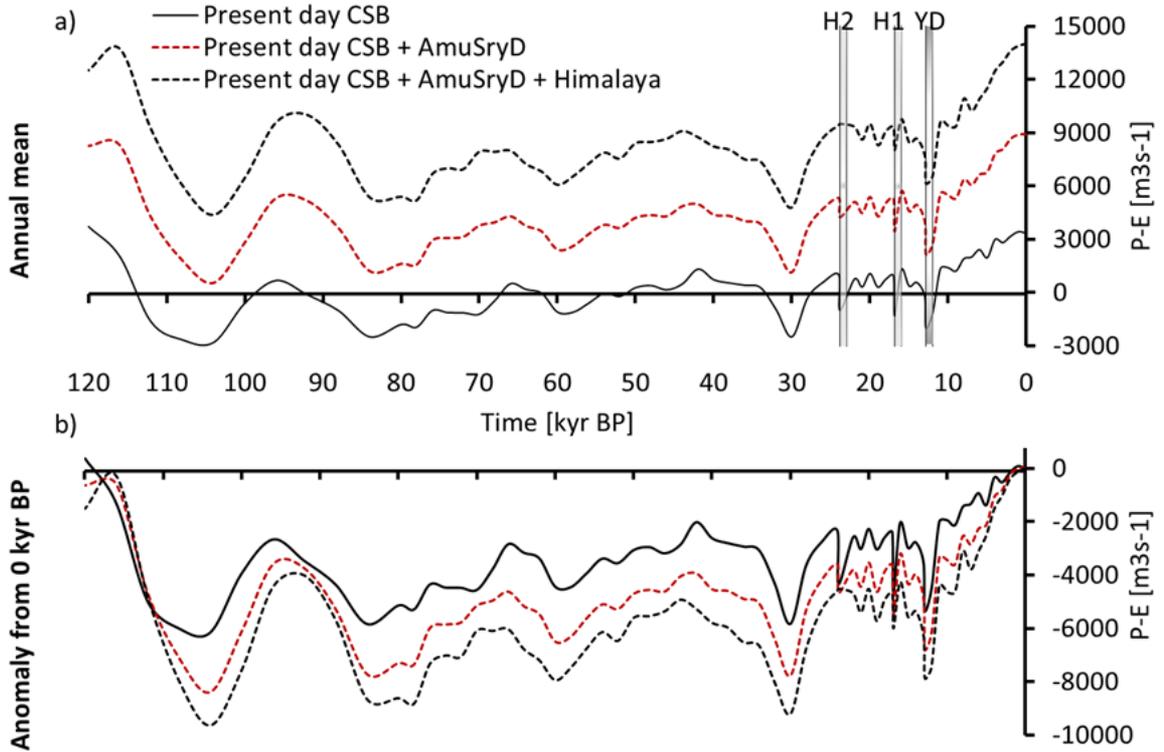
Figure S6.1. Caspian Sea, Amu-Syr Darya and the whole Himalayan drainage basins water budget (P-E) based on HadCM3 climate for all time-slice simulations covering the last 120 kyr: a) Annual mean precipitation minus evaporation (P-E), b) annual mean P-E anomalies from pre-industrial. Some key climate events are indicated by shaded bars and their common names (Younger Dryas – YD, and Heinrich – H).
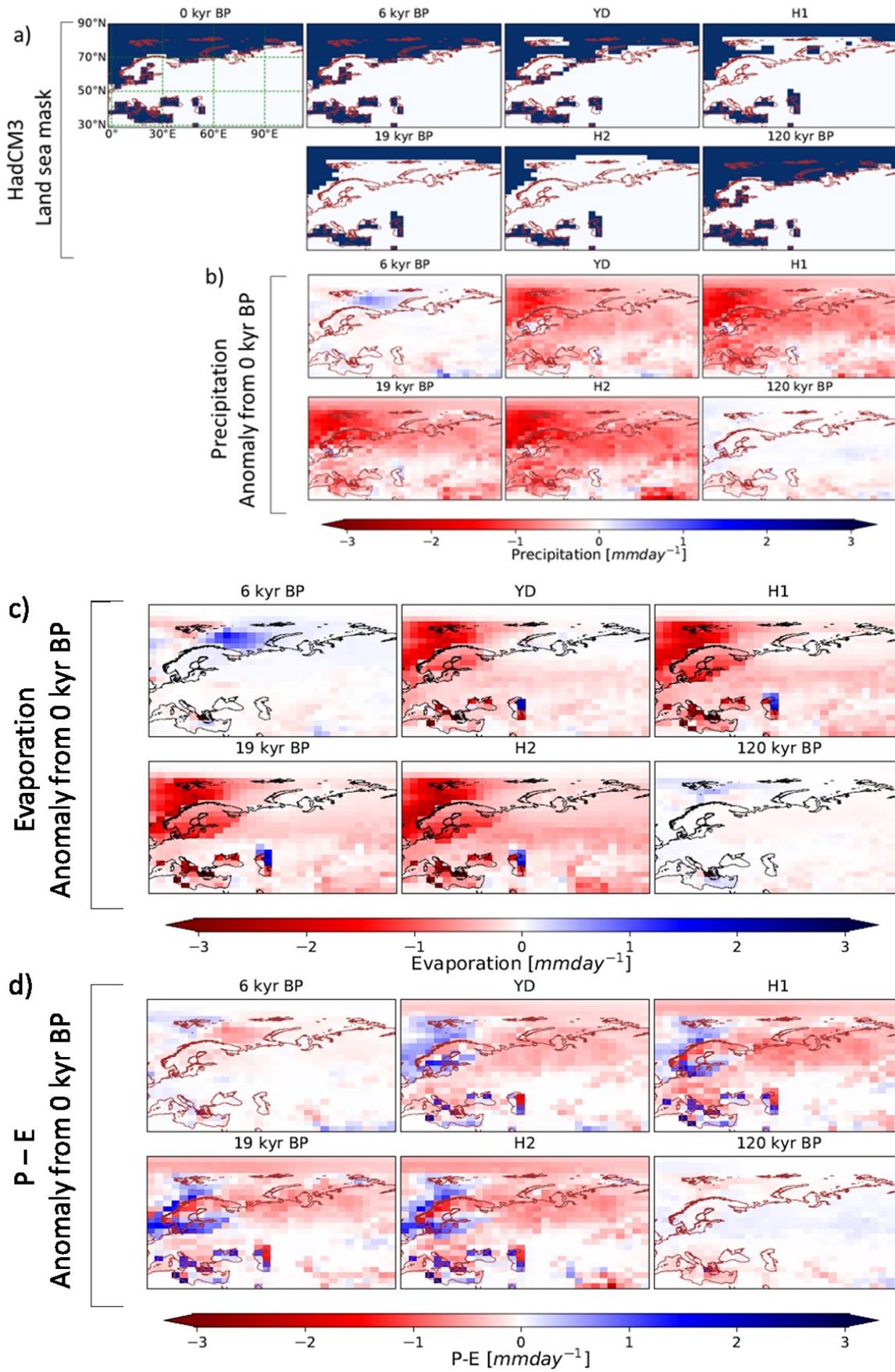
Figure S6.2. Spatial map showing (a) HadCM3 land sea mask, (b) annual mean precipitation anomalies from pre-industrial, (c) annual mean evaporation anomalies from pre-industrial, and (d) annual mean P-E anomalies from pre-industrial for 6k, YD-Younger Dryas, H1- Heinrich event 1, 19k, H2- Heinrich event 2 and 120k years before present.
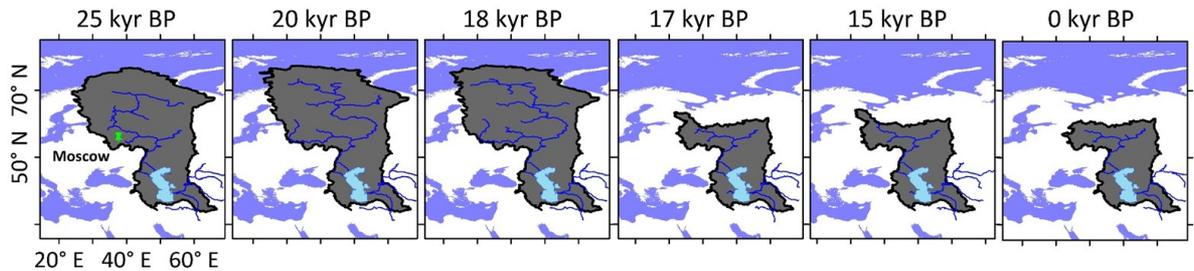
Figure S6.3. Spatial map showing Caspian Sea basin outline and river network for 0k, 15k, 17k, 18k, 20k and 25k years before present. The spatial map is based on ICE-6G_C topography data corrected for glacial isostatic adjustment using algorithm described by Kendall et al. (2005) and combined with present day high resolution digital elevation model (DEM). Drainage basins are delimited in dark grey shaded area and blue lines represent the respective river flow direction. The white and blue colour backgrounds are present day land and sea mask respectively.
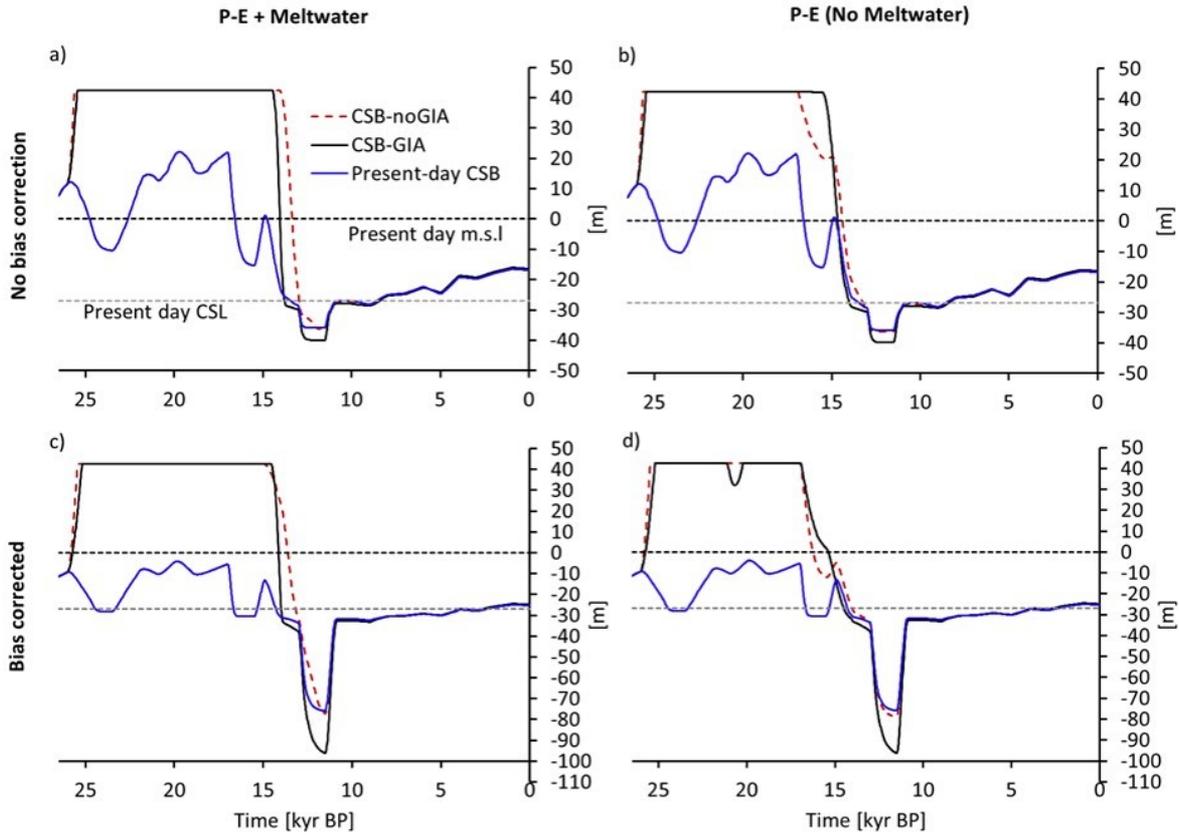
Figure S6.4. Caspian Sea level variation using HadCM3 P-E, ICE-6G_C ice melt, and basin shape changes identified as CSB-noGIA, CSB-GIA (see Fig. 2.7) and Present-day CSB (see Fig. 2.2). Without (a) and with (c) bias-correction of simulated Caspian Sea level using HadCM3 P-E integrated over palaeo CSB-noGIA and CSB-GIA plus ice-sheet melt. Without (b) and with (d) bias-correction of simulated Caspian Sea level using HadCM3 P-E integrated over palaeo CSB-noGIA and CSB-GIA without ice-sheet melt contribution. The blue line is used as control and it represents Caspian Sea level based on HadCM3 P-E within present day Caspian Sea basin.

136
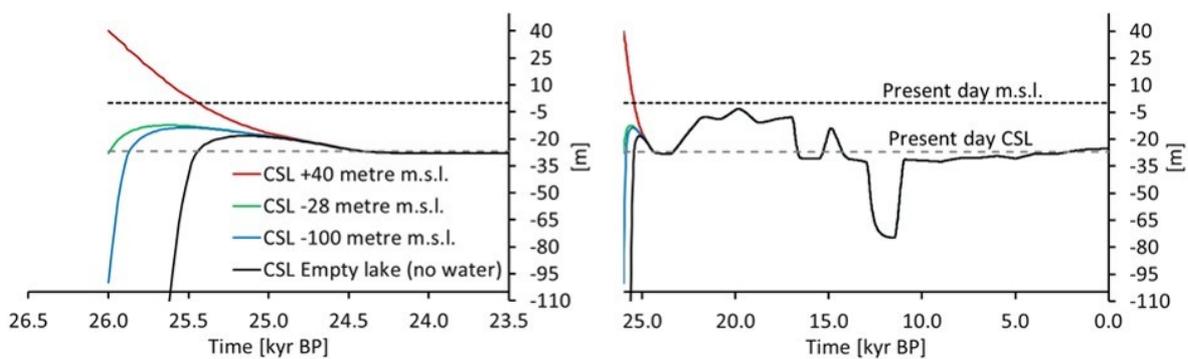
Figure S6.5. Tests of the lake model response to different initial conditions for lake volume.

6.2 Appendix 2: Supplementary information for 'Impacts of variations in Caspian Sea surface area on catchment-scale and large-scale climate'
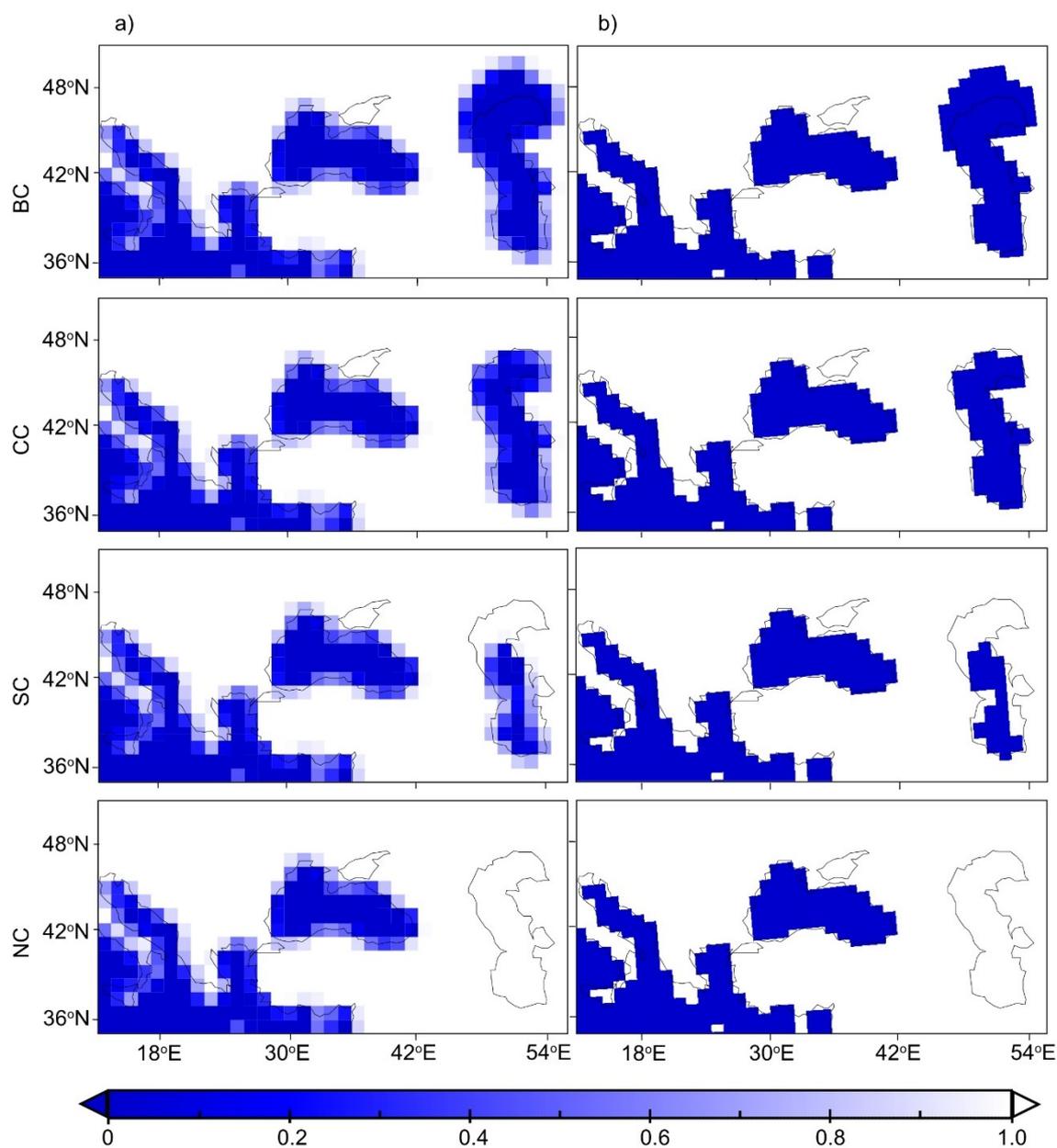
Figure S6.6. Caspian Sea land-sea mask: a) as in atmospheric model, and b) as in ocean model. (Key: BC – Large Caspian Sea, CC – Present-day Caspian Sea, SC – small Caspian Sea, NC – No-Caspian Sea).
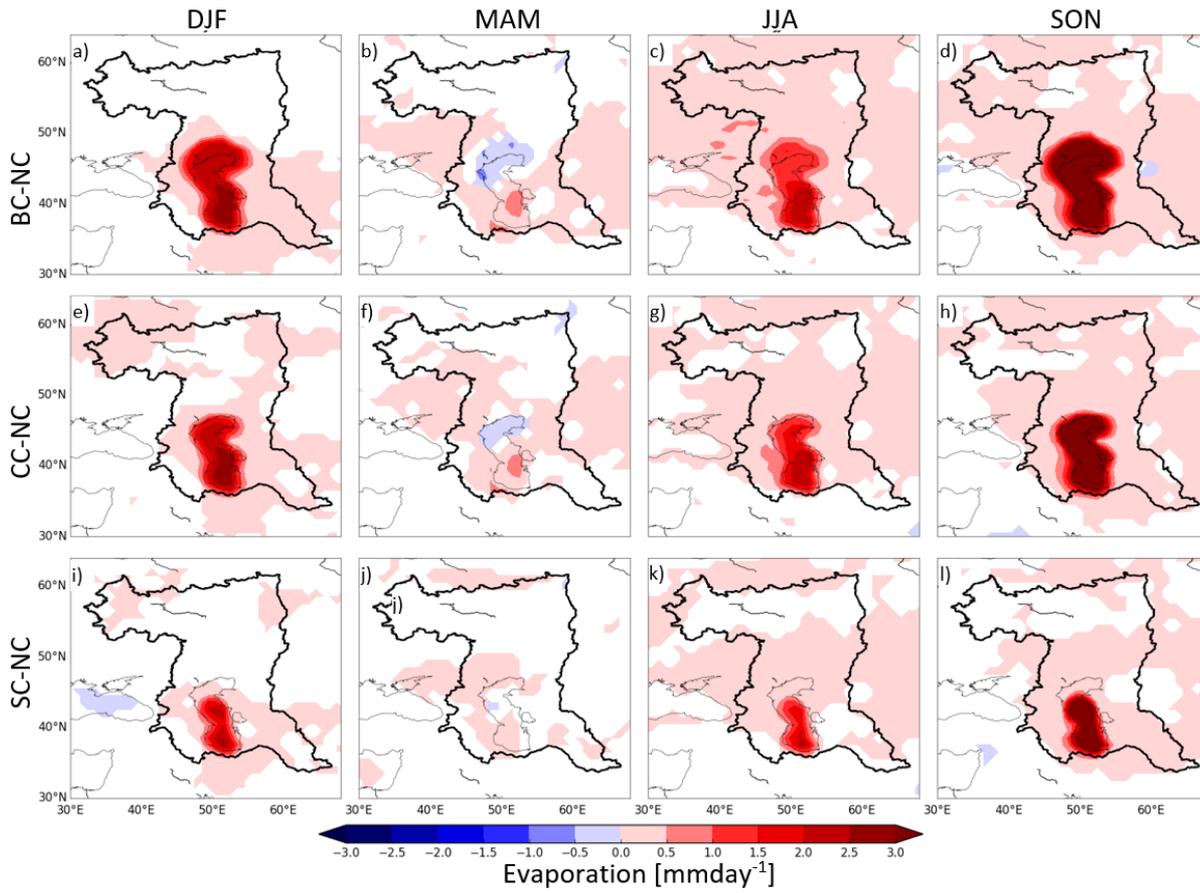
Figure S6.7. Statistically significant changes in seasonal mean evaporation of large (BC), current (CC) and small (SC) CS with respect to no-Caspian Sea scenario. The shaded colours are areas where mean anomaly is different from zero at 95% confidence level.
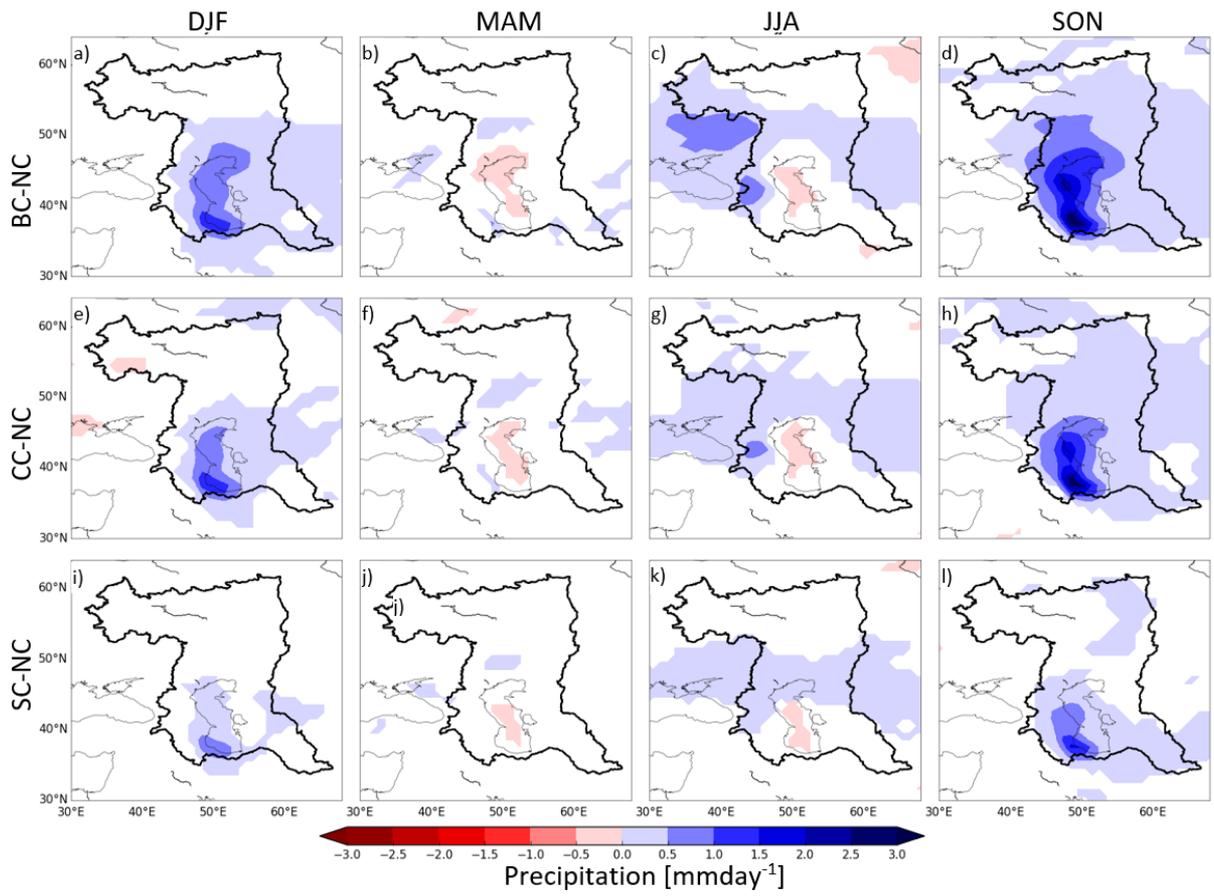
Figure S6.8. Same as 6.70 but for precipitation changes.
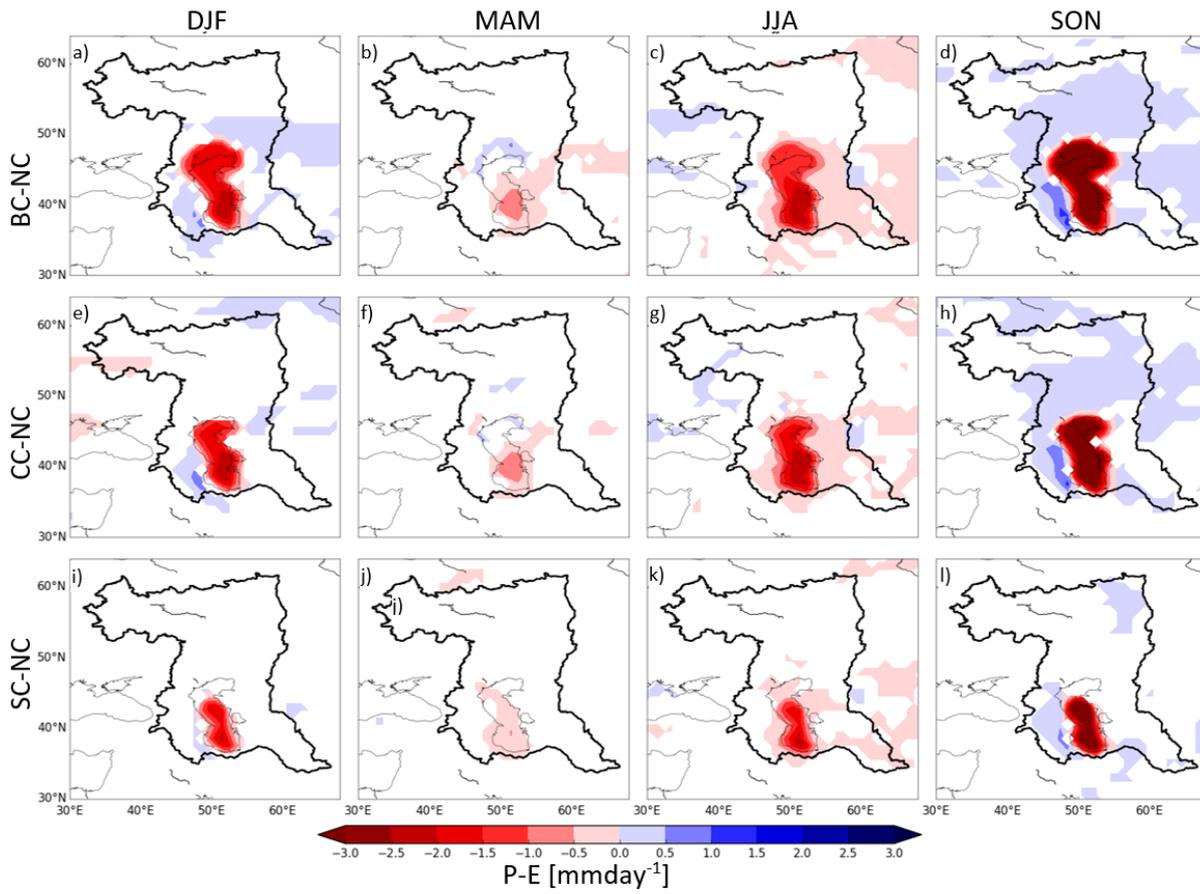
Figure S6.9. Same as 6.70 but for precipitation minus evaporation (P-E) changes.
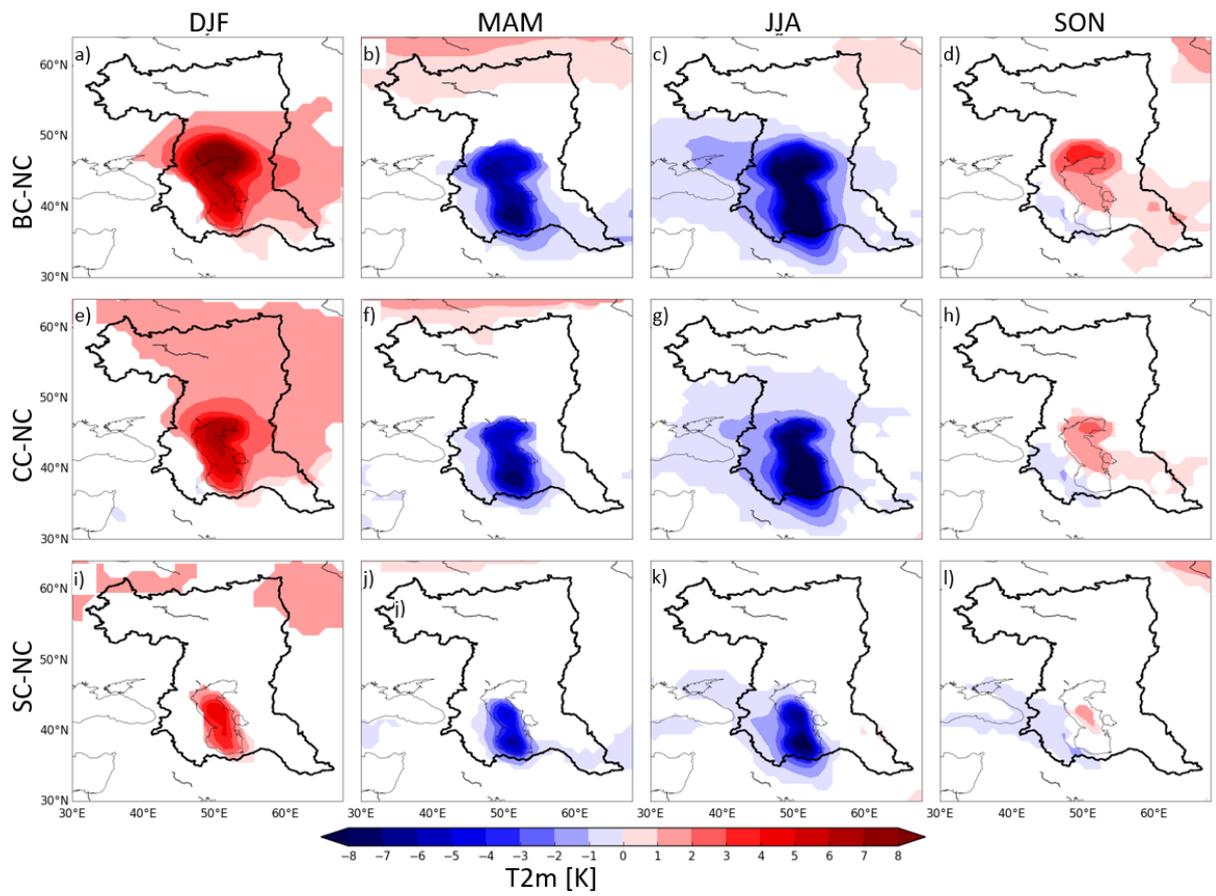
Figure S6.10. Same as 6.70 but for 2-m air temperature (T2m) changes.
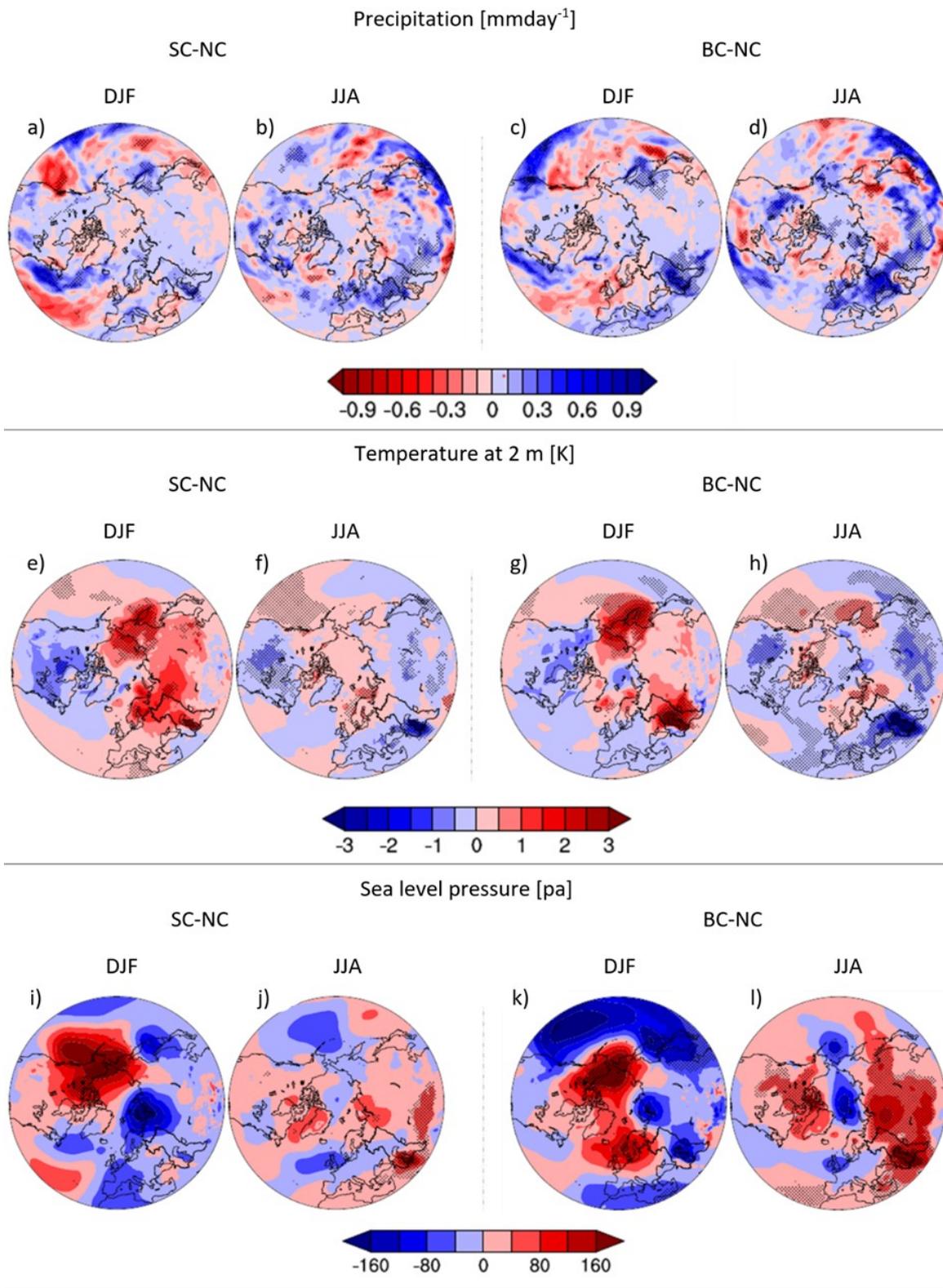
Figure S6.11. Statistically significant changes in seasonal mean precipitation (a-d), 2-m air temperature (e-h) and sea level pressure (i-l) for small Caspian (SC) and big Caspian (BC) with

respect to no-Caspian (NC) scenario. Stippling indicates regions where the change is statistically significant at the 95% level based on a Student's t-test.
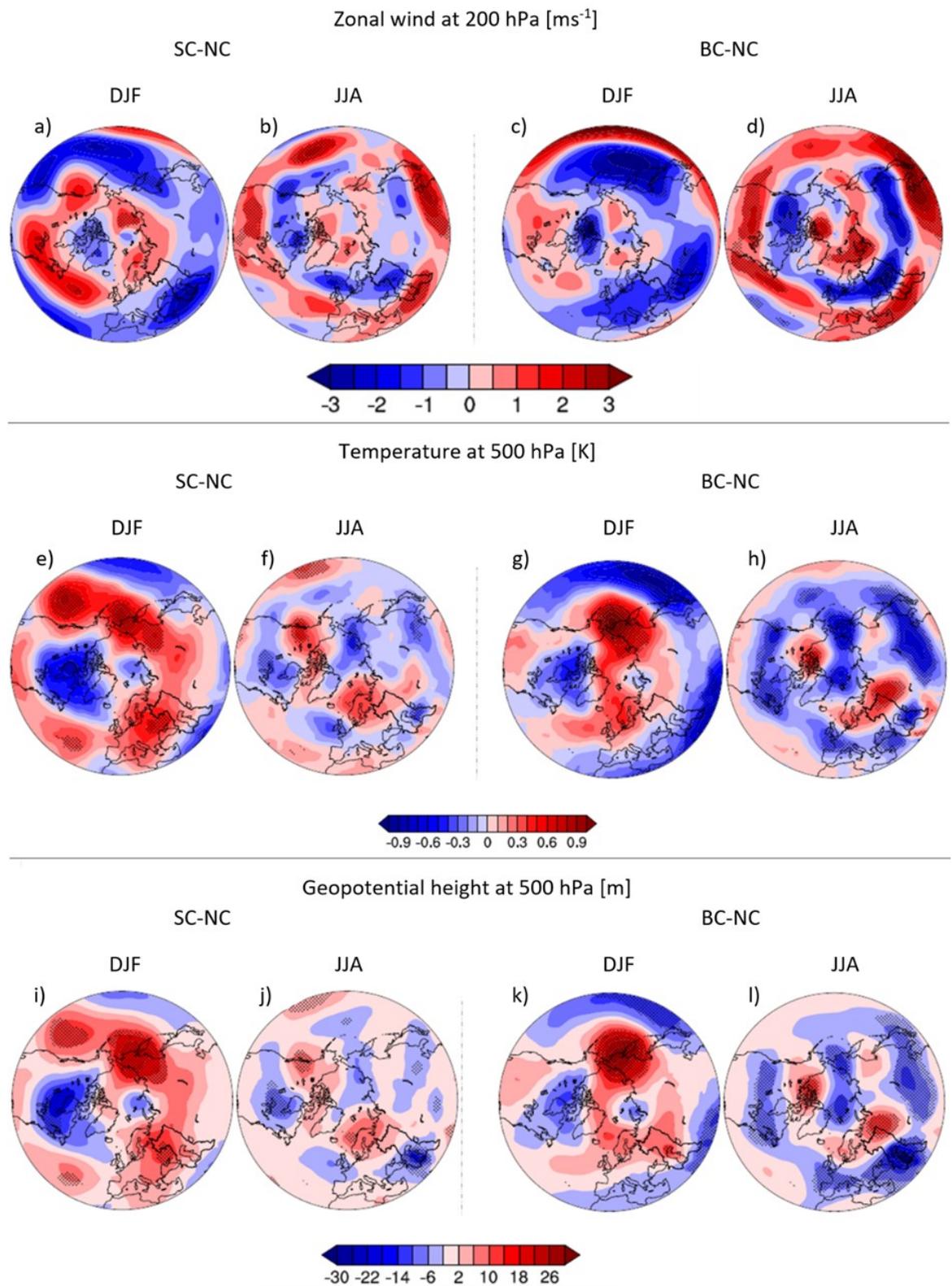
Figure S6.12. Same as 6.11 but for zonal wind at 200 hPa (a-d), temperature at 500 hPa (e-h) and geopotential height at 500 hPa (i-l).
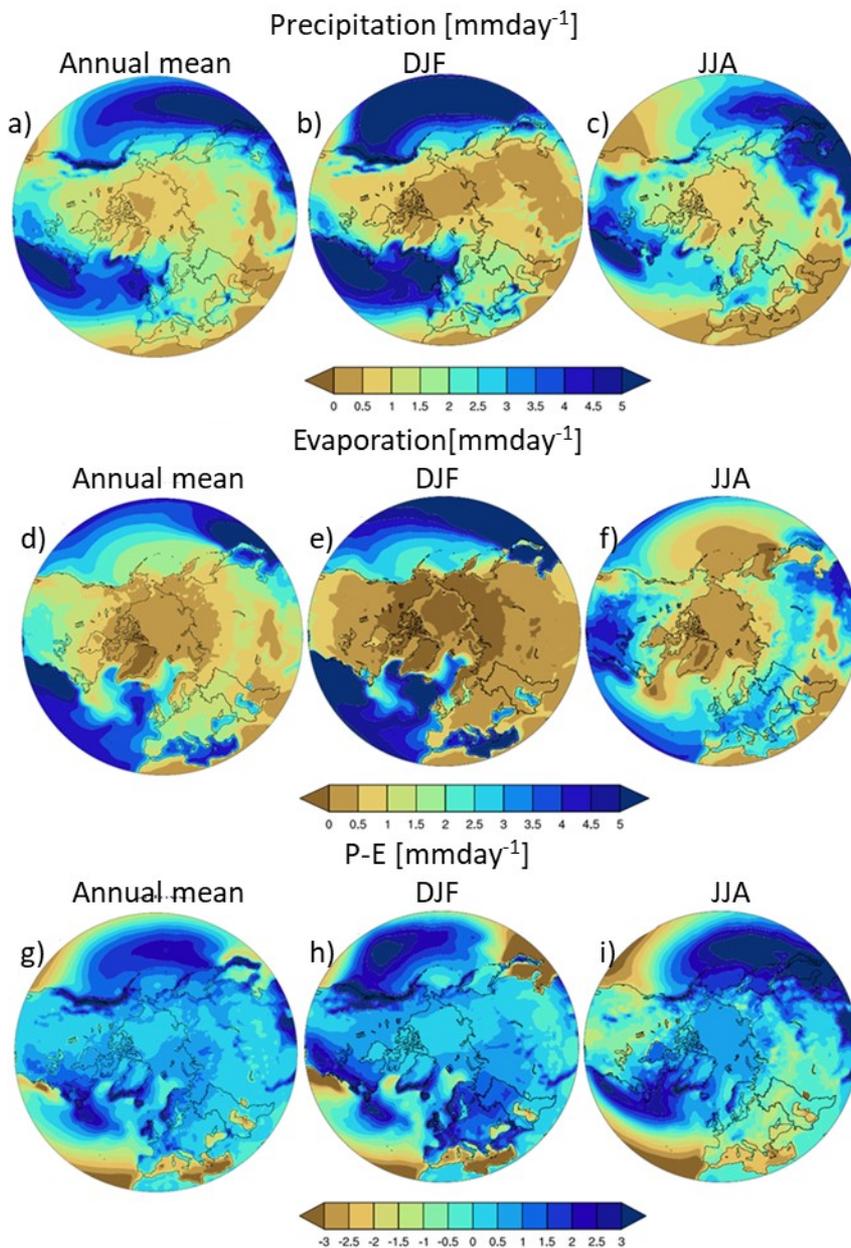
Figure S 6.13. Annual, winter (DJF-December/January/February), and summer (JJA-June/July/August) mean climatologies for the Current Caspian simulated fields of precipitation (a-c), evaporation (d-f), and precipitation-evaporation (P-E) (g-i) in mm/day.
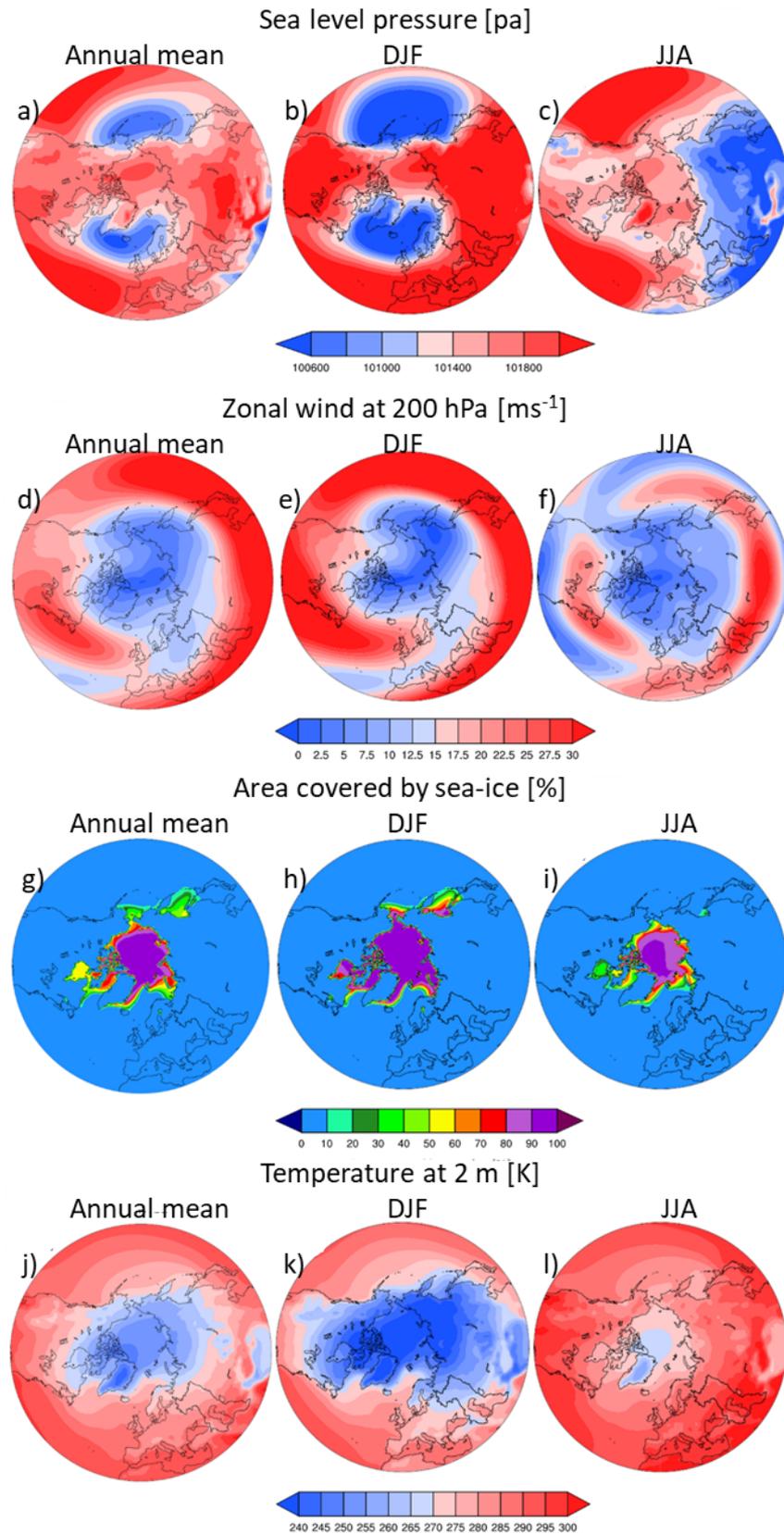
Figure S6.14. Same as 6.13 but for sea level pressure in Pa (a-c), zonal wind a 200 hPa in m/s (d-f), percentage area covered by sea-ice (g-i), and 2-m air temperature in Kelvin (j-l).

6.3 Appendix 3: Supplementary information for 'The fate of the Caspian Sea under projected climate change and water extraction during the 21st century'

Table S6.2. List of CMIP6 models used in this study. Asterisks indicate the models used for evaluating the historical and future water budget change, and simulating projected CS level for the 21st century.

Model	Institution	Resolution (Lon×Lat)
AWI-CM-1-1-MR*	The Alfred Wegener Institute	384×256
CESM2	National Center for Atmospheric Research (NCAR), USA	288×192
CESM-WACCM		288×192
CMCC-CM2-SR5*	Centro Euro-Mediterraneo per i Cambiamenti, Italy	362×292
EC-Earth3*	EC-Earth-Consortium	512×256
EC-Earth3-Veg*		512×256
FGOALS-f3-L	Chines Academy of Sciences, China	288×180
GFDL-ESM4	Geophysical Fluid Dynamics Laboratory, USA	288×180
INM-CM4-8*	Institute for Numerical Mathematics, Russia	180×120
INM-CM5-0*		180×120
MPI-ESM1-2-HR*	Max Planck Institute for Meteorology, Germany	384×192
MRI-ESM2-0	Meteorological Research Institute, Japan	320×160
NorESM2-MM	NorESM climate modeling Consortium of CICERO, MET-Norway, NERSC, NILU, UiB, UiO and UNI, Norway	288×192

Table S6.3. List of CMIP5 models used in this study. Asterisks indicate the models used for evaluating the historical and future water budget change, and simulating projected CS level for the 21st century.

Model	Institution	Resolution (Lon×Lat)
ACCESS1-0	Commonwealth Scientific and Industrial Research Organisation and Bureau of Meteorology, Australia	192×145
ACCESS1-3		192×145
bcc-csm1-1	Beijing Climate Center, China Meteorological Administration, China	128×64
BNU-ESM	Beijing Normal University, China	128×64
CanESM2	Canadian Centre for Climate Modelling and Analysis, Canada	128×64
CESM1-BGC*	National Center for Atmospheric Research (NCAR), USA	288×192
CESM1-CAM5*		288×192
CESM1-WACCM		144×96
CMCC-CM*	Centro Euro-Mediterraneo per i Cambiamenti, Italy	480×240
CMCC-CMS		192×96
CNRM-CM5	Centre National de Recherches Meteorologiques, Meteo-France, France	256×128
CSIRO-Mk3-6-0*	Australian Commonwealth Scientific and Industrial Research Organization, Australia	192×96
EC-EARTH	EC-Earth (European Earth System Model)	320×160
FGOALS-g2	Institute of Atmospheric Physics, Chinese Academy of Sciences, China	128×60
FGOALS-s2		128×108
GFDL-CM3	Geophysical Fluid Dynamics Laboratory, USA	144×90

Model	Institution	Resolution (Lon×Lat)
GFDL-ESM2G		144×90
GISS-E2-H	Goddard Institute for Space Studies, USA	144×90
GISS-E2-H-CC		144×90
GISS-E2-R		144×90
HadGEM2-CC*	Met Office Hadley Centre, UK	192×145
HadGEM2-ES*		192×145
inmcm4*	Institute for Numerical Mathematics, Russia	180×120
IPSL-CM5A-LR	Institut Pierre-Simon Laplace, France	96×96
IPSL-CM5A-MR		144×143
IPSL-CM5B-LR		96×96
MIROC5	AORI (Atmosphere and Ocean Research Institute), NIES (National Institute for Environmental Studies), JAMSTEC (Japan Agency for Marine-Earth Science and Technology), Japan	256×128
MIROC-ESM*		128×64
MIROC-ESM-CHEM*		128×64
MPI-ESM-LR*	Max Planck Institute for Meteorology, Germany	192×96
MPI-ESM-MR*		192×96
MRI-CGCM3	Meteorological Research Institute, Japan	320×160
NorESM1-M	Norwegian Climate Centre, Norway	144×96

Table S6.4. Projected population numbers for the 21st century for countries in the CS catchment, taken from Vollset et al. (2020) using their 'pace' scenario that hits the United Nations Sustainable Development Goals. These are used to form the third water extraction scenario, FWE3, described in section 2.3. From the numbers we estimate a peak population

in the countries that are within the Caspian catchment to be ~ 410 million at approximately 2050, before then declining to 310 million by 2100.

Country	2017 population (millions)	2100 pace scenario pop. (millions)	Peak pop. (peak pop. year)
Azerbaijan	10.23	5.75	11.46 (2045)
Iran	82.18	62.23	95 (2049)
Kazakhstan	17.9	23.24	
Russia	146.19	89.37	146.19 (2017)
Turkmenistan	4.98	5.94	
Armenia	3.03	1.33	(2022)
Georgia	3.69	1.85	3.69 (2017)
Turkey	80.46	86.10	112 (2068)
Uzbekistan	32.24	34.38	45 (2076)
Total	**380.9**	**310.2**	
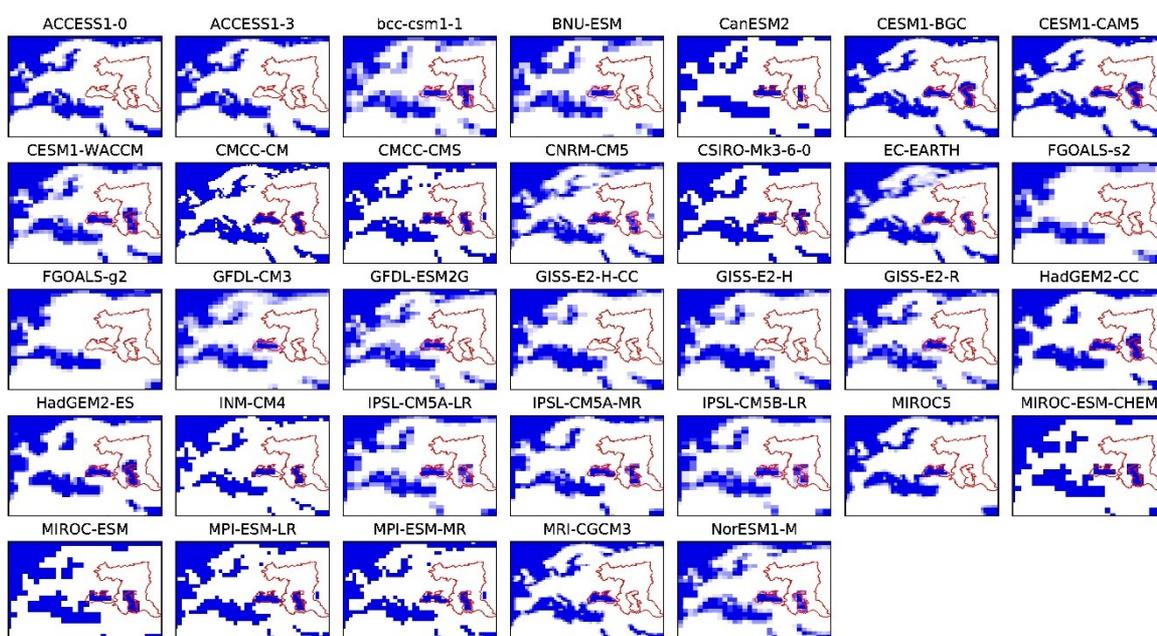
Figure S6.15. Land-sea mask map for CMIP5 models.
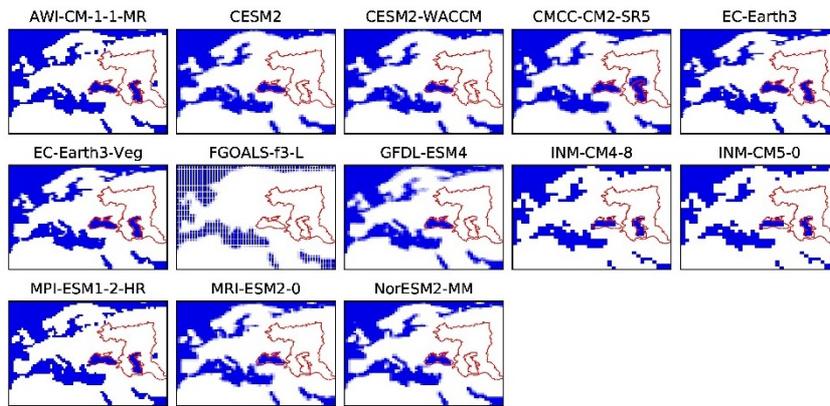
Figure S6.16. Land-sea mask map for CMIP6 models available at the time of the study.
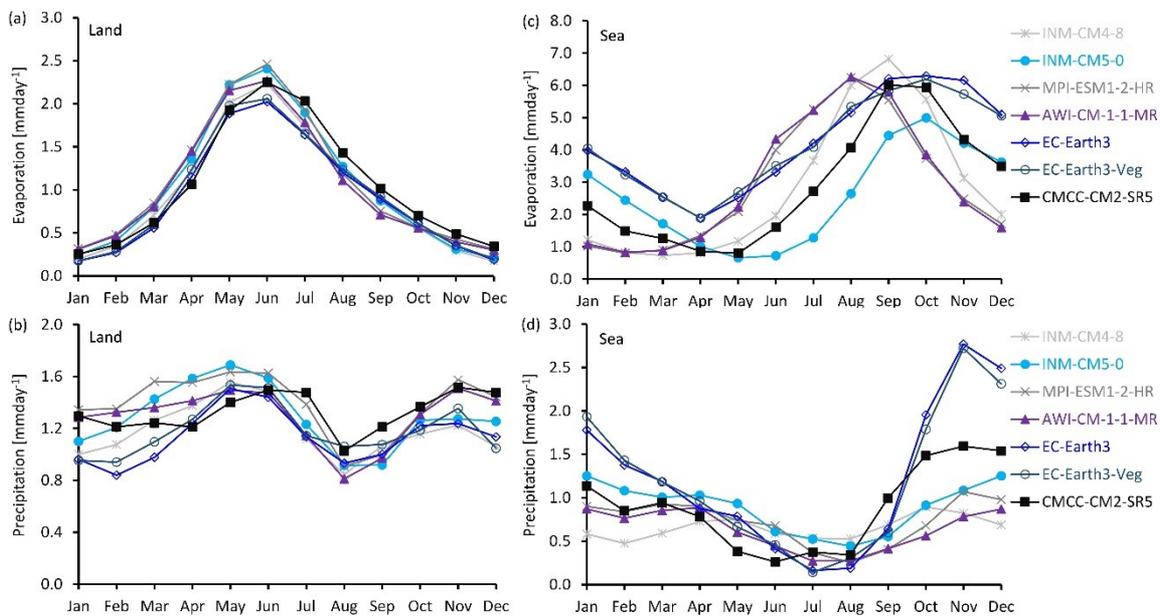
Figure S6.17. CMIP6 mean Seasonal cycle for the historical period from 1979 to 2001 over land and sea, (a) evaporation and (b) precipitation.
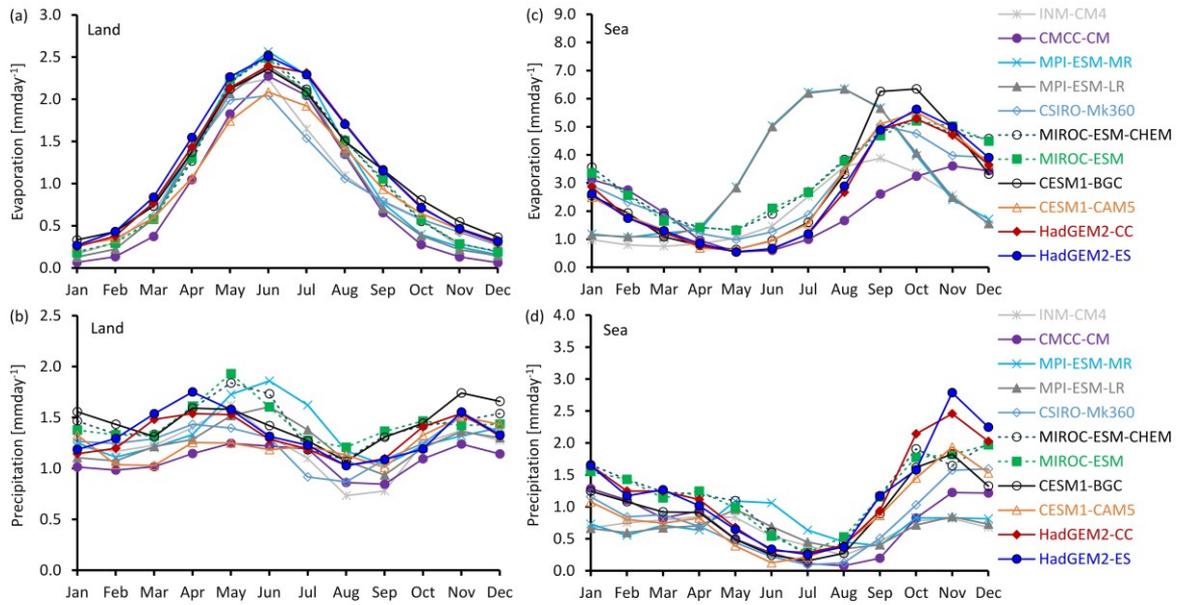
Figure S6.18. CMIP5 mean Seasonal cycle for the historical period from 1979 to 2001 over land and sea, (a) evaporation and (b) precipitation.
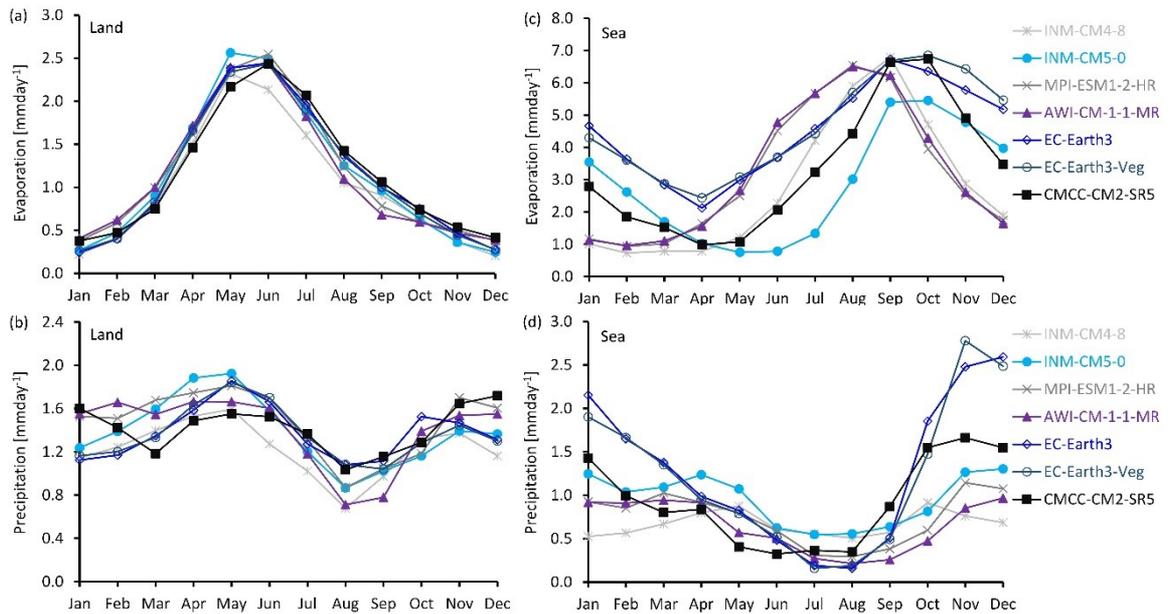
Figure S6.19. CMIP6-ssp245 mean Seasonal cycle for the future period from 2070 to 2100 over land and sea, (a) evaporation and (b) precipitation.
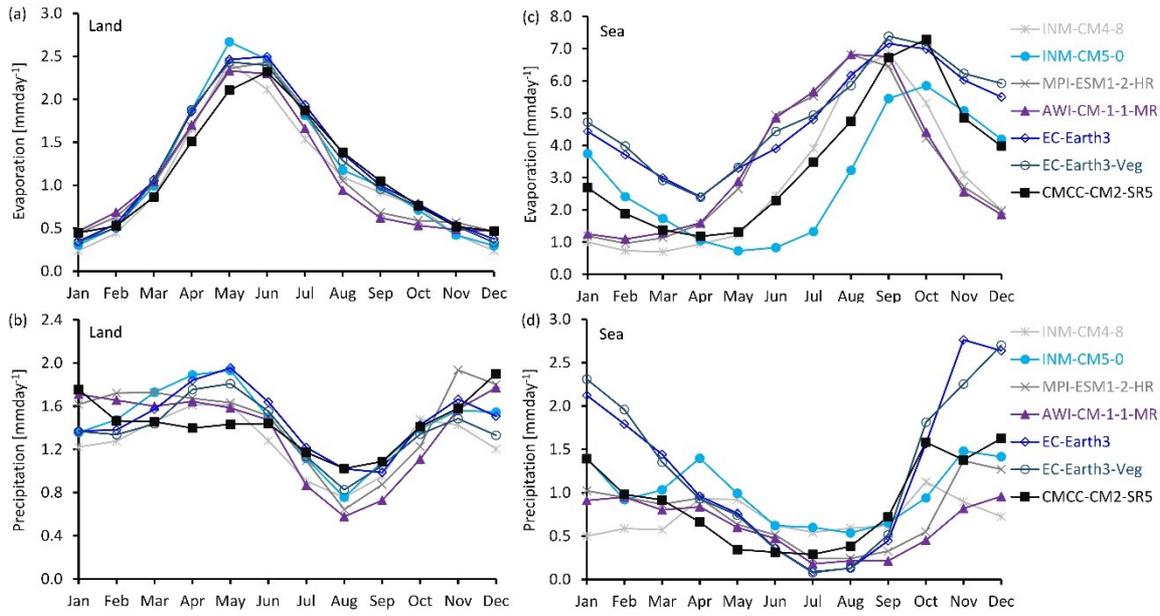
Figure S6.20. CMIP6-ssp585 mean Seasonal cycle for the future period from 2070 to 2100 over land and sea, (a) evaporation and (b) precipitation.
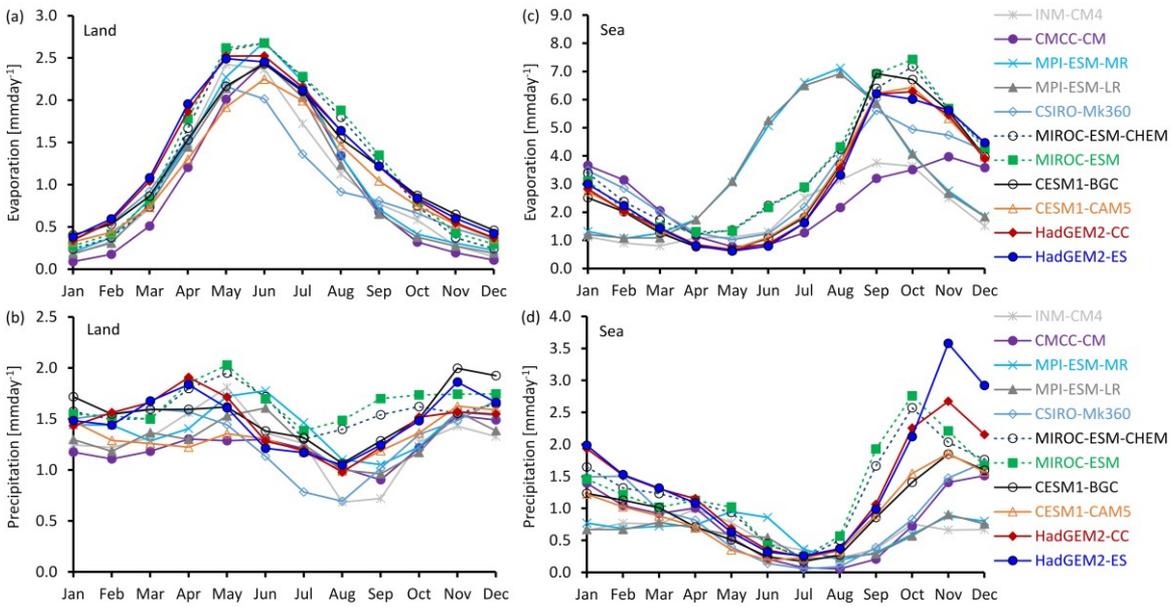
Figure S6.21. CMIP5-rcp45 mean Seasonal cycle for the future period from 2070 to 1998 over land and sea, (a) evaporation and (b) precipitation.
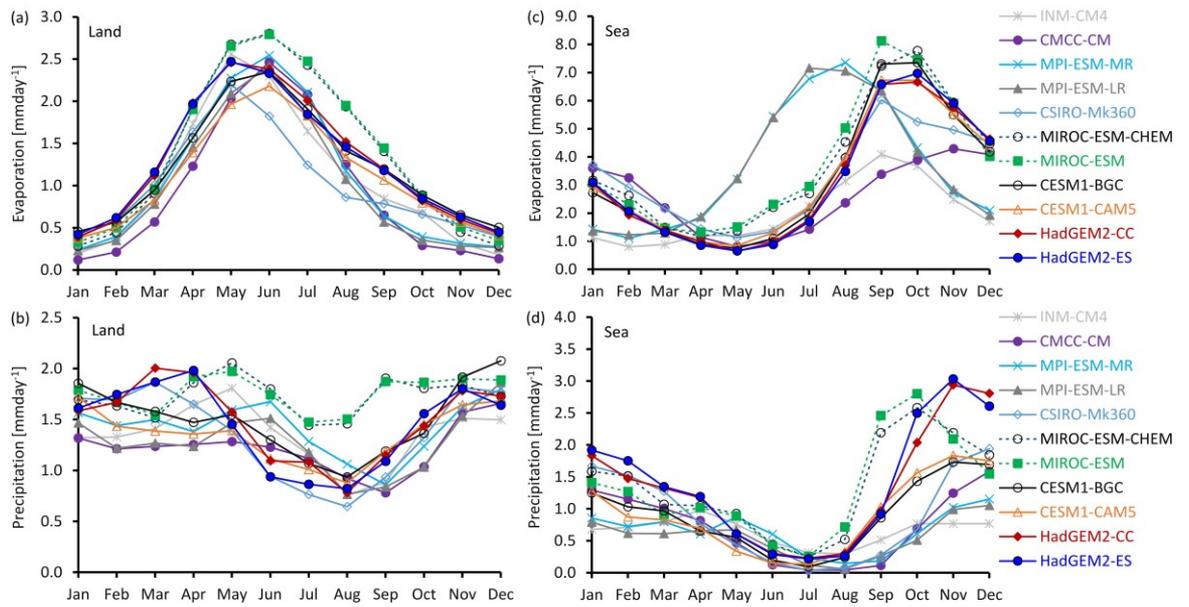
Figure S6.22. CMIP5-rcp85 mean Seasonal cycle for the future period from 2070 to 1998 over land and sea, (a) evaporation and (b) precipitation.
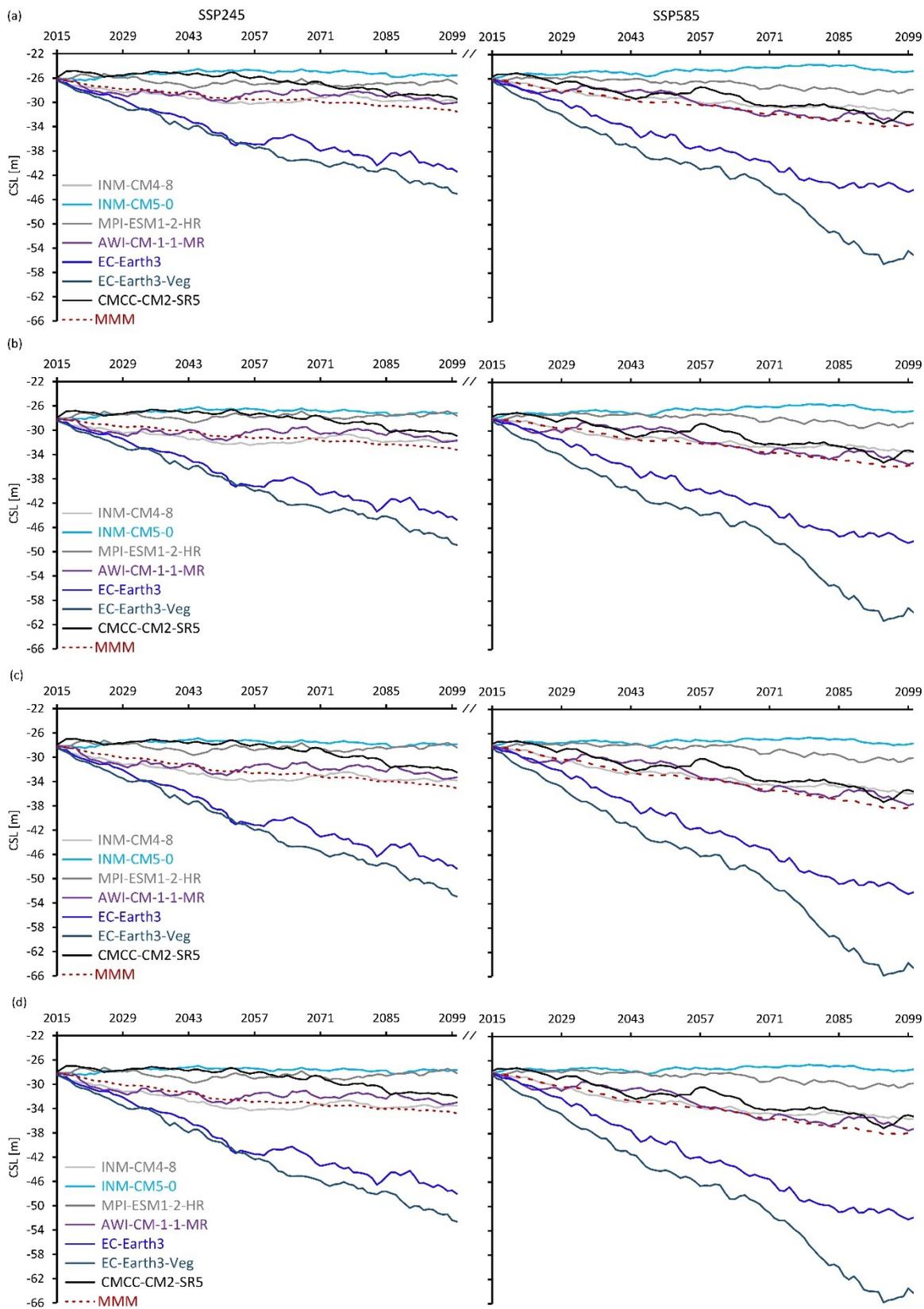
Figure S6.23. Projected CS level of the 21st century based on CMIP6 medium and extreme

emission scenarios and with and without water extraction. (a) NoWE – no-water extraction,

(b) 20 km3 future water extraction per year, (c) 40 km3 future water extraction, and (d) population-based water extraction scenarios.
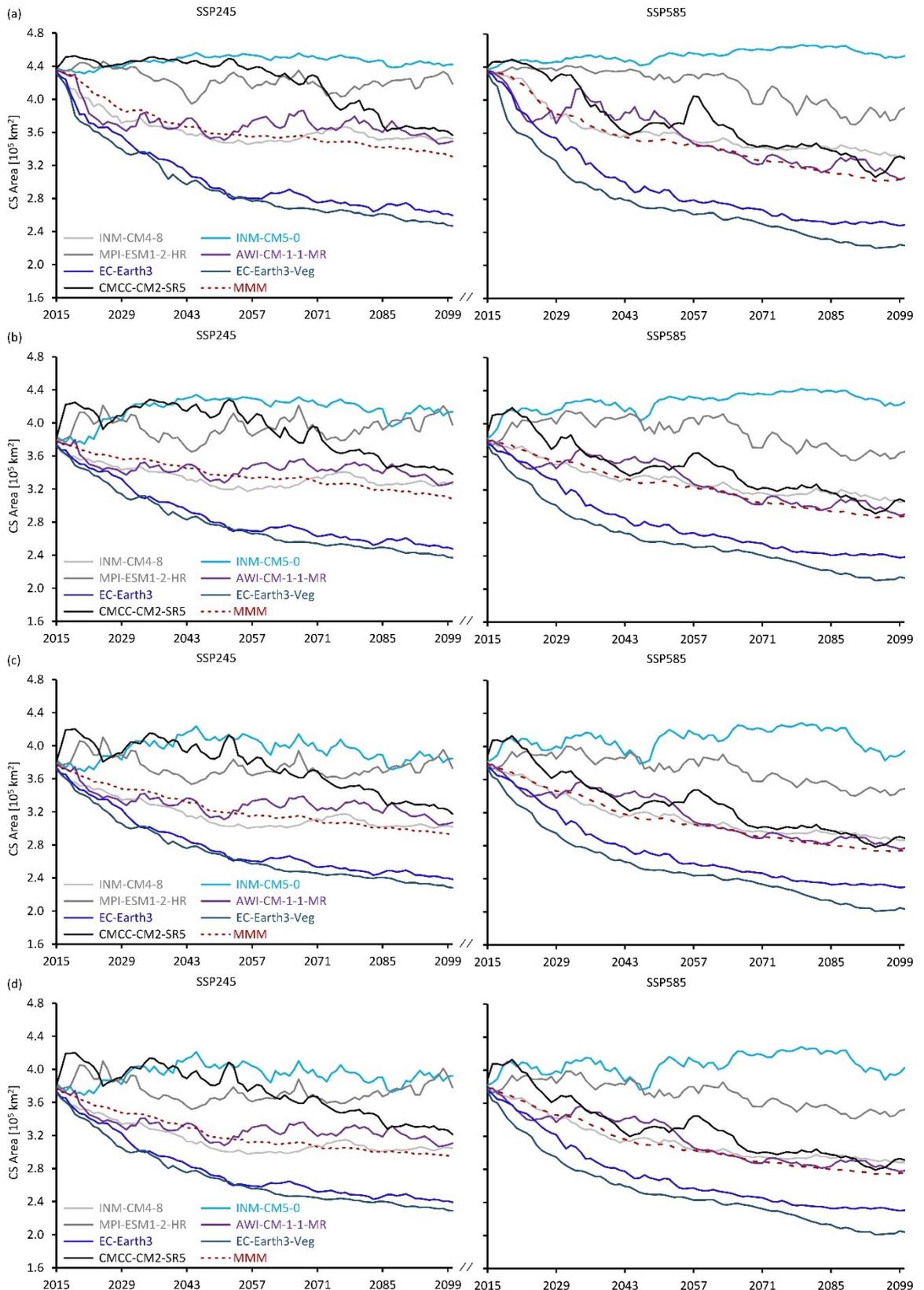
Figure S6.24. Projected CS area of the 21st century based on CMIP6 medium and extreme emission scenarios and with and without water extraction. (a) NoWE – no-water extraction, (b) 20 km3 future water extraction per year, (c) 40 km3 future water extraction, and (d) population-based water extraction scenarios.

References

Akbari, M., Baubekova, A., Roozbahani, A., Gafurov, A., Shiklomanov, A., Rasouli, K., Ivkina, N., Klove, B., Haghighi, A.T., 2020. Vulnerability of the Caspian Sea shoreline to changes in hydrology and climate. Environmental Research Letters 15.

Allen, R.G., Pereira, L.S., Raes, D., Smith, M., 1998. Crop evapotranspiration-Guidelines for computing crop water requirements-FAO Irrigation and drainage paper 56. Fao, Rome 300, D05109.

Alley, R.B., Mayewski, P.A., Sowers, T., Stuiver, M., Taylor, K.C., Clark, P.U., 1997. Holocene climatic instability: A prominent, widespread event 8200 yr ago. Geology 25, 483-486.

Amante, C., Eakins, B.W., 2009. ETOPO1 1 Arc-minute global relief model: procedures, data sources and analysis. NOAA Technical Memorandum NESDIS NGDC-24. National Geophysical Data Center, NOAA., in: Center, N.G.D. (Ed.). National Centers for Environmental Information, NESDIS, NOAA, U.S. Department of Commerce, Boulder, Colorado.

Argus, D.F., Peltier, W.R., Drummond, R., Moore, A.W., 2014. The Antarctica component of postglacial rebound model ICE-6G_C (VM5a) based on GPS positioning, exposure age dating of ice thicknesses, and relative sea level histories. Geophysical Journal International 198, 537-563.

Arnell, N.W., Kay, A.L., Freeman, A., Rudd, A.C., Lowe, J.A., 2021. Changing climate risk in the UK: A multi-sectoral analysis using policy-relevant indicators. Climate Risk Management 31, 100265.

Arpe, K., Bengtsson, L., Golitsyn, G., Mokhov, I., Semenov, V., Sporyshev, P., 1999. Analysis and modeling of the hydrological regime variations in the Caspian Sea basin, Doklady Earth Sciences C/C Of Doklady-Akademiia Nauk. Interperiodica Publishing, pp. 552-556.

References

Arpe, K., Bengtsson, L., Golitsyn, G.S., Mokhov, I.I., Semenov, V.A., Sporyshev, P.V., 2000. Connection between Caspian Sea level variability and ENSO. Geophys Res Lett 27, 2693-2696.

Arpe, K., Leroy, S.A.G., 2007. The Caspian Sea Level forced by the atmospheric circulation, as observed and modelled. Quaternary International 173-174, 144-152.

Arpe, K., Leroy, S.A.G., Lahijani, H., Khan, V., 2012. Impact of the European Russia drought in 2010 on the Caspian Sea level. Hydrol. Earth Syst. Sci. 16, 19-27.

Arpe, K., Leroy, S.A.G., Wetterhall, F., Khan, V., Hagemann, S., Lahijani, H., 2014. Prediction of the Caspian Sea level using ECMWF seasonal forecasts and reanalysis. Theor Appl Climatol 117, 41-60.

Arpe, K., Molavi-Arabshahi, M., Leroy, S.A.G., 2020. Wind variability over the Caspian Sea, its impact on Caspian seawater level and link with ENSO. International Journal of Climatology.

Arpe, K., Tsuang, B.J., Tseng, Y.H., Liu, X.Y., Leroy, S.A.G., 2019. Quantification of climatic feedbacks on the Caspian Sea level variability and impacts from the Caspian Sea on the large-scale atmospheric circulation. Theor Appl Climatol 136, 475-488.

Arslanov, K.A., Yanina, T.A., Chepalyga, A.L., Svitoch, A.A., Makshaev, R.R., Maksimov, F.E., Chernov, S.B., Tertychniy, N.I., Starikova, A.A., 2016. On the age of the Khvalynian deposits of the Caspian Sea coasts according to 14C and 230Th/234U methods. Quaternary International 409, 81-87.

Badertscher, S., Fleitmann, D., Cheng, H., Edwards, R.L., Göktürk, O.M., Zumbühl, A., Leuenberger, M., Tüysüz, O., 2011. Pleistocene water intrusions from the Mediterranean and Caspian seas into the Black Sea. Nature Geoscience 4, 236-239.

Bamber, J.L., Riva, R.E.M., Vermeersen, B.L.A., LeBrocq, A.M., 2009. Reassessment of the Potential Sea-Level Rise from a Collapse of the West Antarctic Ice Sheet. Science 324, 901-903.

Bartlein, P.J., Harrison, S.P., Izumi, K., 2017. Underlying causes of Eurasian midcontinental aridity in simulations of mid-Holocene climate. Geophys Res Lett 44, 9020-9028.

References

Belousov, T., Enman, S., 1999. Morphostructural plan and the tectonic movements of Stavropol Plateau during Quarternary and modern stages of development. Geomorphology 4, 56-69.

Berger, A., Loutre, M.F., 1991. Insolation values for the climate of the last 10 million years. Quaternary Science Reviews 10, 297-317.

Bezrodnykh, Y., Yanina, T., Sorokin, V., Romanyuk, B., 2020. The Northern Caspian Sea: Consequences of climate change for level fluctuations during the Holocene. Quaternary International 540, 68-77.

Bezrodnykh, Y.P., Deliya, S.V., Romanyuk, B.F., Sorokin, V.M., Yanina, T.A., 2015. New data on the upper quaternary stratigraphy of the North Caspian Sea. Doklady Earth Sciences 462, 479-483.

Bezrodnykh, Y.P., Romanyuk, B.F., Deliya, S.V., Magomedov, R.D., Sorokin, V.M., Parunin, O.B., Babak, E., 2004. Biostratigraphy, structure of the upper quaternary deposits and some paleogeographic features of the north Caspian region. Geology, pp. 102-111.

Bezrodnykh, Y.P., Sorokin, V.M., 2016. On the age of the Mangyshlakian deposits of the northern Caspian Sea. Quaternary Research 85, 245-254.

Braconnot, P., Harrison, S.P., Kageyama, M., Bartlein, P.J., Masson-Delmotte, V., Abe-Ouchi, A., Otto-Bliesner, B., Zhao, Y., 2012. Evaluation of climate models using palaeoclimatic data. Nature Climate Change 2, 417-424.

Branstetter, M.L., 2001. Development of a parallel river transport algorithm and applications to climate studies. The University of Texas at Austin.

Briley, L.J., Rood, R.B., Notaro, M., 2021. Large lakes in climate models: A Great Lakes case study on the usability of CMIP5. Journal of Great Lakes Research.

Broström, A., Coe, M., Harrison, S.P., Gallimore, R., Kutzbach, J.E., Foley, J., Prentice, I.C., Behling, P., 1998. Land surface feedbacks and palaeomonsoons in northern Africa. Geophys Res Lett 25, 3615-3618.

References

Carrivick, J.L., Tweed, F.S., 2013. Proglacial lakes: character, behaviour and geological importance. Quaternary Science Reviews 78, 34-52.

Chen, D., Chen, H.W., 2013. Using the Köppen classification to quantify climate variation and change: An example for 1901-2010. Environmental Development 6, 69-79.

Chen, J.L., Pekker, T., Wilson, C.R., Tapley, B.D., Kostianoy, A.G., Cretaux, J.F., Safarov, E.S., 2017a. Long-term Caspian Sea level change. Geophys Res Lett 44, 6993-7001.

Chen, J.L., Wilson, C.R., Tapley, B.D., Save, H., Cretaux, J.F., 2017b. Long-term and seasonal Caspian Sea level change from satellite gravity and altimeter measurements. J Geophys Res-Sol Ea 122, 2274-2290.

Coe, M.T., 1998. A linked global model of terrestrial hydrologic processes: simulation of modern rivers, lakes, and wetlands. J. Geophys. Res. D Atmos. 103, 8885-8899.

Coe, M.T., 2000. Modeling terrestrial hydrological systems at the continental scale: Testing the accuracy of an atmospheric GCM. Journal of Climate 13, 686-704.

Coe, M.T., Bonan, G.B., 1997. Feedbacks between climate and surface water in northern Africa during the middle Holocene. J. Geophys. Res. D Atmos. 102, 11087-11101.

Contoux, C., Jost, A., Ramstein, G., Sepulchre, P., Krinner, G., Schuster, M., 2013. Megalake chad impact on climate and vegetation during the late Pliocene and the mid-Holocene. Climate of the Past 9, 1417-1430.

Cox, P.M., Betts, R.A., Bunton, C.B., Essery, R.L.H., Rowntree, P.R., Smith, J., 1999. The impact of new land surface physics on the GCM simulation of climate and climate sensitivity. Climate Dynamics 15, 183-203.

Dadson, S., Blyth, E., Clark, D., Hughes, A., Hannaford, J., Lawrence, B., Polcher, J., Reynard, N., 2019. Hydro-JULES: Next Generation Land-surface and Hydrological Predictions, Geophysical Research Abstracts.

References

Davies-Barnard, T., Ridgwell, A., Singarayer, J., Valdes, P., 2017. Quantifying the influence of the terrestrial biosphere on glacial–interglacial climate dynamics. Clim. Past 13, 1381-1401.

Demin, A.P., 2007. Present-day changes in water consumption in the Caspian Sea basin. Water Resources 34, 237-253.

Diansky, N.A., Fomin, V.V., Vyruchalkina, T.Y., Gusev, A.V., 2018. Numerical Simulation of the Caspian Sea Circulation Using the Marine and Atmospheric Research System. Water Resources 45, 706-718.

Dolukhanov, P.M., Chepalyga, A.L., Lavrentiev, N.V., 2010. The Khvalynian transgressions and early human settlement in the Caspian basin. Quaternary International 225, 152-159.

Dyakonov, G.S., Ibrayev, R.A., 2019. Long-term evolution of Caspian Sea thermohaline properties reconstructed in an eddy-resolving ocean general circulation model. Ocean Sci. 15, 527-541.

Elguindi, N., Giorgi, F., 2006a. Projected changes in the Caspian Sea level for the 21st century based on the latest AOGCM simulations. Geophys Res Lett 33.

Elguindi, N., Giorgi, F., 2006b. Simulating multi-decadal variability of Caspian Sea level changes using regional climate model outputs. Climate Dynamics 26, 167-181.

Elguindi, N., Giorgi, F., 2007. Simulating future Caspian sea level changes using regional climate model outputs. Climate Dynamics 28, 365-379.

Elguindi, N., Somot, S., Déqué, M., Ludwig, W., 2011. Climate change evolution of the hydrological balance of the Mediterranean, Black and Caspian Seas: impact of climate model resolution. Climate Dynamics 36, 205-228.

Eyring, V., Bony, S., Meehl, G.A., Senior, C.A., Stevens, B., Stouffer, R.J., Taylor, K.E., 2016. Overview of the Coupled Model Intercomparison Project Phase 6 (CMIP6) experimental design and organization. Geoscientific Model Development 9, 1937-1958.

References

Farrow, A.R., 2012. On the mechanisms of climate, vegetation and lake change in Late Quaternary Africa. Ph.D Thesis. University of Bristol, U.K.

Forte, A.M., Cowgill, E., 2013. Late Cenozoic base-level variations of the Caspian Sea: A review of its history and proposed driving mechanisms. Palaeogeography, Palaeoclimatology, Palaeoecology 386, 392-407.

Golitsyn, G.S., 1995. The Caspian Sea-Level as a Problem of Diagnosis and Prognosis of the Regional Climate-Change. Izv an Fiz Atmos Ok+ 31, 385-391.

Golovanova, O.V., 2015. Groundwater of the Pleistocene aquifer system in the north Caspian and near-Caspian regions: Communication 1. Character of water exchange and factors of sedimentary water integrity. Lithology and Mineral Resources 50, 231-247.

Gong, X., Knorr, G., Lohmann, G., Zhang, X., 2013. Dependence of abrupt Atlantic meridional ocean circulation changes on climate background states. Geophys Res Lett 40, 3698-3704.

Gordon, C., Cooper, C., Senior, C.A., Banks, H., Gregory, J.M., Johns, T.C., Mitchell, J.F.B., Wood, R.A., 2000. The simulation of SST, sea ice extents and ocean heat transports in a version of the Hadley Centre coupled model without flux adjustments. Climate Dynamics 16, 147-168.

Grigorovich, I.A., Therriault, T.W., MacIsaac, H.J., 2003. History of aquatic invertebrate invasions in the Caspian Sea. Biological Invasions 5, 103-115.

Hampton, S.E., McGowan, S., Ozersky, T., Virdis, S.G.P., Vu, T.T., Spanbauer, T.L., Kraemer, B.M., Swann, G., Mackay, A.W., Powers, S.M., Meyer, M.F., Labou, S.G., O'Reilly, C.M., DiCarlo, M., Galloway, A.W.E., Fritz, S.C., 2018. Recent ecological change in ancient lakes. Limnology and Oceanography 63, 2277-2304.

Hausfather, Z., 2019. CMIP6: the next generation of climate models explained., Climate modelling. CarbonBrief.

Hays, J.D., Imbrie, J., Shackleton, N.J., 1976. Variations in the Earth's Orbit: Pacemaker of the Ice Ages. Science 194, 1121-1132.

References

Hersbach, H., Bell, B., Berrisford, P., Hirahara, S., Horányi, A., Muñoz-Sabater, J., Nicolas, J., Peubey, C., Radu, R., Schepers, D., Simmons, A., Soci, C., Abdalla, S., Abellan, X., Balsamo, G., Bechtold, P., Biavati, G., Bidlot, J., Bonavita, M., De Chiara, G., Dahlgren, P., Dee, D., Diamantakis, M., Dragani, R., Flemming, J., Forbes, R., Fuentes, M., Geer, A., Haimberger, L., Healy, S., Hogan, R.J., Hólm, E., Janisková, M., Keeley, S., Laloyaux, P., Lopez, P., Lupu, C., Radnoti, G., de Rosnay, P., Rozum, I., Vamborg, F., Villaume, S., Thépaut, J.-N., 2020. The ERA5 global reanalysis. Quarterly Journal of the Royal Meteorological Society n/a.

Hoogakker, B.A.A., Smith, R.S., Singarayer, J.S., Marchant, R., Prentice, I.C., Allen, J.R.M., Anderson, R.S., Bhagwat, S.A., Behling, H., Borisova, O., Bush, M., Correa-Metrio, A., de Vernal, A., Finch, J.M., Fréchette, B., Lozano-Garcia, S., Gosling, W.D., Granoszewski, W., Grimm, E.C., Grüger, E., Hanselman, J., Harrison, S.P., Hill, T.R., Huntley, B., Jiménez-Moreno, G., Kershaw, P., Ledru, M.P., Magri, D., McKenzie, M., Müller, U., Nakagawa, T., Novenko, E., Penny, D., Sadori, L., Scott, L., Stevenson, J., Valdes, P.J., Vandergoes, M., Velichko, A., Whitlock, C., Tzedakis, C., 2016. Terrestrial biosphere changes over the last 120 kyr. Clim. Past 12, 51-73.

Hoskins, B.J., Karoly, D.J., 1981. The steady linear response of a spherical atmosphere to thermal and orographic forcing. Journal of the Atmospheric Sciences 38, 1179-1196.

Huang, L., Lee, S.-S., Timmermann, A., 2021. Caspian Sea and Black Sea Response to Greenhouse Warming in a High-Resolution Global Climate Model. Geophys Res Lett 48, e2020GL090270.

Hughes, A.L.C., Gyllencreutz, R., Lohne, Ø.S., Mangerud, J., Svendsen, J.I., 2016. The last Eurasian ice sheets – a chronological database and time-slice reconstruction, DATED-1. Boreas 45, 1-45.

Hurrell, J.W., Holland, M.M., Gent, P.R., Ghan, S., Kay, J.E., Kushner, P.J., Lamarque, J.F., Large, W.G., Lawrence, D., Lindsay, K., Lipscomb, W.H., Long, M.C., Mahowald, N., Marsh, D.R., Neale, R.B., Rasch, P., Vavrus, S., Vertenstein, M., Bader, D., Collins, W.D., Hack, J.J., Kiehl, J., Marshall, S., 2013. The community earth system model: A framework for collaborative research. Bulletin of the American Meteorological Society 94, 1339-1360.

References

Interim Secretariat of the Framework Convention for the Protection of the Marine Environment of the Caspian Sea, 2012. Caspian Sea: State of the Environment 2011., Geneva and Arendal.

Interim Secretariat of the Framework Convention for the Protection of the Marine Environment of the Caspian Sea, 2020. Caspian Sea: State of the Environment 2019., Geneva and Arendal.

Jamshidi, S., 2017. Assessment of thermal stratification, stability and characteristics of deep water zone of the southern Caspian Sea. Journal of Ocean Engineering and Science 2, 203-216.

Jones, P.W., 1999. First-and second-order conservative remapping schemes for grids in spherical coordinates. Monthly Weather Review 127, 2204-2210.

Jorissen, E.L., Abels, H.A., Wesselingh, F.P., Lazarev, S., Aghayeva, V., Krijgsman, W., 2020. Amplitude, frequency and drivers of Caspian Sea lake-level variations during the Early Pleistocene and their impact on a protected wave-dominated coastline. Sedimentology 67, 649-676.

Kakroodi, A.A., Kroonenberg, S.B., Goorabi, A., Yamani, M., 2014. Shoreline Response to Rapid 20th Century Sea-Level Change along the Iranian Caspian Coast. Journal of Coastal Research 30, 1243-1250.

Kakroodi, A.A., Kroonenberg, S.B., Hoogendoorn, R.M., Mohammd Khani, H., Yamani, M., Ghassemi, M.R., Lahijani, H.A.K., 2012. Rapid Holocene sea-level changes along the Iranian Caspian coast. Quaternary International 263, 93-103.

Kakroodi, A.A., Leroy, S.A.G., Kroonenberg, S.B., Lahijani, H.A.K., Alimohammadian, H., Boomer, I., Goorabi, A., 2015. Late Pleistocene and Holocene sea-level change and coastal paleoenvironment evolution along the Iranian Caspian shore. Marine Geology 361, 111-125.

References

Kislov, A., Toropov, P., 2007. East European river runoff and Black Sea and Caspian Sea level changes as simulated within the Paleoclimate modeling intercomparison project. Quaternary International 167-168, 40-48.

Kislov, A.V., 2018. Secular Variability of the Caspian Sea Level. Russ Meteorol Hydro+ 43, 679-685.

Kislov, A.V., Panin, A., Toropov, P., 2014. Current status and palaeostages of the Caspian Sea as a potential evaluation tool for climate model simulations. Quaternary International 345, 48-55.

Komatsu, G., Baker, V.R., Arzhannikov, S.G., Gallagher, R., Arzhannikova, A.V., Murana, A., Oguchi, T., 2016. Catastrophic flooding, palaeolakes, and late Quaternary drainage reorganization in northern Eurasia. International Geology Review 58, 1693-1722.

Komijani, F., Chegini, V., Siadatmousavi, S.M., 2019. Seasonal variability of circulation and air-sea interaction in the Caspian Sea based on a high resolution circulation model. Journal of Great Lakes Research 45, 1113-1129.

Kondratjeva, K.A., Khrutzky, S.F., Romanovsky, N.N., 1993. Changes in the extent of permafrost during the late quaternary period in the territory of the former Soviet Union. Permafrost and Periglacial Processes 4, 113-119.

Koriche, S.A., Nandini-Weiss, S.D., Prange, M., Singarayer, J.S., Arpe, K., Cloke, H.L., Schulz, M., Bakker, P., Leroy, S.A.G., Coe, M., 2020b. Impacts of variations in Caspian Sea surface area on catchment-scale and large-scale climate. Under review at JGR: Atmospheres

Koriche, S.A., Singarayer, J.S., Cloke, H.L., Valdes, P.J., Wesselingh, F.P., Kroonenberg, S.B., Wickert, A.D., Yanina, T.A., 2020a. What are the drivers of Caspian Sea level variation during the late Quaternary? Under review at Journal of Quaternary Science Review.

Kosarev, A.N., 2005. Physico-geographical conditions of the Caspian Sea, The Caspian Sea Environment. Springer, pp. 5-31.

Kosarev, A.N., Kostianoy, A.G., Zonn, I.S., 2009. Kara-Bogaz-Gol Bay: Physical and Chemical Evolution. Aquatic Geochemistry 15, 223-236.

References

Krijgsman, W., Tesakov, A., Yanina, T., Lazarev, S., Danukalova, G., Van Baak, C.G.C., Agustí, J., Alçiçek, M.C., Aliyeva, E., Bista, D., Bruch, A., Büyükmeriç, Y., Bukhsianidze, M., Flecker, R., Frolov, P., Hoyle, T.M., Jorissen, E.L., Kirscher, U., Koriche, S.A., Kroonenberg, S.B., Lordkipanidze, D., Oms, O., Rausch, L., Singarayer, J., Stoica, M., van de Velde, S., Titov, V.V., Wesselingh, F.P., 2019. Quaternary time scales for the Pontocaspian domain: Interbasinal connectivity and faunal evolution. Earth-Science Reviews 188, 1-40.

Krinner, G., Mangerud, J., Jakobsson, M., Crucifix, M., Ritz, C., Svendsen, J.I., 2004. Enhanced ice sheet growth in Eurasia owing to adjacent ice-dammed lakes. Nature 427, 429-432.

Kroonenberg, S., 2012. Rapid Caspian Sea level oscillations in the Holocene: synchronicity with global climate change. Quaternary International 279-280, 257.

Kroonenberg, S.B., Alekseevski, N.I., Aliyeva, E., Allen, M.B., Aybulatov, D.N., Baba-Zadeh, A., Badyukova, E.N., Davies, C.E., Hinds, D.J., Hoogendoorn, R.M., Huseynov, D., Ibrahimov, B., Mamedov, P., Overeem, I., Rusakov, G.V., Suleymanova, S., Svitoch, A.A., Vincent, S.J., Giosan, L., Bhattacharya, J.P., 2005. Two Deltas, Two Basins, One River, One Sea: The Modern Volga Delta as an Analogue of the Neogene Productive Series, South Caspian Basin, River Deltas–Concepts, Models, and Examples. SEPM Society for Sedimentary Geology, p. 0.

Kroonenberg, S.B., Badyukova, E.N., Storms, J.E.A., Ignatov, E.I., Kasimov, N.S., 2000. A full sea-level cycle in 65 years: barrier dynamics along Caspian shores. Sedimentary Geology 134, 257-274.

Kroonenberg, S.B., Kasimov, N.S., Lychagin, M.Y., 2008. The Caspian Sea, a natural laboratory for sea-level change. Geography, environment, sustainability 1, 22-37.

Kroonenberg, S.B., Rusakov, G.V., Svitoch, A.A., 1997. The wandering of the Volga delta: a response to rapid Caspian sea-level change. Sedimentary Geology 107, 189-209.

Kudekov, T., 2006. Climate change and vulnerability assessment report for the Republic of Kazakhstan., Caspian Environmental Programme.

References

Lahijani, H.A.K., Rahimpour-Bonab, H., Tavakoli, V., Hosseindoost, M., 2009. Evidence for late Holocene highstands in Central Guilan–East Mazanderan, South Caspian coast, Iran. Quaternary International 197, 55-71.

Lattuada, M., Albrecht, C., Wilke, T., 2019. Differential impact of anthropogenic pressures on Caspian Sea ecoregions. Marine Pollution Bulletin 142, 274-281.

Latypov, Y.Y., 2015. The Bivalve Mollusc Abra ovata: role in succession of soft bottom communities on newly flooded area of the Caspian Sea. American Journal of Climate Change 4, 239.

Le Pichon, X., Şengör, A.C., Kende, J., İmren, C., Henry, P., Grall, C., Karabulut, H., 2016. Propagation of a strike-slip plate boundary within an extensional environment: the westward propagation of the North Anatolian Fault. Can J Earth Sci 53, 1416-1439.

Leroy, S.A., Lahijani, H.A., Crétaux, J.-F., Aladin, N.V., Plotnikov, I.S., 2020. Past and current changes in the largest lake of the world: The Caspian Sea, Large Asian Lakes in a Changing World. Springer, pp. 65-107.

Leroy, S.A.G., Marret, F., Gibert, E., Chalié, F., Reyss, J.L., Arpe, K., 2007. River inflow and salinity changes in the Caspian Sea during the last 5500 years. Quaternary Science Reviews 26, 3359-3383.

Leroy, S.A.G., Tudryn, A., Chalié, F., López-Merino, L., Gasse, F., 2013. From the Allerød to the mid-Holocene: palynological evidence from the south basin of the Caspian Sea. Quaternary Science Reviews 78, 77-97.

Lodh, A., 2015. Impact of Caspian Sea Drying on Indian Monsoon Precipitation and Temperature as Simulated by RegCM4 Model. Hydrol Current Res 6.

Lofgren, B.M., 1997. Simulated effects of idealized Laurentian Great Lakes on regional and large-scale climate. Journal of Climate 10, 2847-2858.

Long, Z., Perrie, W., Gyakum, J., Caya, D., Laprise, R., 2007. Northern lake impacts on local seasonal climate. J. Hydrometeor. 8, 881-896.

References

Love, R., Milne, G.A., Tarasov, L., Engelhart, S.E., Hijma, M.P., Latychev, K., Horton, B.P., Törnqvist, T.E., 2016. The contribution of glacial isostatic adjustment to projections of sea-level change along the Atlantic and Gulf coasts of North America. Earth's Future 4, 440-464.

Lysa, A., Jensen, M.A., Larsan, E., Fredin, O., Demidov, I.N., 2011. Ice-distal landscape and sediment signatures evidencing damming and drainage of large pro-glacial lakes, northwest Russia. Boreas 40, 481-497.

MacKay, M.D., Neale, P.J., Arp, C.D., De Senerpont Domis, L.N., Fang, X., Gal, G., Jöhnk, K.D., Kirillin, G., Lenters, J.D., Litchman, E., MacIntyre, S., Marsh, P., Melack, J., Mooij, W.M., Peeters, F., Quesada, A., Schladow, S.G., Schmid, M., Spence, C., Stokesr, S.L., 2009. Modeling lakes and reservoirs in the climate system. Limnology and Oceanography 54, 2315-2329.

Mamedov, A.V., 1997. The Late Pleistocene-Holocene history of the Caspian Sea. Quaternary International 41, 161-166.

Mangerud, J., Astakhov, V., Jakobsson, M., Svendsen, J.I., 2001. Huge Ice-age lakes in Russia. Journal of Quaternary Science 16, 773-777.

Mangerud, J., Jakobsson, M., Alexanderson, H., Astakhov, V., Clarke, G.K.C., Henriksen, M., Hjort, C., Krinner, G., Lunkka, J.-P., Möller, P., Murray, A., Nikolskaya, O., Saarnisto, M., Svendsen, J.I., 2004. Ice-dammed lakes and rerouting of the drainage of northern Eurasia during the Last Glaciation. Quaternary Science Reviews 23, 1313-1332.

Marret, F., Leroy, S., Chalié, F., Françoise, F., 2004. New organic-walled dinoflagellate cysts from recent sediments of Central Asian seas. Review of Palaeobotany and Palynology 129, 1-20.

Marsicek, J., Shuman, B.N., Bartlein, P.J., Shafer, S.L., Brewer, S., 2018. Reconciling divergent trends and millennial variations in Holocene temperatures. Nature 554, 92-96.

Masson-Delmotte, V., Schulz, M., Abe-Ouchi, A., Beer, J., Ganopolski, A., González Rouco, J.F., Jansen, E., Lambeck, K., Luterbacher, J., Naish, T., Osborn, T., Otto-Bliesner, B., Quinn, T.,

Ramesh, R., Rojas, M., Shao, X., Timmermann, A., 2013. Information from Paleoclimate Archives, in: Stocker, T.F., Qin, D., Plattner, G.-K., Tignor, M., Allen, S.K., Doschung, J., Nauels, A., Xia, Y., Bex, V., Midgley, P.M. (Eds.), Climate Change 2013 – The Physical Science Basis: Working Group I Contribution to the Fifth Assessment Report of the Intergovernmental Panel on Climate Change. Cambridge University Press, Cambridge, pp. 383-464.

Meinshausen, M., Smith, S.J., Calvin, K., Daniel, J.S., Kainuma, M.L.T., Lamarque, J.F., Matsumoto, K., Montzka, S.A., Raper, S.C.B., Riahi, K., Thomson, A., Velders, G.J.M., van Vuuren, D.P.P., 2011. The RCP greenhouse gas concentrations and their extensions from 1765 to 2300. Climatic Change 109, 213.

Metz, M., Mitasova, H., Harmon, R.S., 2011. Efficient extraction of drainage networks from massive, radar-based elevation models with least cost path search. Hydrol. Earth Syst. Sci. 15, 667-678.

Micklin, P.P., 1988. Desiccation of the Aral Sea: A Water Management Disaster in the Soviet Union. Science 241, 1170-1176.

Molavi-Arabshahi, M., Arpe, K., Leroy, S.A.G., 2016. Precipitation and temperature of the southwest Caspian Sea region during the last 55 years: their trends and teleconnections with large-scale atmospheric phenomena. International Journal of Climatology 36, 2156-2172.

Naderi Beni, A., Lahijani, H., Mousavi Harami, R., Arpe, K., Leroy, S.A.G., Marriner, N., Berberian, M., Andrieu-Ponel, V., Djamali, M., Mahboubi, A., Reimer, P.J., 2013. Caspian sea-level changes during the last millennium: historical and geological evidence from the south Caspian Sea. Clim. Past 9, 1645-1665.

Nadirov, R.S., Bagirov, E., Tagiyev, M., Lerche, I., 1997. Flexural plate subsidence, sedimentation rates, and structural development of the super-deep South Caspian Basin. Marine and Petroleum Geology 14, 383-400.

References

Nandini-Weiss, S.D., Prange, M., Arpe, K., Merkel, U., Schulz, M., 2020. Past and future impact of the winter North Atlantic Oscillation in the Caspian Sea catchment area. International Journal of Climatology 40, 2717-2731.

Nativi, S., Craglia, M., 2020. Destination Earth: Use Cases Analysis, EUR 30437 EN, Publications Office of the European Union, Luxembourg.

Neteler, M., Bowman, M.H., Landa, M., Metz, M., 2012. GRASS GIS: A multi-purpose open source GIS. Environmental Modelling & Software 31, 124-130.

Nevesskaja, L.A., 2007. History of the genus Didacna (Bivalvia: Cardiidae). Paleontological Journal 41, 861-949.

Nicholls, J.F., Toumi, R., 2014. On the lake effects of the Caspian Sea. Quarterly Journal of the Royal Meteorological Society 140, 1399-1408.

NOAA, n.d. Abrupt Climate Change: A Paleo Perspective, Glacial-Interglacial Cycles.

Notaro, M., Holman, K., Zarrin, A., Fluck, E., Vavrus, S., Bennington, V., 2013. Influence of the laurentian great lakes on regional climate. Journal of Climate 26, 789-804.

PAGES, P.I.W.G.o., 2016. Interglacials of the last 800,000 years. Reviews of Geophysics 54, 162-219.

Panin, A.V., Astakhov, V.I., Lotsari, E., Komatsu, G., Lang, J., Winsemann, J., 2020. Middle and Late Quaternary glacial lake-outburst floods, drainage diversions and reorganization of fluvial systems in northwestern Eurasia. Earth-Science Reviews 201, 103069.

Panin, G.N., Diansky, N.A., 2014. On the correlation between oscillations of the Caspian Sea level and the North Atlantic climate. Izvestiya, Atmospheric and Oceanic Physics 50, 266-277.

Peixoto, J.P., Oort, A.H., 1992. Physics of climate. American Institute of Physics, College Park, Md, United States.

References

Peltier, W.R., 2004. GLOBAL GLACIAL ISOSTASY AND THE SURFACE OF THE ICE-AGE EARTH: The ICE-5G (VM2) Model and GRACE. Annual Review of Earth and Planetary Sciences 32, 111-149.

Peltier, W.R., Argus, D.F., Drummond, R., 2015. Space geodesy constrains ice age terminal deglaciation: The global ICE-6G_C (VM5a) model. Journal of Geophysical Research: Solid Earth 120, 450-487.

Pokhrel, Y.N., Hanasaki, N., Yeh, P.J.F., Yamada, T.J., Kanae, S., Oki, T., 2012. Model estimates of sea-level change due to anthropogenic impacts on terrestrial water storage. Nature Geoscience 5, 389-392.

Poli, P., Hersbach, H., Dee, D.P., Berrisford, P., Simmons, A.J., Vitart, F., Laloyaux, P., Tan, D.G.H., Peubey, C., Thépaut, J.-N., Trémolet, Y., Hólm, E.V., Bonavita, M., Isaksen, L., Fisher, M., 2016. ERA-20C: An Atmospheric Reanalysis of the Twentieth Century. Journal of Climate 29, 4083-4097.

Pope, V.D., Gallani, M.L., Rowntree, P.R., Stratton, R.A., 2000. The impact of new physical parametrizations in the Hadley Centre climate model: HadAM3. Climate Dynamics 16, 123-146.

Popov, S.V., Shcherba, I.G., Ilyina, L.B., Nevesskaya, L.A., Paramonova, N.P., Khondkarian, S.O., Magyar, I., 2006. Late Miocene to Pliocene palaeogeography of the Paratethys and its relation to the Mediterranean. Palaeogeography, Palaeoclimatology, Palaeoecology 238, 91-106.

Prange, M., Wilke, T., Wesselingh, F.P., 2020. The other side of sea level change. Communications Earth & Environment 1, 69.

Renssen, H., Lougheed, B.C., Aerts, J.C.J.H., de Moel, H., Ward, P.J., Kwadijk, J.C.J., 2007. Simulating long-term Caspian Sea level changes: The impact of Holocene and future climate conditions. Earth Planet Sc Lett 261, 685-693.

Riahi, K., van Vuuren, D.P., Kriegler, E., Edmonds, J., O'Neill, B.C., Fujimori, S., Bauer, N., Calvin, K., Dellink, R., Fricko, O., Lutz, W., Popp, A., Cuaresma, J.C., Kc, S., Leimbach, M., Jiang, L.,

Kram, T., Rao, S., Emmerling, J., Ebi, K., Hasegawa, T., Havlik, P., Humpenöder, F., Da Silva, L.A., Smith, S., Stehfest, E., Bosetti, V., Eom, J., Gernaat, D., Masui, T., Rogelj, J., Strefler, J., Drouet, L., Krey, V., Luderer, G., Harmsen, M., Takahashi, K., Baumstark, L., Doelman, J.C., Kainuma, M., Klimont, Z., Marangoni, G., Lotze-Campen, H., Obersteiner, M., Tabeau, A., Tavoni, M., 2017. The Shared Socioeconomic Pathways and their energy, land use, and greenhouse gas emissions implications: An overview. Global Environmental Change 42, 153-168.

Richards, K., Mudie, P., Rochon, A., Athersuch, J., Bolikhovskaya, N., Hoogendoorn, R., Verlinden, V., 2017. Late Pleistocene to Holocene evolution of the Emba Delta, Kazakhstan, and coastline of the north-eastern Caspian Sea: Sediment, ostracods, pollen and dinoflagellate cyst records. Palaeogeography, Palaeoclimatolgy, Palaeoecology 468, 427-452.

Ritz, C., Edwards, T.L., Durand, G., Payne, A.J., Peyaud, V., Hindmarsh, R.C.A., 2015. Potential sea-level rise from Antarctic ice-sheet instability constrained by observations. Nature 528, 115-118.

Rodell, M., Famiglietti, J.S., Wiese, D.N., Reager, J.T., Beaudoing, H.K., Landerer, F.W., Lo, M.H., 2018. Emerging trends in global freshwater availability. Nature 557, 651-659.

Rodionov, S.N., 1994. Global and regional climate interaction: the Caspian Sea experience. Springer Science & Business Media, Dordrecht.

Roshan, G., Moghbel, M., Grab, S., 2012. Modeling Caspian Sea water level oscillations under different scenarios of increasing atmospheric carbon dioxide concentrations. Iranian Journal of Environmental Health Science & Engineering 9, 24.

Rychagov, G., 1997a. Pleistocene history of the Caspian Sea. Moscow State University, Moscow, pp. 1e267 (in Russian).

Rychagov, G.I., 1997b. Holocene oscillations of the Caspian Sea, and forecasts based on palaeogeographical reconstructions. Quaternary International 41, 167-172.

Samuelsson, P., Kourzeneva, E., Mironov, D., 2010. The impact of lakes on the European climate as simulated by a regional climate model. Boreal Environment Research 15, 113-129.

Sánchez-Goñi, M.a.F., Turon, J.-L., Eynaud, F., Gendreau, S., 2000. European Climatic Response to Millennial-Scale Changes in the Atmosphere–Ocean System during the Last Glacial Period. Quaternary Research 54, 394-403.

Seidov, D., Maslin, M., 1999. North Atlantic deep water circulation collapse during Heinrich events. Geology 27, 23-26.

Shepherd, T.G., 2014. Atmospheric circulation as a source of uncertainty in climate change projections. Nature Geoscience 7, 703-708.

Shiklomanov, I.A., 1981. The effects of man on basin runoff, and on the water balance and water stage of the Caspian Sea / Influence de l'homme sur l'écoulement du basin fluvial, sur le bilan hydrologique et sur les niveaux de la Mer Caspienne. Hydrological Sciences Bulletin 26, 321-328.

Shkatova, V.K., 2010. Paleogeography of the Late Pleistocene Caspian Basins: Geochronometry, paleomagnetism, paleotemperature, paleosalinity and oxygen isotopes. Quaternary International 225, 221-229.

Sillmann, J., Shepherd, T.G., van den Hurk, B., Hazeleger, W., Martius, O., Slingo, J., Zscheischler, J., 2021. Event-Based Storylines to Address Climate Risk. Earth's Future 9, e2020EF001783.

Singarayer, J.S., Burrough, S.L., 2015. Interhemispheric dynamics of the African rainbelt during the late Quaternary. Quaternary Science Reviews 124, 48-67.

Singarayer, J.S., Valdes, P.J., 2010. High-latitude climate sensitivity to ice-sheet forcing over the last 120kyr. Quaternary Science Reviews 29, 43-55.

Singarayer, J.S., Valdes, P.J., Roberts, W.H.G., 2017. Ocean dominated expansion and contraction of the late Quaternary tropical rainbelt. Scientific Reports 7, 9382.

References

Small, E.E., Giorgi, F., Sloan, L.C., Hostetler, S., 2001. The Effects of Desiccation and Climatic Change on the Hydrology of the Aral Sea. Journal of Climate 14, 300-322.

Sorokin, V.M., 2011. Correlation of upper quaternary deposits and paleogeography of the Black and Caspian seas. Stratigraphy and Geological Correlation 19, 563.

Soulet, G., Ménot, G., Bayon, G., Rostek, F., Ponzevera, E., Toucanne, S., Lericolais, G., Bard, E., 2013. Abrupt drainage cycles of the Fennoscandian Ice Sheet. Proceedings of the National Academy of Sciences 110, 6682-6687.

Sousa, P.M., Ramos, A.M., Raible, C.C., Messmer, M., Tomé, R., Pinto, J.G., Trigo, R.M., 2020. North Atlantic Integrated Water Vapor Transport—From 850 to 2100 CE: Impacts on Western European Rainfall. Journal of Climate 33, 263-279.

Sousounis, P.J., Fritsch, J.M., 1994. Lake-aggregate mesoscale disturbances. Part II: a case study of the effects on regional and synoptic-scale weather systems. Bulletin - American Meteorolgoical Society 75, 1793-1811.

Steffensen, J.P., Andersen, K.K., Bigler, M., Clausen, H.B., Dahl-Jensen, D., Fischer, H., Goto-Azuma, K., Hansson, M., Johnsen, S.J., Jouzel, J., Masson-Delmotte, V., Popp, T., Rasmussen, S.O., Röthlisberger, R., Ruth, U., Stauffer, B., Siggaard-Andersen, M.-L., Sveinbjörnsdóttir, Á.E., Svensson, A., White, J.W.C., 2008. High-Resolution Greenland Ice Core Data Show Abrupt Climate Change Happens in Few Years. Science 321, 680-684.

Stuhne, G.R., Peltier, W.R., 2015. Reconciling the ICE-6G_C reconstruction of glacial chronology with ice sheet dynamics: The cases of Greenland and Antarctica. Journal of Geophysical Research: Earth Surface 120, 1841-1865.

Svendsen, J.I., Alexanderson, H., Astakhov, V.I., Demidov, I., Dowdeswell, J.A., Funder, S., Gataullin, V., Henriksen, M., Hjort, C., Houmark-Nielsen, M., Hubberten, H.W., Ingólfsson, Ó., Jakobsson, M., Kjær, K.H., Larsen, E., Lokrantz, H., Lunkka, J.P., Lyså, A., Mangerud, J., Matiouchkov, A., Murray, A., Möller, P., Niessen, F., Nikolskaya, O., Polyak, L., Saarnisto, M., Siegert, C., Siegert, M.J., Spielhagen, R.F., Stein, R., 2004. Late Quaternary ice sheet history of northern Eurasia. Quaternary Science Reviews 23, 1229-1271.

Svitoch, A.A., 2009. Khvalynian transgression of the Caspian Sea was not a result of water overflow from the Siberian Proglacial lakes, nor a prototype of the Noachian flood. Quaternary International 197, 115-125.

Svitoch, A.A., 2010. The Neoeuxinian basin of the Black Sea and the Khvalinian transgression of the Caspian Sea. Quaternary International 225, 230-234.

Svitoch, A.A., 2013. The Pleistocene Manych straits: Their structure, evolution and role in the Ponto-Caspian basin development. Quaternary International 302, 101-109.

Svitoch, A.A., Makshaev, R.R., 2011. Neotectonics of the Manych Trough. Doklady Earth Sciences 441, 1572-1575.

Svitoch, A.A., Yanina, T.A., 2001. New Data on the Mollusk Fauna from the Marine Pleistocene of Manych. Doklady Biological Sciences 380, 478-481.

Taylor, K.E., Stouffer, R.J., Meehl, G.A., 2012. An Overview of CMIP5 and the Experiment Design. Bulletin of the American Meteorological Society 93, 485-498.

Tokarska, K.B., Stolpe, M.B., Sippel, S., Fischer, E.M., Smith, C.J., Lehner, F., Knutti, R., 2020. Past warming trend constrains future warming in CMIP6 models. Science Advances 6, eaaz9549.

Torres, M.A., Yilmaz, P.O., Isaksen, G.H., 2007. The Petroleum Geology of Western Turkmenistan: The Gograndag-Okarem Province, Oil and Gas of the Greater Caspian Area. American Association of Petroleum Geologists, p. 0.

Tsuang, B.J., Tu, C.Y., Arpe, K., 2001. Lake parameterization for climate models. Max Planck Institute for Meteorology, 316.

Tudryn, A., Chalié, F., Lavrushin, Y.A., Antipov, M.P., Spiridonova, E.A., Lavrushin, V., Tucholka, P., Leroy, S.A.G., 2013. Late Quaternary Caspian Sea environment: Late Khazarian and Early Khvalynian transgressions from the lower reaches of the Volga River. Quaternary International 292, 193-204.

Tudryn, A., Leroy, S.A.G., Toucanne, S., Gibert-Brunet, E., Tucholka, P., Lavrushin, Y.A., Dufaure, O., Miska, S., Bayon, G., 2016. The Ponto-Caspian basin as a final trap for southeastern Scandinavian Ice-Sheet meltwater. Quaternary Science Reviews 148, 29-43.

Turuncoglu, U.U., Elguindi, N., Giorgi, F., Fournier, N., Giuliani, G., 2013a. Development and validation of a regional coupled atmosphere lake model for the Caspian Sea Basin. Climate Dynamics 41, 1731-1748.

Turuncoglu, U.U., Giuliani, G., Elguindi, N., Giorgi, F., 2013b. Modelling the Caspian Sea and its catchment area using a coupled regional atmosphere-ocean model (RegCM4-ROMS): model design and preliminary results. Geoscientific Model Development 6, 283-299.

Valdes, P.J., Armstrong, E., Badger, M.P.S., Bradshaw, C.D., Bragg, F., Crucifix, M., Davies-Barnard, T., Day, J.J., Farnsworth, A., Gordon, C., Hopcroft, P.O., Kennedy, A.T., Lord, N.S., Lunt, D.J., Marzocchi, A., Parry, L.M., Pope, V., Roberts, W.H.G., Stone, E.J., Tourte, G.J.L., Williams, J.H.T., 2017. The BRIDGE HadCM3 family of climate models: HadCM3@Bristol v1.0. Geosci. Model Dev. 10, 3715-3743.

van Baak, C.G.C., Stoica, M., Grothe, A., Aliyeva, E., Krijgsman, W., 2016. Mediterranean-Paratethys connectivity during the Messinian salinity crisis: The Pontian of Azerbaijan. Global and Planetary Change 141, 63-81.

Varuschenko, S., Varuschenko, A., Klige, R., 1987. Changes in the regime of the Caspian Sea and non-terminal water bodies in paleotime. Nauka, Moscow.

Vincent, S.J., Davies, C.E., Richards, K., Aliyeva, E., 2010. Contrasting Pliocene fluvial depositional systems within the rapidly subsiding South Caspian Basin; a case study of the palaeo-Volga and palaeo-Kura river systems in the Surakhany Suite, Upper Productive Series, onshore Azerbaijan. Marine and Petroleum Geology 27, 2079-2106.

Vollset, S.E., Goren, E., Yuan, C.-W., Cao, J., Smith, A.E., Hsiao, T., Bisignano, C., Azhar, G.S., Castro, E., Chalek, J., Dolgert, A.J., Frank, T., Fukutaki, K., Hay, S.I., Lozano, R., Mokdad, A.H., Nandakumar, V., Pierce, M., Pletcher, M., Robalik, T., Steuben, K.M., Wunrow, H.Y., Zlavog, B.S., Murray, C.J.L., 2020. Fertility, mortality, migration, and population scenarios

for 195 countries and territories from 2017 to 2100: a forecasting analysis for the Global Burden of Disease Study. The Lancet 396, 1285-1306.

Wickert, A.D., 2016. Reconstruction of North American drainage basins and river discharge since the Last Glacial Maximum. Earth Surf. Dynam. 4, 831-869.

Woldemeskel, F.M., Sharma, A., Sivakumar, B., Mehrotra, R., 2016. Quantification of precipitation and temperature uncertainties simulated by CMIP3 and CMIP5 models. Journal of Geophysical Research: Atmospheres 121, 3-17.

Wyser, K., Kjellström, E., Koenigk, T., Martins, H., Döscher, R., 2020. Warmer climate projections in EC-Earth3-Veg: the role of changes in the greenhouse gas concentrations from CMIP5 to CMIP6. Environmental Research Letters 15, 054020.

Xue, P.F., Pal, J.S., Ye, X.Y., Lenters, J.D., Huang, C.F., Chu, P.Y., 2017. Improving the Simulation of Large Lakes in Regional Climate Modeling: Two-Way Lake-Atmosphere Coupling with a 3D Hydrodynamic Model of the Great Lakes. Journal of Climate 30, 1605-1627.

Yanchilina, A.G., Ryan, W.B.F., Kenna, T.C., McManus, J.F., 2019. Meltwater floods into the Black and Caspian Seas during Heinrich Stadial 1. Earth-Science Reviews 198, 102931.

Yanina, T., Bolikhovskaya, N., Sorokin, V., Romanyuk, B., Berdnikova, A., Tkach, N., 2020. Paleogeography of the Atelian regression in the Caspian Sea (based on drilling data). Quaternary International.

Yanina, T., Sorokin, V., Bezrodnykh, Y., Romanyuk, B., 2018. Late Pleistocene climatic events reflected in the Caspian Sea geological history (based on drilling data). Quaternary International 465, 130-141.

Yanina, T.A., 2012. Correlation of the Late Pleistocene paleogeographical events of the Caspian Sea and Russian Plain. Quaternary International 271, 120-129.

Yanina, T.A., 2014. The Ponto-Caspian region: Environmental consequences of climate change during the Late Pleistocene. Quaternary International 345, 88-99.

References

Yanko-Hombach, V., Kislov, A., 2018. Late Pleistocene – Holocene sea-level dynamics in the Caspian and Black Seas: Data synthesis and Paradoxical interpretations. Quaternary International 465, 63-71.

Zavialov, P.O., Kostianoy, A.G., Emelianov, S.V., Ni, A.A., Ishniyazov, D., Khan, V.M., Kudyshkin, T.V., 2003. Hydrographic survey in the dying Aral Sea. Geophys Res Lett 30.

Zekster, I.S., 1995. Groundwater discharge into lakes: A review of recent studies with particular regard to large saline lakes in central Asia. International Journal of Salt Lake Research 4, 233-249.

[dataset] Harrison, S., Dennisenko, O., Prentice, C., Sykes, M., 1991. Lake Status Records, Caspian and Aral Seas. IGBP PAGES/World Data Center-A for Paleoclimatology Data Contribution Series # 91-008. NOAA/NGDC Paleoclimatology Program, Boulder CO, USA.

[dataset] Copernicus Climate Change Service (C3S), 2017. ERA5: Fifth generation of ECMWF atmospheric reanalyses of the global climate. Copernicus Climate Change Service Climate Data Store (CDS), accessed on 21-03-2020. https://cds.climate.copernicus.eu/cdsapp#!/home

[dataset] GEBCO Compilation Group, 2019. The GEBCO_2019 Grid - a continuous terrain model of the global oceans and land. British Oceanographic Data Centre, National Oceanography Centre, NERC, UK. https://doi.org/10/c33m.